# Detectors in Nuclear and Particle Physics

Prof. Dr. Johanna Stachel

Department of Physics und Astronomy
University of Heidelberg

June 3, 2015

# 4. Semiconductor Detectors

4 Semiconductor Detectors
- Principle of operation
- p-n junction
- Signal generation in semiconductor detectors
- Ionization yield and Fano factor
- Energy measurement with semiconductor detectors
  - Ion implanted or diffusion barrier detectors
  - Surface barrier detectors
  - p-i-n detectors Ge(Li), Si(Li)
  - High purity or intrinsic Ge detectors
  - Bolometers
- Position measurement with semiconductor detectors
  - Principle
  - Micro-strip detectors (about 1983)
  - Double-sided micro-strip detectors
  - Silicon drift detectors
  - Pixel detectors (Si)
  - putting it all together: the LHC experiments use Si pixels, strips, and drift
  - CCD, charge-coupled device
- Radiation damage

Main applications:

- $\gamma$ spectroscopy with high energy resolution
- vertex detectors with high spatial resolution
- energy measurement of charged particles (few MeV) and PID via dE/dx (multiple layers)

- use microchip technology; structures with few $\mu$m precision can be produced at low cost; read-out electronics can be directly bonded to detector
- only a few eV per electron-hole pair
- high density compared to gases - need only thin layers

# 4.1 Principle of operation

in semiconductors like Si, Ge, GaAs
lower edge of conduction band $E_C$ only a few eV above upper edge of valence band $E_V$.

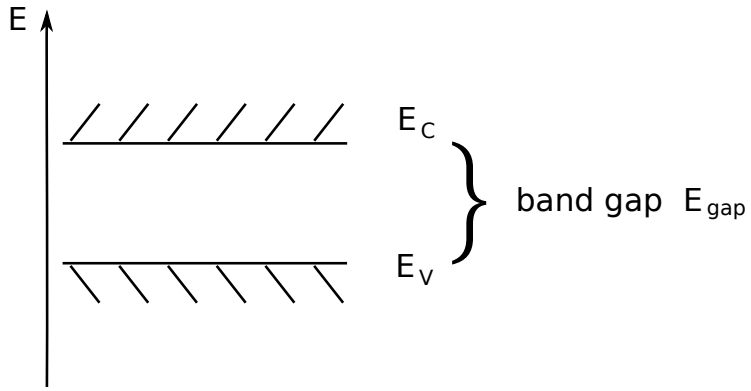


- detector operates like solid state ionization chamber
- charged particle creates electron-hole pairs
- crystal between two electrodes that set up electric field in which charge carriers drift and induce signal
- primary ionization electron has high energy, up to 20 keV $\rightarrow$ many secondary electron-hole pairs and lattice excitations (phonons)
- effect: along track of primary ionizing particle plasma tube of electrons and holes with very high concentration ($10^{15} - 10^{17}$ cm$^{-3}$)
- challenge: need to collect charge carriers before they recombine $\rightarrow$ very high purity semiconductor needed

# Primer Semiconductors - only what is needed here

**Introduction to band structure:**
in a metal an electron interacts with a large number of atoms (order $N_A$)
$\rightarrow$ discrete atomic levels form a group of $N$ very closely spaced levels, 'band'
electrons in a band similar to particles in a box or potential well $\rightarrow$ Fermi gas model

$$E \propto k^2, \text{ density of states} \qquad g(E) = \frac{g(\lambda)}{dE/d\lambda} = \frac{2m}{\hbar^2\lambda} = \frac{(2m)^{3/2}}{2\pi^2\hbar^3}\sqrt{E}$$

number of electrons as function of energy $E$ is determined by a distribution function, the Fermi-Dirac distribution function

$$f(E) = \frac{1}{1+\exp((E-E_F)/kT)}$$

and the number of electrons per energy interval

$$n(E)\mathrm{d}E = g(E)f(E)\mathrm{d}E$$

characteristics of solid determined by location of Fermi energy relative to energy bands

- metal: $E_F$ below top of an energy band
- insulator: $E_F$ at top of valence band and gap to next allowed band too large to be bridged by optical or thermal excitation or electric force at normal E-field
- semiconductor: gap smaller so that electrons can be excited across thermally or optically, $E_F$ between valence and conduction band

# Distribution of electrons and energy levels in semiconductors

Fermi distribution

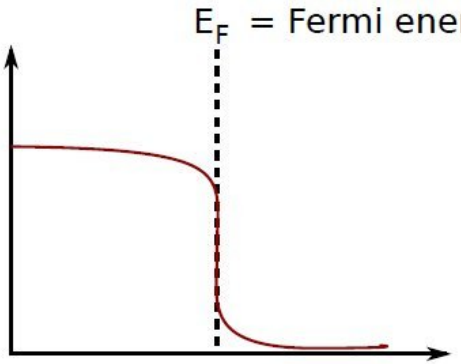


$$f(E) \approx \exp[-(E - E_F)/kT] \qquad E > E_F$$
$$1 - f(E) \approx \exp[-(E_F - E)/kT] \qquad E < E_F$$

Fermi gas model

phase space density g(E)

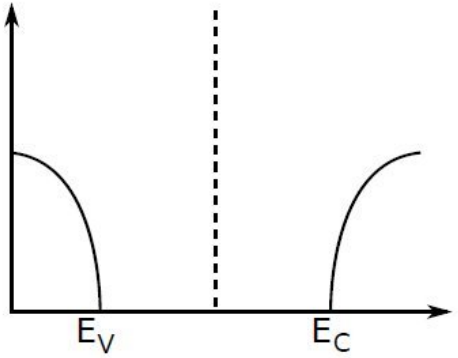


$$g_c(E) = \frac{(2m_n^*)^{3/2}}{2\pi^2\hbar^3}\sqrt{E - E_C} \qquad E > E_C$$
$$g_V(E) = \frac{(2m_p^*)^{3/2}}{2\pi^2\hbar^3}\sqrt{E_V - E} \qquad E < E_V$$

charge carrier distribution

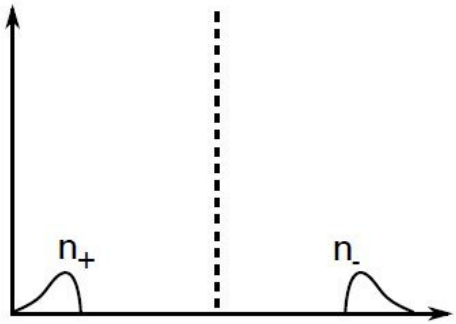


$$n_-(E) = f \cdot g_C$$
$$n_+(E) = (1 - f) \cdot g_V$$

# Intrinsic and extrinsic semiconductors

intrinsic semiconductor:

- very pure material, charge carriers are created by thermal or optical excitation of electrons to conduction band $N_- = N_+$

impurity or extrinsic semiconductor:

- majority of charge carriers provided by impurity atoms at lattice sites of crystal
- impurity atom provides either an extra electron above number required for covalent bonds $\rightarrow$ majority charge carriers are electrons **'n-type semiconductor'**
  or
- impurity atom has insufficient number of electrons for covalent bonds, free hole at impurity site $\rightarrow$ majority charge carriers are holes **'p-type semiconductor'**

most common:

- crystal of element of group IV such as Si or Ge
- impurities of group V (P, As, Sb) or of group III (Al, Ga, In)
- but also GaAs or CdS

in semiconductors like Si, Ge, GaAs, lower edge of conduction band $E_c$ only a few eV above upper edge of valence band $E_v$.

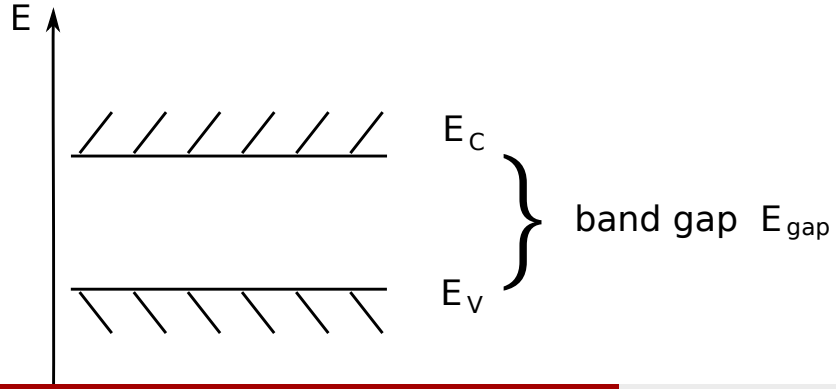


| | $E_{gap}$ |
|---|---|
| Si | 1.12 eV |
| Ge | 0.66 eV |
| GaAs | 1.43 eV |

acceptor and donor levels very close to valence and conduction bands (drawing not to scale!)

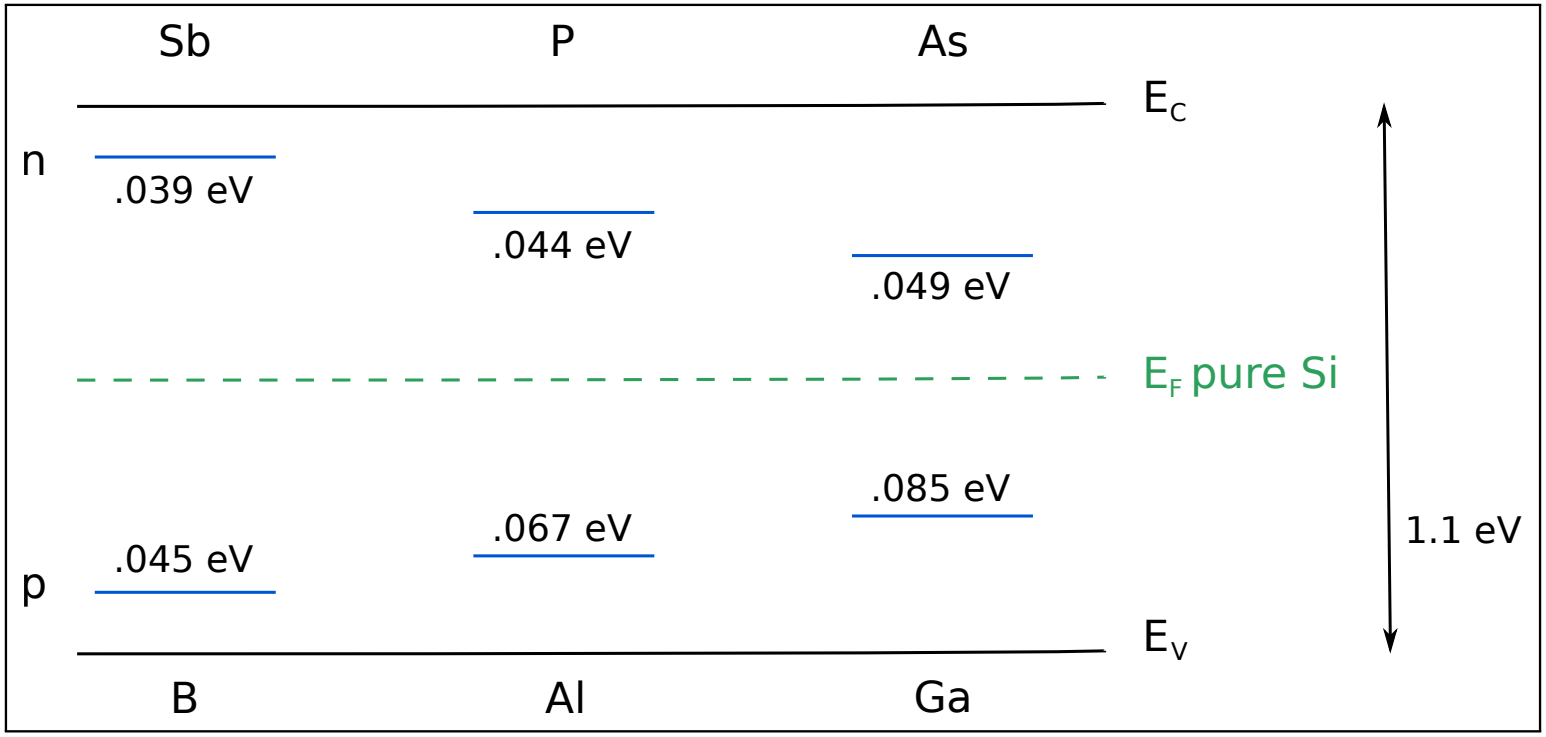


electron donors (P, Sb, ...): $5^{th}$ electron bound only weakly in Si-crystal
can easily be promoted into conduction band (Li-like)

electron acceptors (B, Al, ...): only valence electrons, one unsaturated binding in Si-crystal
tendency to 'accept' an electron from Si leaving behind
a 'hole' in valence band

# Intrinsic and extrinsic semiconductors

intrinsic semiconductor:

the smaller the band gap, the larger the number of charge carriers

$n = \int n_- \mathrm{d}E$

$p = \int n_+ \mathrm{d}E$

$n = p$

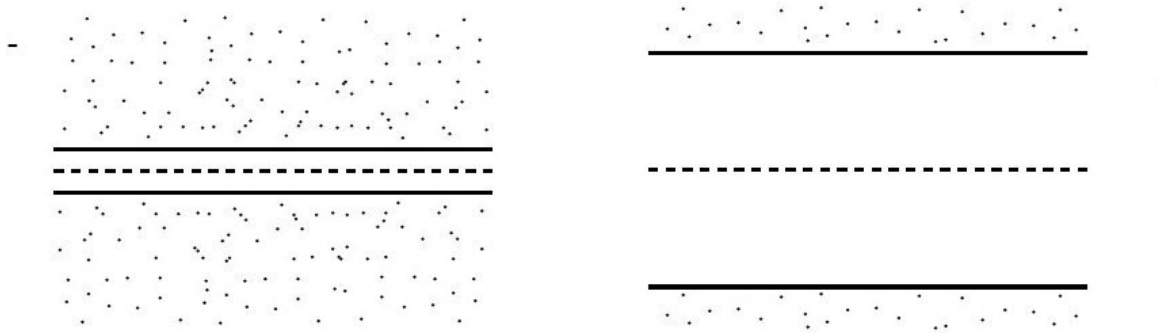

doped semiconductor:

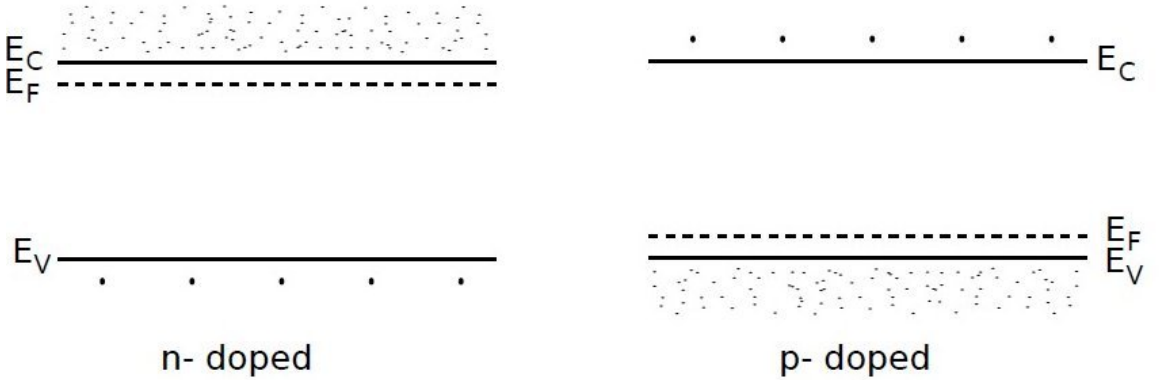


| | | | |
|---|---|---|---|
| $T = 0$ | $Si + P$ | $Si + B$ | not conducting |
| $T \neq 0$ | $Si + P^+ + e^-$ | $Si + B^- + \oplus$ | |
| | n conducting | p conducting | |

# Intrinsic and extrinsic semiconductors

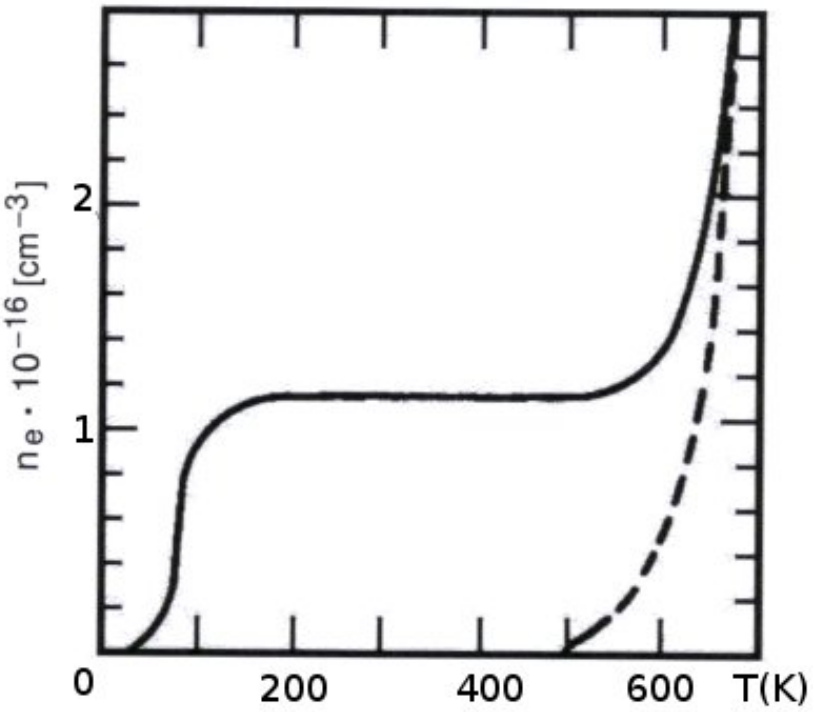


electron density in conduction band
in pure Si (dashed)
and in Si doped with As ($10^{16}/cm^3$)

electrical behavior determined by mobility of charge carriers $\mu$ ($m^2/Vs$)

- drift velocity $v_D = \mu E$
- specific resistance $\rho$ ($\Omega m$)
- resistance $R = \rho\, l/A$ with length $l$ and area $A$ transverse to $E$

# Intrinsic semiconductors I

- density of electrons in conduction band

$$n = \int n_- \, dE = \int_{E_c}^{\infty} f \, g_c \, dE = N_c \exp[-(E_c - E_F)/kT]$$

and correspondingly density of holes in valence band

$$p = \int n_+ dE = \int_{-\infty}^{E_v} (1 - f) \, g_v \, dE = N_v \exp[-(E_F - E_v)/kT]$$

$N_c, N_v$: effective density of states at edge of conduction with valence bands and $N_{c,v} = 2 \left( \frac{m^*_{n,p} kT}{2\pi\hbar^2} \right)^{\frac{3}{2}}$ with effective masses $m^*$ of electrons and holes
i.e. much weaker $T$-dependence than exponential,
looks like only levels at $E_c$ and $E_v$ present, not broad bands

- for pure or intrinsic semiconductors

$$\begin{aligned} E_c - E_F &= E_F - E_v \quad \Rightarrow \quad n_i = p_i \\ np &= N_c N_v \exp\left( -\frac{(E_c - E_v)}{kT} \right) = n_i^2 \end{aligned}$$

note: product of $n$ and $p$ at a given $T$ has fixed value characterized by effective masses and band gap (often called 'law of mass action')

typical values at 300 K :

Si $n_i = 1.5 \cdot 10^{10}$ cm$^{-3}$ raise $T$ by 8 K $\rightarrow$ $n_i$ doubles
Ge $n_i = 2.5 \cdot 10^{13}$ cm$^{-3}$

- drift of charge carriers: as in gases, random thermal motion plus drift in electric field

$$\text{mobility} \quad \mu \cong \text{const. for } E < 10^3 \text{ V/cm}$$

$$\mu \propto \frac{1}{\sqrt{E}} \text{ for } 10^3 \text{ V/cm} < E < 10^4 \text{ V/cm}$$

$$\mu \propto \frac{1}{E} \text{ for } E > 10^4 \text{ V/cm} \quad \Rightarrow \quad \boxed{v_D = \mu \cdot E \rightarrow \text{const.}}$$

saturates at about 10 cm/$\mu$s (similar to gases)
$\rightarrow$ fast collection of charges (10 ns for 100 $\mu$m)
but: $v_h \cong 0.3 - 0.5\, v_e$ (very different from gases!)

- conductivity: $$I = \underbrace{e \cdot n_i(\mu_e + \mu_h)}_{\sigma = 1/\rho} E$$

# Properties of Intrinsic Silicon and Germanium

| | | Si | Ge |
|---|---|---|---|
| Atomic number | | 14 | 32 |
| Atomic weight | u | 28.09 | 72.60 |
| Stable isotope mass numbers | | 28-29-30 | 70-72-73-74-76 |
| Density (300 K) | $g/cm^3$ | 2.33 | 5.32 |
| Atoms/$cm^3$ | $cm^{-3}$ | $4.96 \cdot 10^{22}$ | $4.41 \cdot 10^{22}$ |
| Dielectric constant | | 12 | 16 |
| Forbidden energy gap (300 K) | eV | 1.115 | 0.665 |
| Forbidden energy gap (0 K) | eV | 1.165 | 0.746 |
| Intrinsic carrier density (300 K) | $cm^{-3}$ | $1.5 \cdot 10^{10}$ | $2.4 \cdot 10^{13}$ |
| Intrinsic resistivity (300 K) | $\Omega$cm | $2.3 \cdot 10^5$ | 47 |
| Electron mobility (300 K) | $cm^2/Vs$ | 1350 | 3900 |
| Hole mobility (300 K) | $cm^2/Vs$ | 480 | 1900 |
| Electron mobility (77 K) | $cm^2/Vs$ | $2.1 \cdot 10^4$ | $3.6 \cdot 10^4$ |
| Hole mobility (77 K) | $cm^2/Vs$ | $1.1 \cdot 10^4$ | $4.2 \cdot 10^4$ |
| Energy per electron-hole pair (300 K) | eV | 3.62 | |
| Energy per electron-hole pair (77 K) | eV | 3.76 | 2.96 |

Source: G. Bertolini an A. Coche (eds.), Semiconductor Detectors, Elsevier-North Holland, Amsterdam, 1968

# Doped semiconductors I

donor atom is either neutral or ionized: $N_D = N_D^0 + N_D^+$
and accordingly $N_A = N_A^0 + N_A^-$ with

$$N_D^+ = N_D\,(1 - f(E_D))$$
$$N_A^- = N_A\,f(E_A)$$

and

$$f(E) = \frac{1}{exp[(E - E_F)/kT + 1}$$

Note: for $T \neq 0$ one should use $\mu$ instead of $E_F$, but follow here solid state textbooks
Fermi energy (chemical potential) temperature dependent and defined by charge neutrality

$$n + N_A^- = p + N_D^+$$

and as above we have

$$n = N_c \exp[-(E_c - E_F)/kT]$$
$$p = N_v \exp[-(E_F - E_v)/kT]$$

$\rightarrow$ location of donor or acceptor levels of doped semiconductor relative to the Fermi energy together with $N_{c,v}$ and $T$ determines properties

for n-type semiconductor: Fermi energy moves with increasing temperature from value between conduction band and donor levels to middle between valence and conduction band

# Doped semiconductors II

at room temperature $E_F$ is close to $E_D$
$\rightarrow kT \approx E_c - E_D = E_d$ and $\exp[-E_d/kT] \approx 1$
charge carriers dominantly electrons of the donor and nearly all donors ionized
$n \cong N_D \approx const. \gg n_i$

p-conducting material: analogous for positively charged holes of acceptor

typical dopant concentration: $\geq 10^{13}$ atoms/cm$^3$ (compare density of Si: $5 \cdot 10^{23}$/cm$^3$)
strong doping: 'n$^+$' or 'p$^+$' $\cong 10^{20}$ atoms/cm$^3$

equilibrium between densities of electrons and holes:

increase of one type of carrier concentration $\rightarrow$ reduction of the other due to recombination following the law of mass action

$$n \cdot p = n_i p_i = A \cdot T^3 \exp\left(-\frac{E_{gap}}{kT}\right)$$

so, for n-doped material concentration of holes is decreased

# Doped semiconductors III

example: at 300 K in Si

$$n_i = p_i = 10^{10}\ \mathrm{cm}^{-3}$$
$$n = 10^{17}\ \mathrm{cm}^{-3} \quad \rightarrow \quad p = 10^{3}\ \mathrm{cm}^{-3}$$

conductivity determined by majority carriers (electrons in n-doped, holes in p-doped)
role of minority carriers negligible with

$$\begin{aligned} n &\cong N_D \\ p &\cong \frac{n_i p_i}{N_D} = \frac{n_i^2}{N_D} \\ \frac{1}{\rho} &= \sigma = e \cdot N_D \cdot \mu_e \end{aligned}$$

typical values:

| pure Si | Si p-type $10^{13}\ \mathrm{cm}^{-3}$ |
|---|---|
| $2.3 \cdot 10^5\ \Omega$cm | 500 $\Omega$cm |

# Doped semiconductors IV

**important for fabrication of semiconductor detectors:**
on a substrate very thin layers ('epitactic layers') of $< 1\,\mu$m thickness can be grown with density of carriers very different from substrate.

e.g. film with low carrier density ($\rho$ large) on high charge carrier density substrate ($\rho$ small):
within $1\,\mu$m density can change by factor $10 - 100$

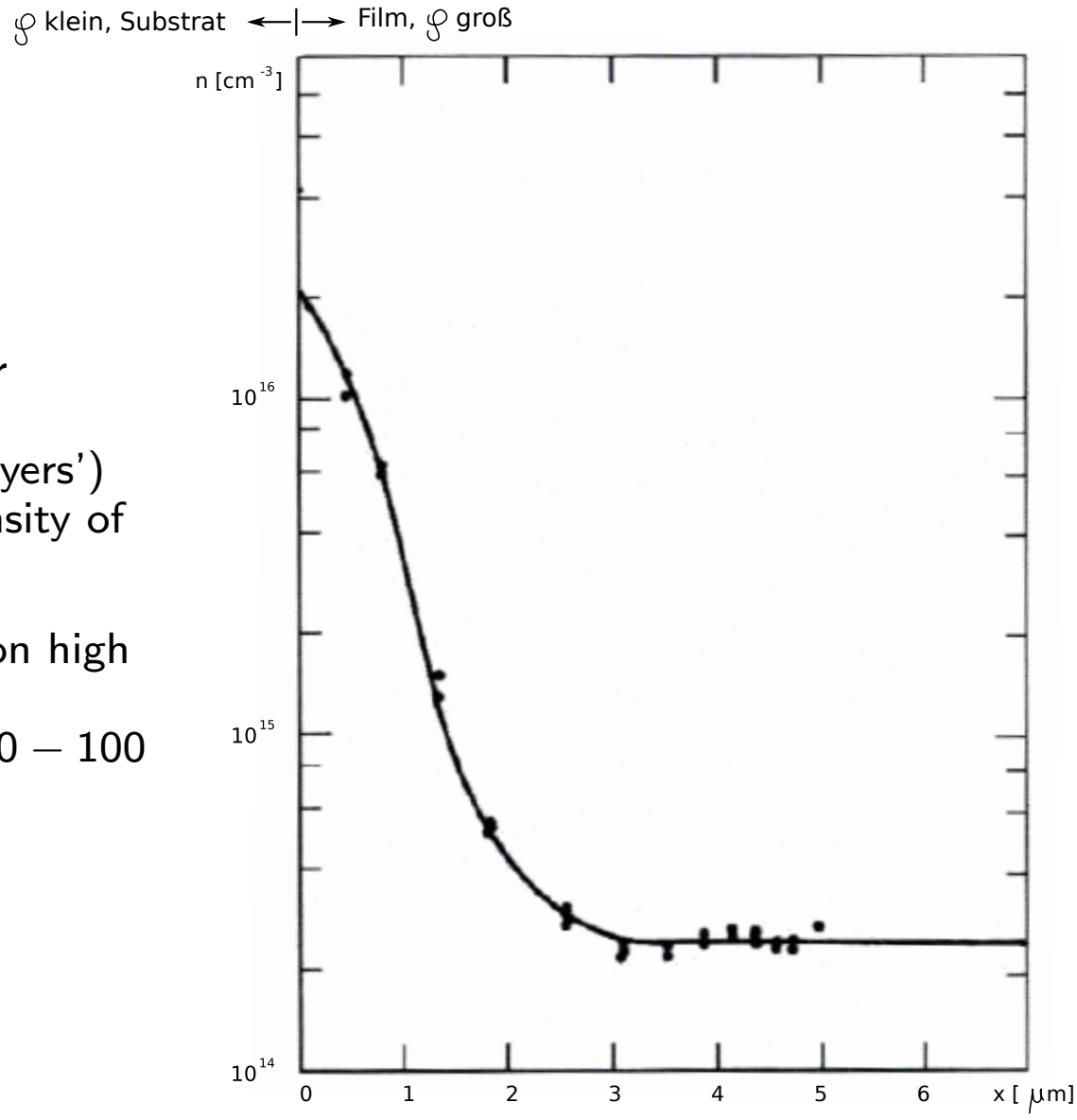

# 4.2 p-n junction

- bring p- and n-semiconductors into contact; thermodynamic equilibrium → Fermi-energies of both systems become equal

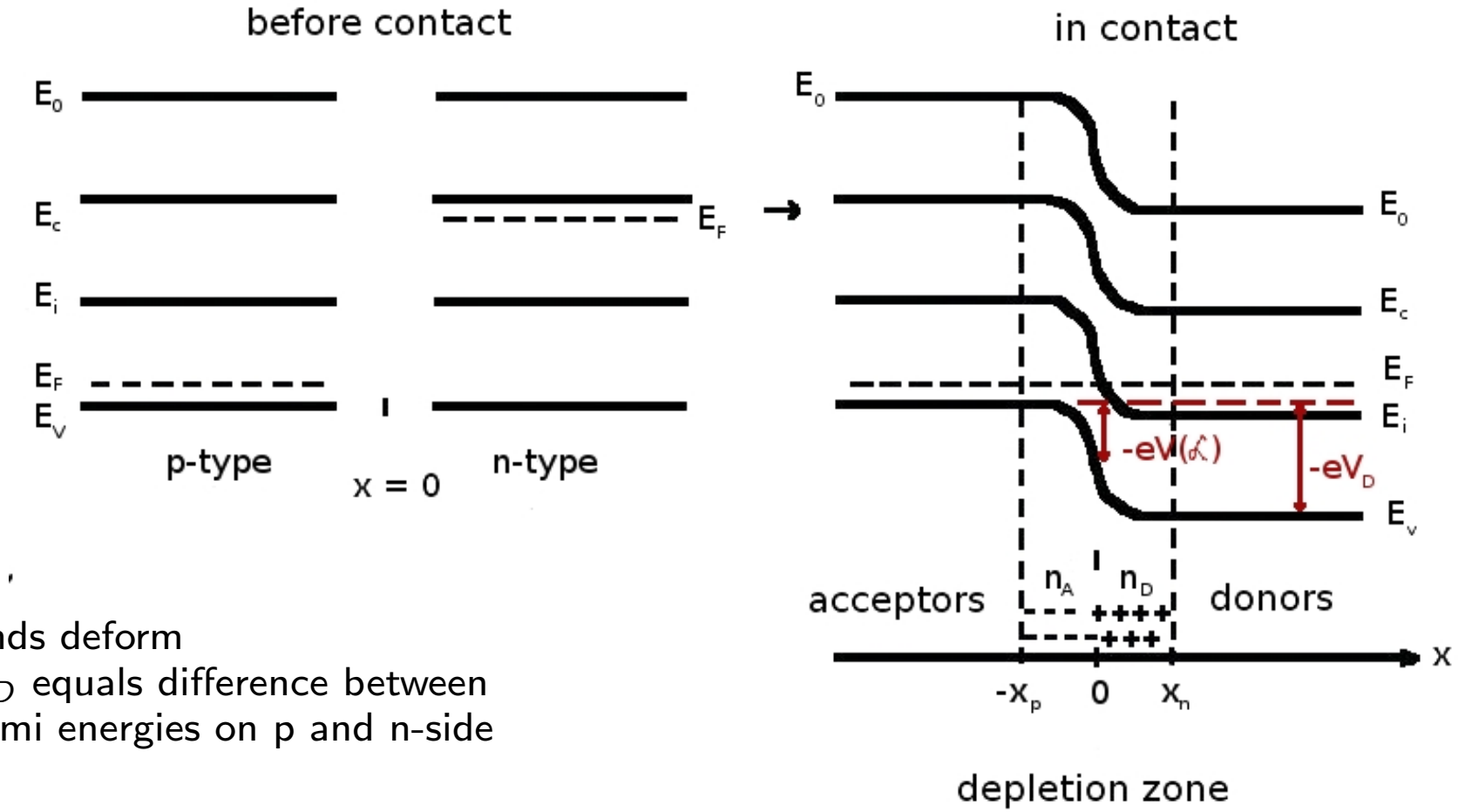


- bands deform
  $eV_D$ equals difference between Fermi energies on p and n-side

- equilibration is achieved by electrons diffusing from n to p semiconductor and holes from p to n
- at the boundary a zone with few free charge carriers (electrons and holes) builds up 'depletion layer'
- fixed charges are left behind (ionized donors and acceptors) $\rightarrow$ space charge
  E-field builds up and counteracts the diffusion which stops eventually (like Hall effect)
  with $n \approx N_D$ and $p \approx N_A$, difference between Fermi energies on both sides gives

$$\begin{aligned} eV_D &= E_c - kT \ln \frac{N_c}{N_D} - E_v - kT \ln \frac{N_v}{N_A} \\ &= E_{gap} - kT \ln \frac{N_c\, N_v}{N_D\, N_A} \end{aligned}$$

$V_D$: diffusion/contact potential

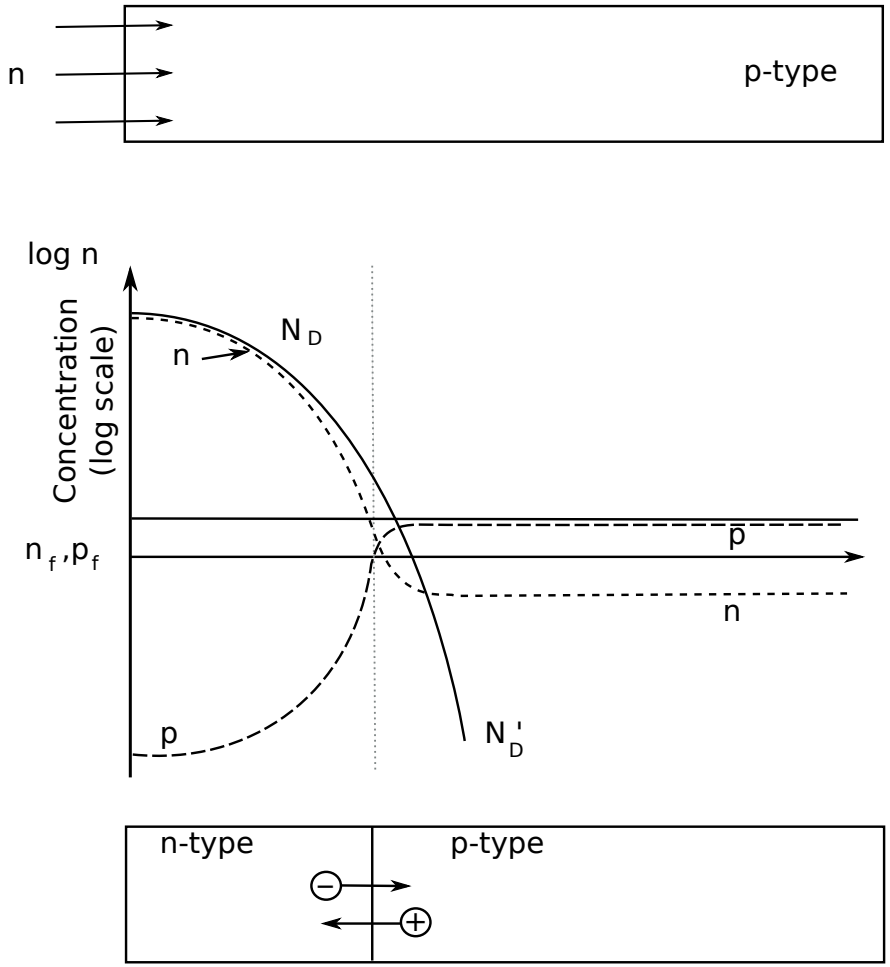


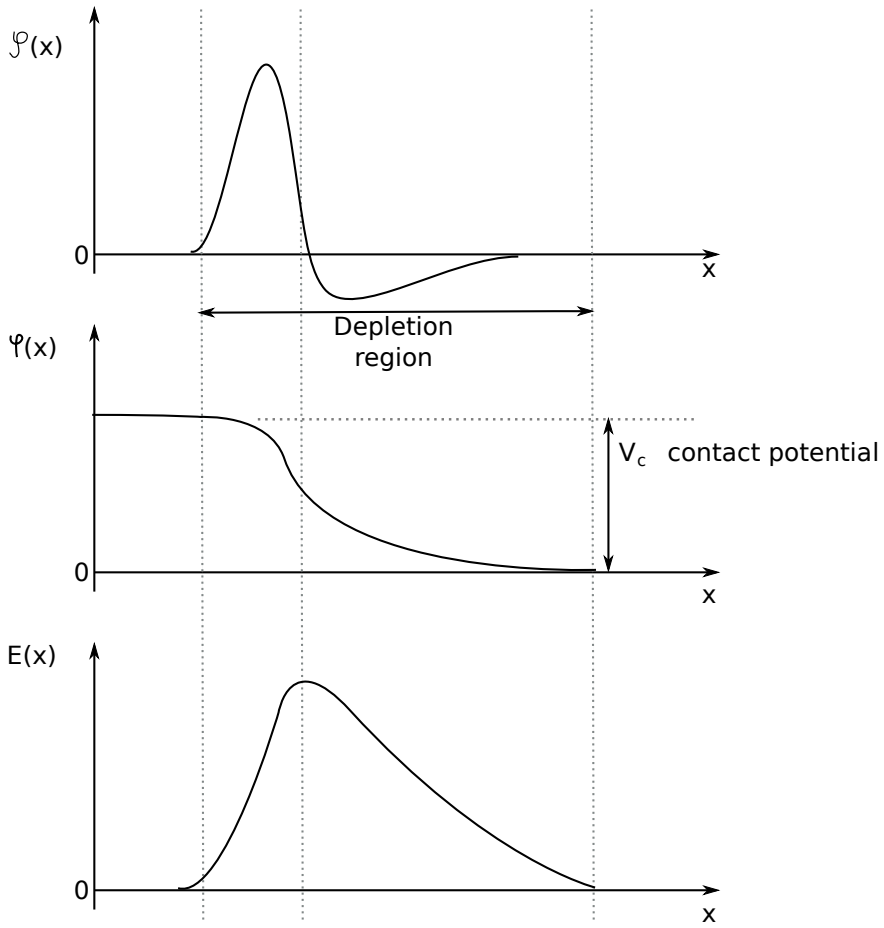


$$\text{n-region} \qquad \rho = e(N_D^+ - n_n(x) + p_n(x))$$

$$\text{p-region} \qquad \rho = -e(N_A^- + n_p(x) - p_p(x))$$

density of majority carriers $n_n, p_p \quad \gg \quad$ density of minority carriers $n_p, p_n$

potential and space charge related by Poisson equation

$$\frac{\partial^2 V(x)}{\partial x^2} = -\frac{\rho(x)}{\epsilon \cdot \epsilon_0}$$

but $\rho(x)$ depends on the potential, need to solve self-consistently

approximation: concentration of free charge carriers in depletion layer very small (approx. 0), abrupt change
$n > 0 \;\rightarrow\; n = p = 0 \;\rightarrow\; p > 0$
in reality over small length
(Debye length, $0.1 - 1\,\mu$m)

for steps in density: Schottky model
area of rectangles such, that overall region space-charge neutral

$$\rho(x) = \begin{cases} 0 & \text{for} \quad x < -d_p \\ -eN_A & -d_p < x < 0 \\ +eN_D & 0 < x < d_n \\ 0 & d_n < x \end{cases}$$

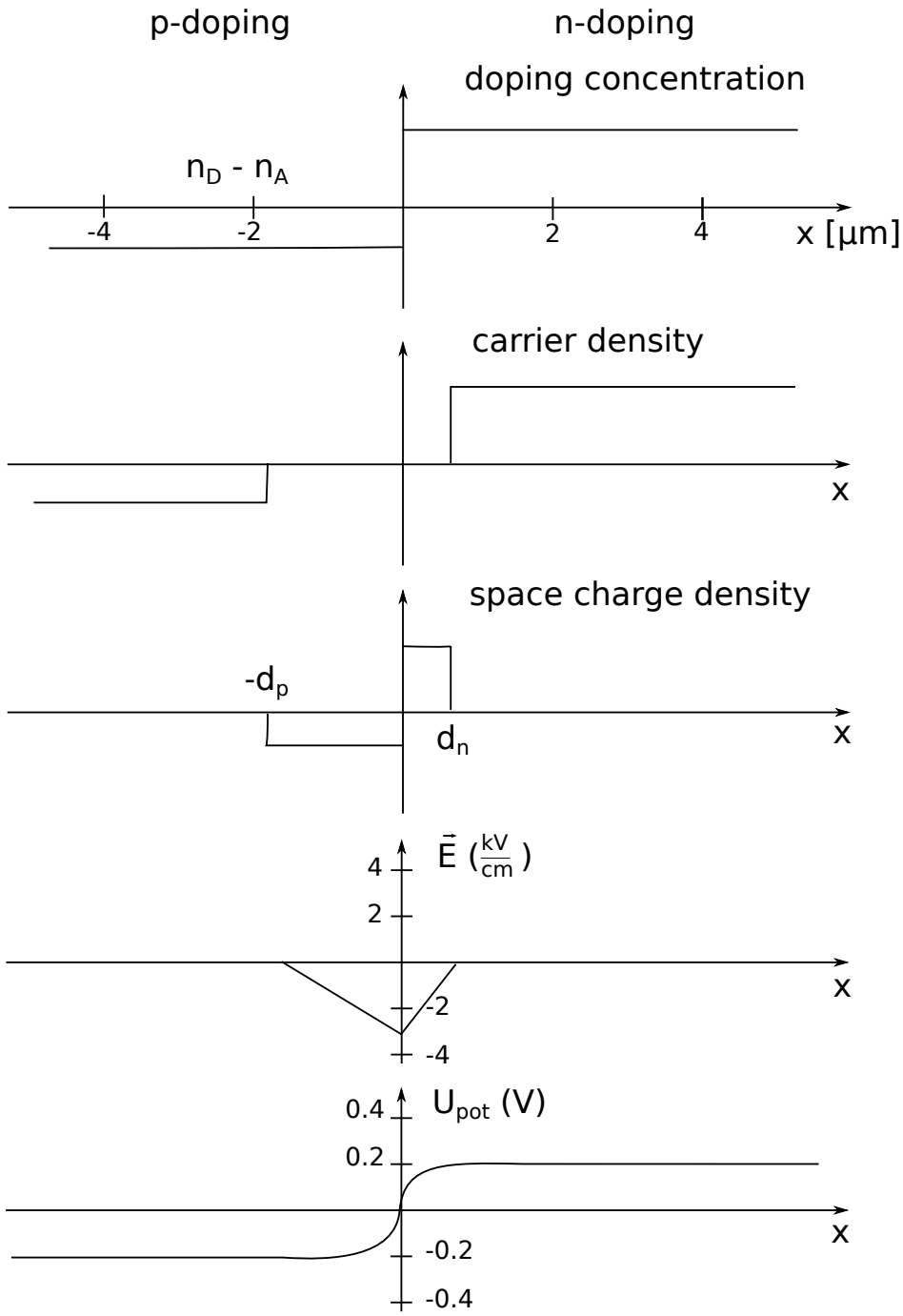

thickness of depletion layer $d_p$ and $d_n$: integrate Poisson equation in pieces
n-doped region:

$$\begin{aligned} \frac{\partial^2 V(x)}{\partial x^2} &= -\frac{eN_D}{\epsilon\epsilon_0} \\ E_x &= -\frac{\partial V}{\partial x} = -\frac{e}{\epsilon\epsilon_0} N_D (d_n - x) \\ V(x) &= V_n(\infty) - \frac{e}{2\epsilon\epsilon_0} N_D (d_n - x)^2 \end{aligned}$$

p-doped region equivalently

condition of neutrality: $N_D d_n = N_A d_p$

continuity of potential $V(x)$ at $x = 0$

$$\frac{e}{2\epsilon\epsilon_0}(N_D d_n^2 + N_A d_p^2) = V_n(\infty) - V_p(-\infty) = V_D$$

$$\Rightarrow \quad d_n = \sqrt{\frac{2\epsilon\epsilon_0 V_D}{e} \frac{N_A/N_D}{N_A + N_D}} \quad \text{and} \quad d_p = \sqrt{\frac{2\epsilon\epsilon_0 V_D}{e} \frac{N_D/N_A}{N_A + N_D}}$$

e.g. $eV_D \cong E_{gap} \cong 1\ \text{eV}$, $N_A \cong N_D = 10^{14}\ \text{cm}^{-3}$ $\Big\}$ $d_n \cong d_p \cong 1\,\mu\text{m}$, $E \cong 10^6\ \text{V/m}$

to achieve large width on one side choose asymmetric doping,
e.g. $N_D = 10^{12}/\text{cm}^3$ and $N_A = 10^{16}/\text{cm}^3$ (need very pure material to start with)

**in presence of external field**

most of the voltage drop $U$ occurs in depletion layer (very few free carriers, large $\rho$)

$$V_n(\infty) - V_p(\infty) = V_D - U$$

choose sign such that positive $U$ is opposite to diffusion potential (contact potential)

**Forward bias** $U > 0$:

holes diffuse in n-direction electrons diffuse in p-direction, potential barrier is lowered

majority carriers recombine in depletion region: 'recombination current',
or penetrate to the other side: 'diffusion current',
depletion zone narrows

$$d_n(U) = d_n(0)\sqrt{1 - \frac{U}{V_D}}$$

$$d_p(U) = d_p(0)\sqrt{1 - \frac{U}{V_D}}$$

**reverse bias** $U < 0$:

electron-hole pairs generated in or near the depletion layer by thermal processes (or in the case of detector by ionization) are separated: 'leakage current'
depletion zone becomes wider (at 300 V order of 1 mm)

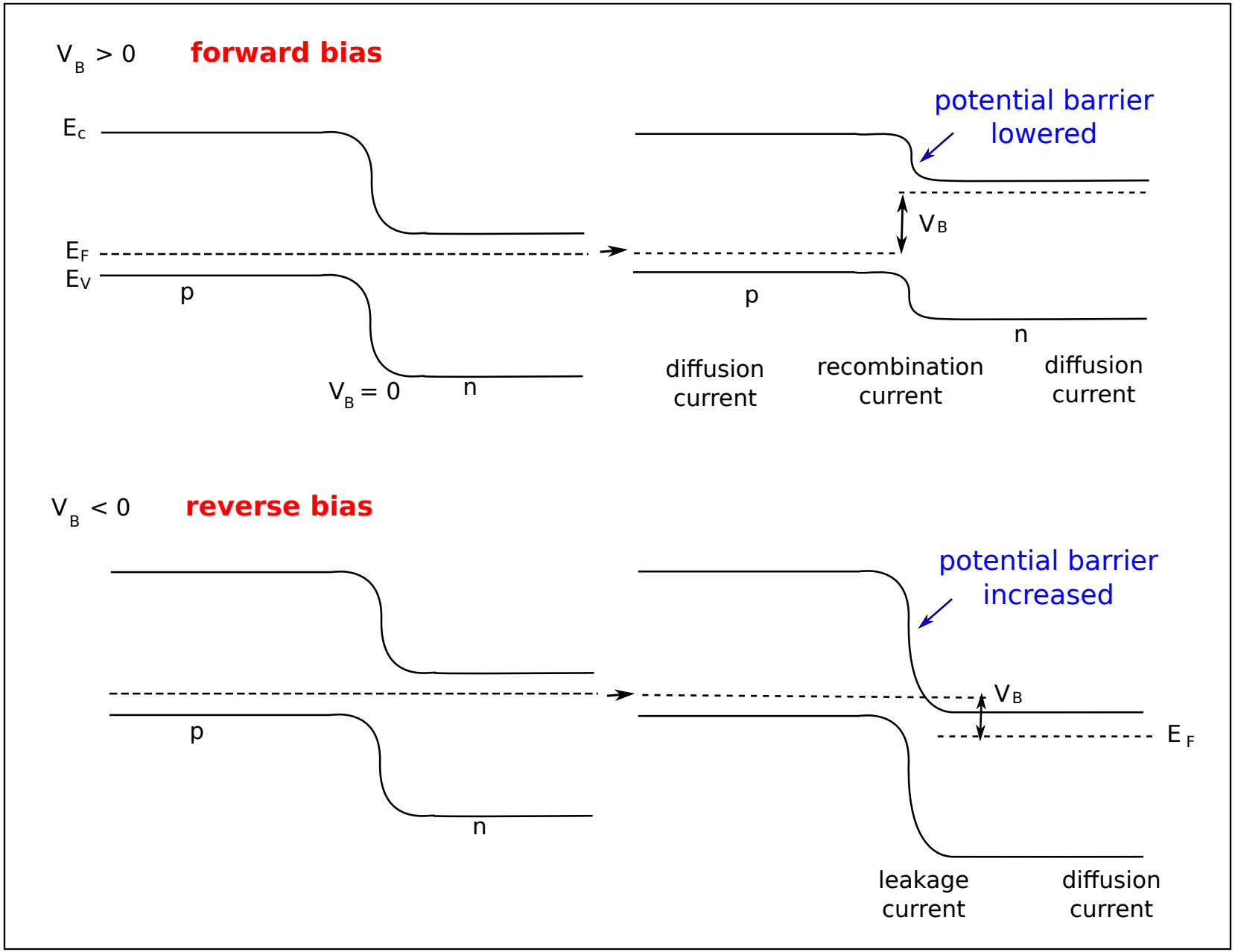


note:
to maximize thickness of depletion layer, need high resistivity (pure material) $d \cong \sqrt{2\epsilon\epsilon_0 U\rho\mu}$

# p-n semiconductor detector

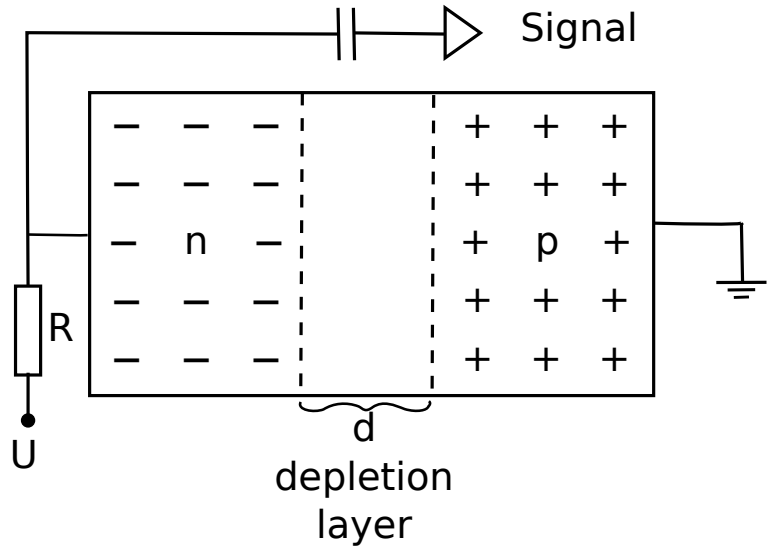


$+++$, $---$: free charge carriers

typical realization:

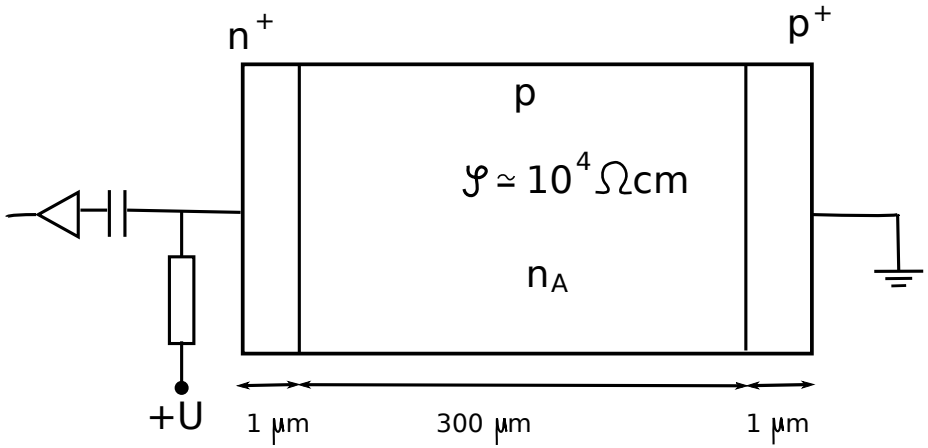


$p^+$, $n^+$: very highly doped, conducting

$$d_p + d_n \cong d_p \cong \sqrt{\frac{2\epsilon\epsilon_0}{e}\frac{U}{N_A}}$$

since $N_A \ll N_D$, $V_D \ll U$

with $N_A \cong 10^{15}$ cm$^{-3}$ $\Rightarrow$

$$U = \frac{e}{2\epsilon\epsilon_0} N_A d_p^2 \cong 100 \text{ V}$$

$$|E| = \frac{100 \text{ V}}{300 \cdot 10^{-6} \text{ m}} = 3 \cdot 10^5 \text{ V/m}$$

(safe; spark limit at $10^7$ V/m)

# 4.3 Signal generation in semiconductor detectors

in principle like ionization chambers:
if $E$ const: each drifting electron contributes to signal current while drifting

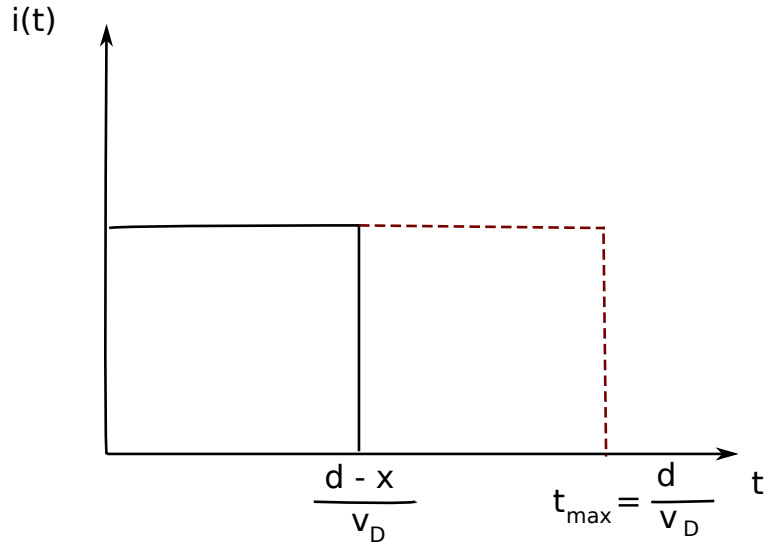


$$i = \frac{\mathrm{d}q}{\mathrm{d}t} = e\frac{\mathrm{d}x}{d}\frac{1}{dx/v_D} = e\frac{v_D}{d}$$

$d$: width of depletion zone
$x$: location where electron was generated

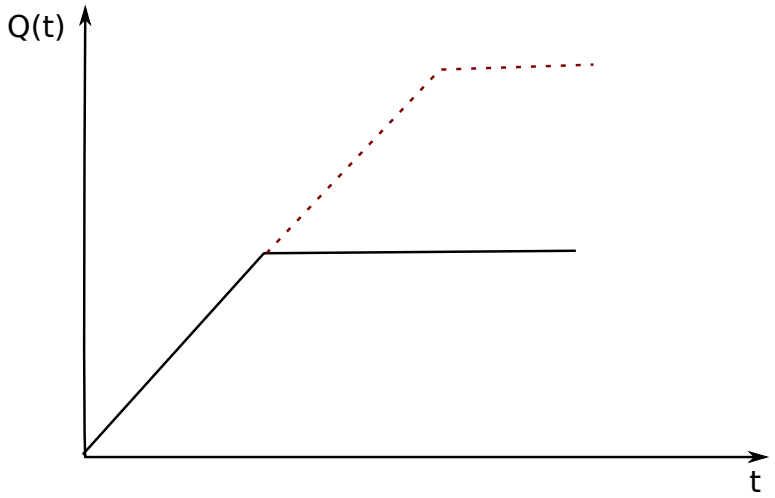


capacitor charges:

$$Q = e\frac{v_D}{d}\cdot t = e\frac{v_D}{d}\frac{d-x}{v_D}$$

line charge of electrons across the depletion layer (constant ionization along track):

$$\begin{aligned} i &= N_0 e \frac{v_D}{d} \left(1 - \frac{t v_D}{d}\right) \Theta \left(1 - \frac{t v_D}{d}\right) \\ Q(t) &= N_0 e \frac{v_D}{d} \left(t - \frac{t^2 v_D}{d}\right) \Theta \left(1 - \frac{t v_D}{d}\right) \end{aligned}$$

integrated:

$$Q\left(t = \frac{d}{v_D}\right) = \frac{N_0 e}{2}$$

same signal for positive carriers (holes), thus in total

$$\boxed{N_0 \cdot e = Q_{tot}}$$

more realistic treatment: E-field depends on $x$

simple ansatz: $|\vec{E}| = \frac{e\,N_A}{\epsilon\epsilon_0} \cdot x$

and with $\sigma = \frac{1}{\rho} = e\,N_A\,\mu_+$ and $\tau = \frac{\epsilon\epsilon_0}{\sigma}$

$$|\vec{E}| = \frac{x}{\mu_+ \tau} \qquad (\tau \cong 1 \text{ ns})$$

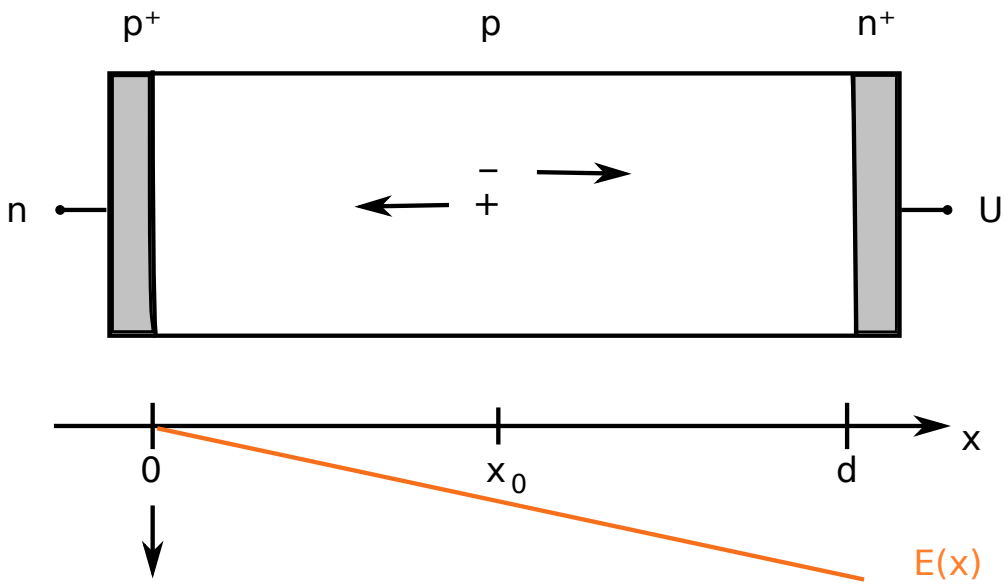


for an electron generated at location $x$ inside depletion zone and mobilities independent of $E$:

$$v_- = -\mu_- E = \frac{\mu_-}{\mu_+}\frac{x}{\tau} \quad \Rightarrow \quad x = x_0 \exp\left(\frac{\mu_- t}{\mu_+ \tau}\right)$$

total drift time of electrons:

$$t_d = \tau \frac{\mu_+}{\mu_-} \ln\left(\frac{d}{x_0}\right)$$

charge signal for $t < t_d$

$$Q_-(t) = -\frac{e}{d}\int \frac{dx}{dt} dt = \frac{e}{d} x_0 \left(1 - \exp\left(\frac{\mu_- t}{\mu_+ \tau}\right)\right)$$

analogously for hole

$$v_+ = \mu_+ E = -\frac{x}{\tau} \quad \Rightarrow \quad x = x_0 \exp\left(-t/\tau\right)$$

$$Q_+(t) = -\tfrac{e}{d} x_0 \left(1 - \exp\left(-t/\tau\right)\right)$$

Total charge signal:

$$Q_-(t_d) + Q_+(t \to \infty) = -e$$

signal rise time essentially determined by

$$\tau = \rho \cdot \epsilon \cdot \epsilon_0$$

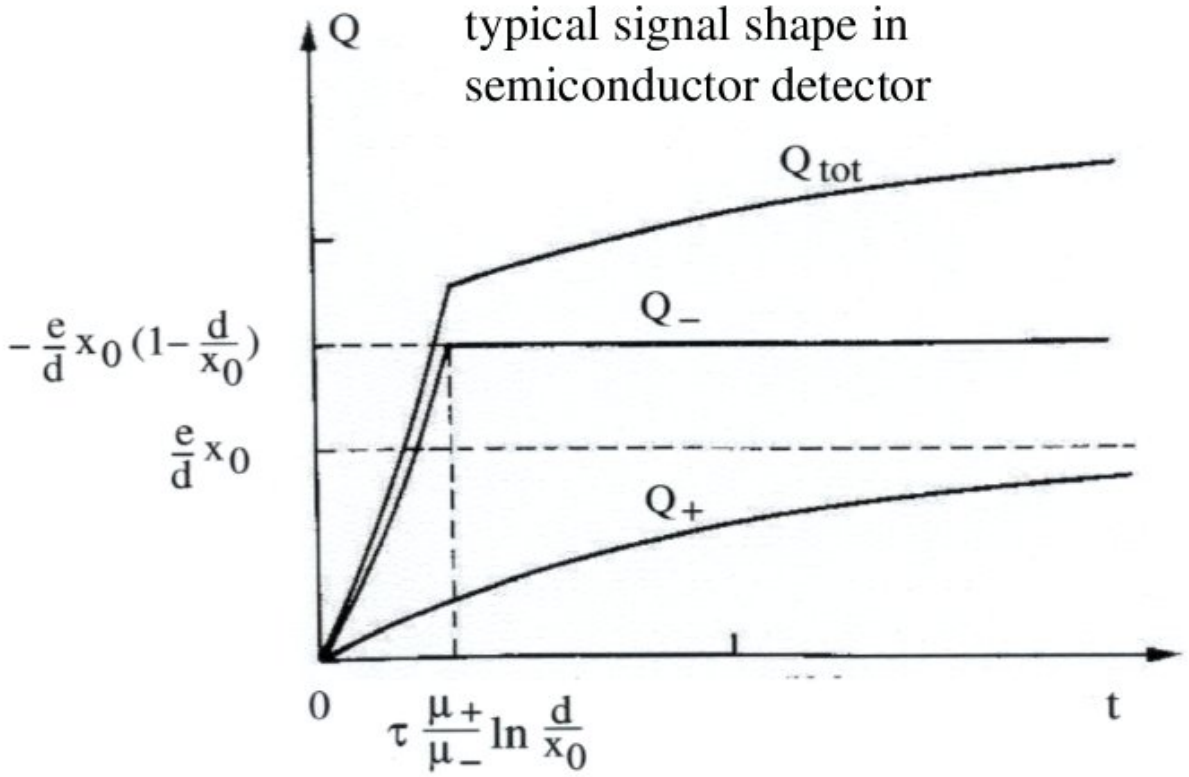


in reality a bit more complicated:

- track not exactly a line charge (distributed over typically 50 $\mu m$ width)
- $\mu_\pm \neq$ constant
- some loss of charges due to recombination at impurities

  for Si $\tau = \rho \cdot 10^{-12}$ s ($\rho$ in $\Omega$cm), $\rho = 1000\ \Omega$cm $\to \tau = 1$ ns

# 4.4 Ionization yield and Fano factor

mean energy per electron-hole pair

| | $E_0^{300\ \mathrm{K}}$ | $E_0^{77\ \mathrm{K}}$ | $E_{\mathrm{gap}}$ |
|---|---|---|---|
| Si | 3.6 eV | 3.8 eV | 1.1 eV |
| Ge | - | 2.9 eV | 0.7 eV |

$\sim \frac{2}{3}$ goes into excitation of crystal lattice

Energy loss $\Delta E \quad \Rightarrow$

- lattice vibrations: generation of phonons, typical quantum energy $E_x = 0.037$ eV
- ionization: characteristic energy $E_i = E_{\mathrm{gap}} = 1.1$ eV in Si
- total: $\Delta E = E_i N_i + E_x N_x$

assume Poisson distributions for both processes with $\sigma_i = \sqrt{N_i} \quad \sigma_x = \sqrt{N_x}$

for a fixed energy loss $\Delta E$:
sharing between ionization and lattice excitation varies as $E_x \Delta N_x + E_i \Delta N_i = 0$

on average: $E_i \sigma_i = E_x \sigma_x$

$$\sigma_i = \frac{E_x}{E_i}\sigma_x = \frac{E_x}{E_i}\sqrt{N_x}$$

using $N_x = (\Delta E - E_i N_i)/E_x$

$$\sigma_i = \frac{E_x}{E_i}\sqrt{\frac{\Delta E}{E_x} - \frac{E_i}{E_x}N_i}$$

$N_i = \dfrac{\Delta E}{E_0}$ in case of ideal charge collection without losses

$$\rightarrow \qquad \sigma_i = \frac{E_x}{E_i}\sqrt{\frac{\Delta E}{E_x} - \frac{E_i}{E_x}\frac{\Delta E}{E_0}} = \underbrace{\sqrt{\frac{\Delta E}{E_0}}}_{\sqrt{N_i}} \; \underbrace{\sqrt{\frac{E_x}{E_i}\left(\frac{E_0}{E_i} - 1\right)}}_{\sqrt{F}}$$

F: Fano factor

Si: $E_0 \cong 3.6$ eV $\quad F \cong 0.1$
Ge: $E_0 \cong 2.9$ eV $\quad F \cong 0.1$

$\boxed{\sigma_i = \sqrt{N_i}\sqrt{F}}$ smaller than naive expectation

due to energy conservation, fluctuations are reduced for a given energy loss $\Delta E$
(the total absorbed energy does not fluctuate)

relative energy resolution

$$\boxed{\frac{\sigma_i}{N_i} = \frac{\sqrt{N_i\,F}}{N_i} = \frac{\sqrt{F}}{\sqrt{N_i}} = \frac{\sqrt{F\,E_0}}{\sqrt{\Delta E}} = \frac{\sigma_{\Delta E}}{\Delta E}}$$

example: photon of 5 keV, $E_\gamma = \Delta E$, $\sigma_{\Delta E} = 40$ eV $\cong 1\%$ instead of 2.7% w/o Fano factor

# Energy resolution of semiconductor detector

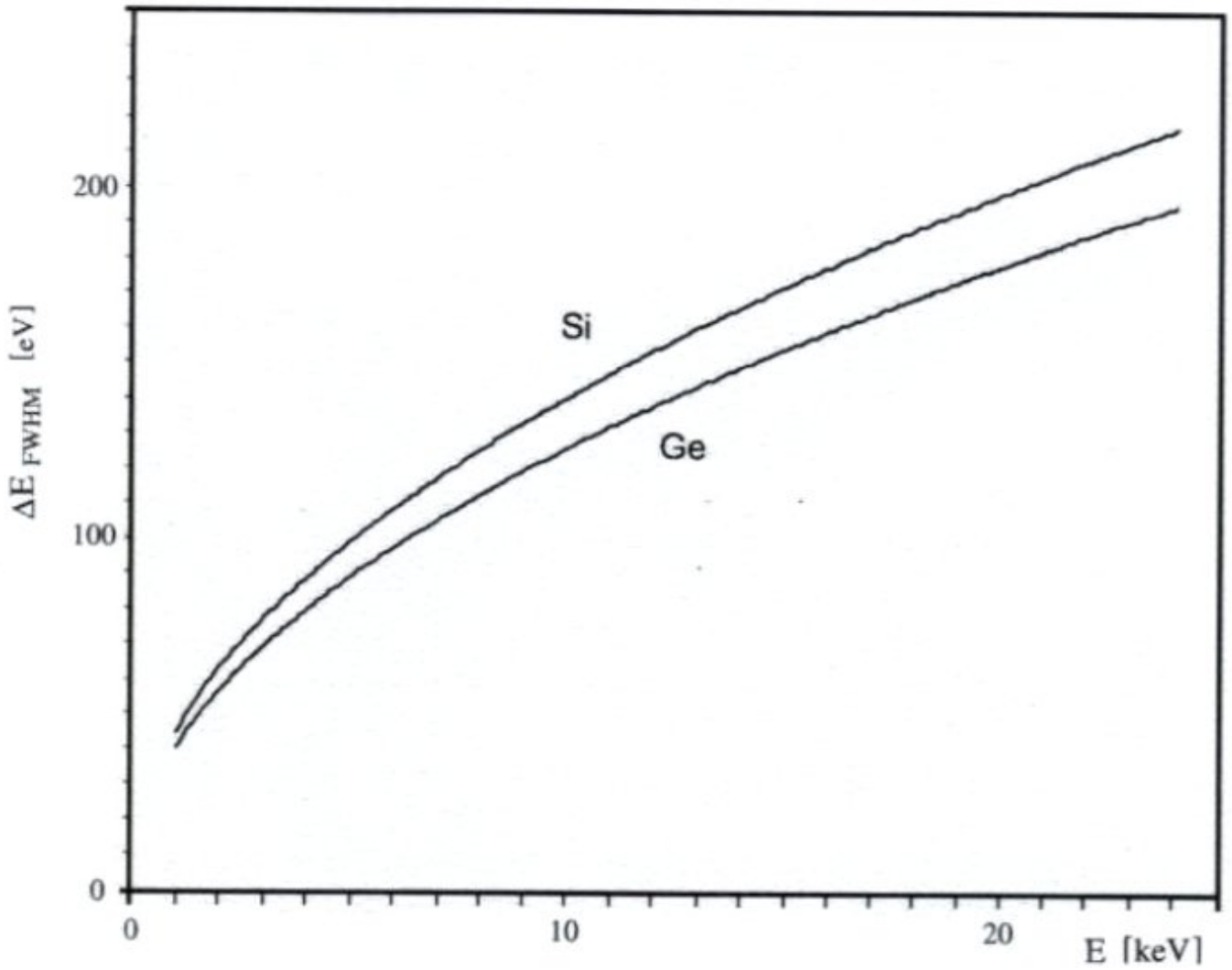


intrinsic resolution due to statistics of charge carriers generated, in addition noise and non-uniformities in charge-collection efficiency

# 4.5 Energy measurement with semiconductor detectors

for low energies, e.g. $\alpha$-particles, low energy electrons or X- and $\gamma$-rays

## 4.5.1 Ion implanted or diffusion barrier detectors

as described in previous paragraph:
p-material with $n^+$ and $p^+$ surface contacts of
50 nm (ion implantation) or
0.1 – 1 $\mu$m (diffusion doping) thickness

$+U$ applied at $n^+$ side

p-layer typically 300 $\mu$m thick, usually
'fully depleted' i.e. depletion layer = p-zone

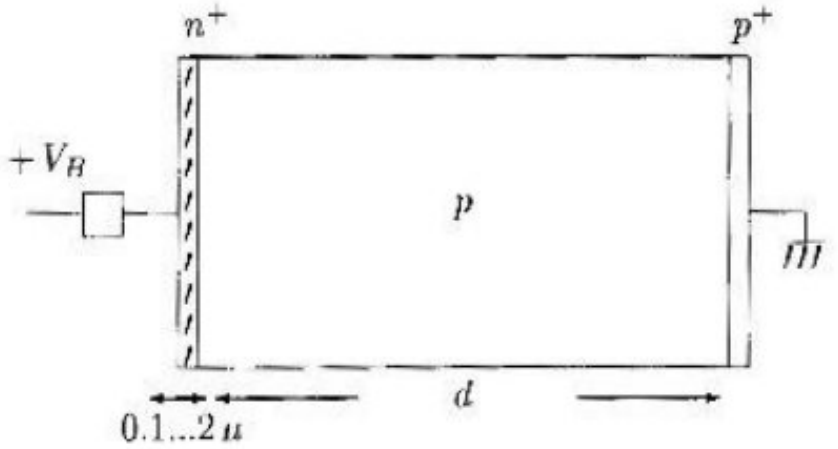


Disadvantage: $n^+$ contact layer acts as dead material for entering particles

- part of energy loss not measured → additional fluctuations
- very soft particles or short range particles like $\alpha$'s may not reach the depletion layer

## 4.5.2 Surface barrier detectors

contacts are very thin evaporated
metal layers, 40 $\mu g/cm^2 \hat{=}$ 20 nm

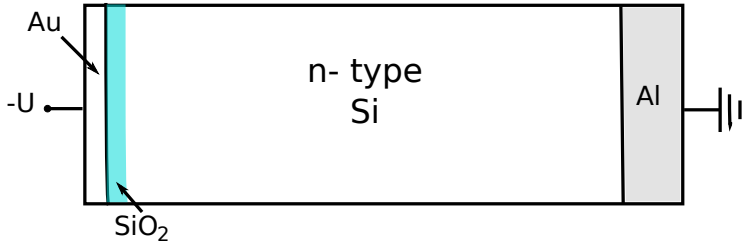

# 2-band model of Schottky diode

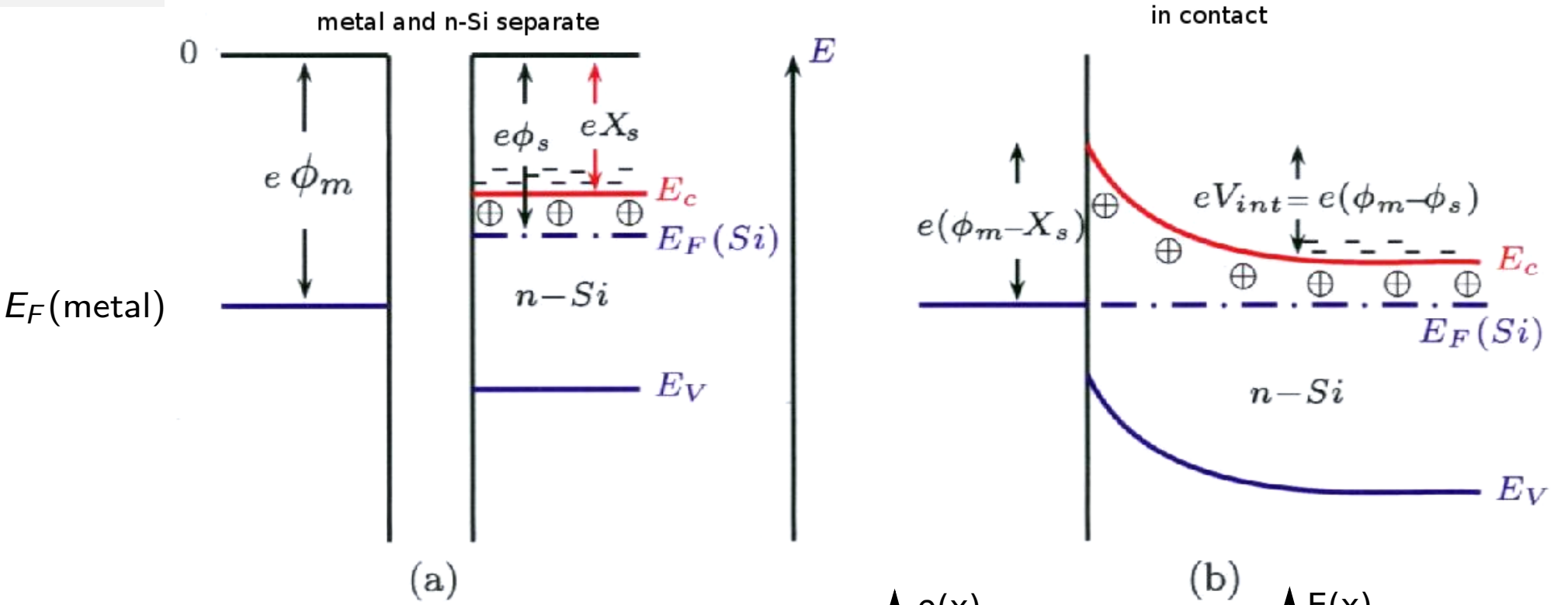


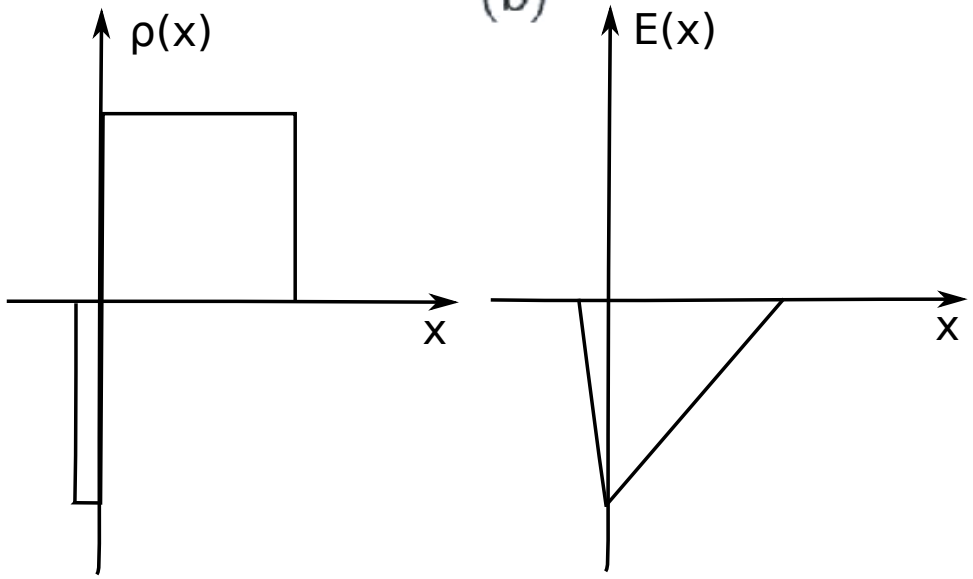


$e\Phi_m$ work function metal
$e\Phi_S$ work function semiconductor $< e\Phi_m$
(otherwise interface would be conducting)
$eX_S$ electron affinity semiconductor

bringing metal in contact with n-Si:
electrons diffuse from Si into metal until
$E_F^{\text{metal}} = E_F^{\text{Si}} \rightarrow$ strong $E$-field at surface

metal – semiconductor junction acts as diode, region with high resistance
$eV_{int} = e(\phi_m - \phi_S)$ potential barrier at surface for electrons in conduction band in Si

applying $-U$ at metal: this barrier is increased $\rightarrow$ no tunneling (dark current)
current only due to ionization

depletion layer in n-Si up to several mm thick
used since the 1960ies for particle detection

advantage of surface barrier detector:
very thin entrance window

- energy loss negligible
- for detection of photons down to eV energy range
  but usually thickness too small for $\gamma$-ray detection above 100 keV,
  i.e. good for X-rays

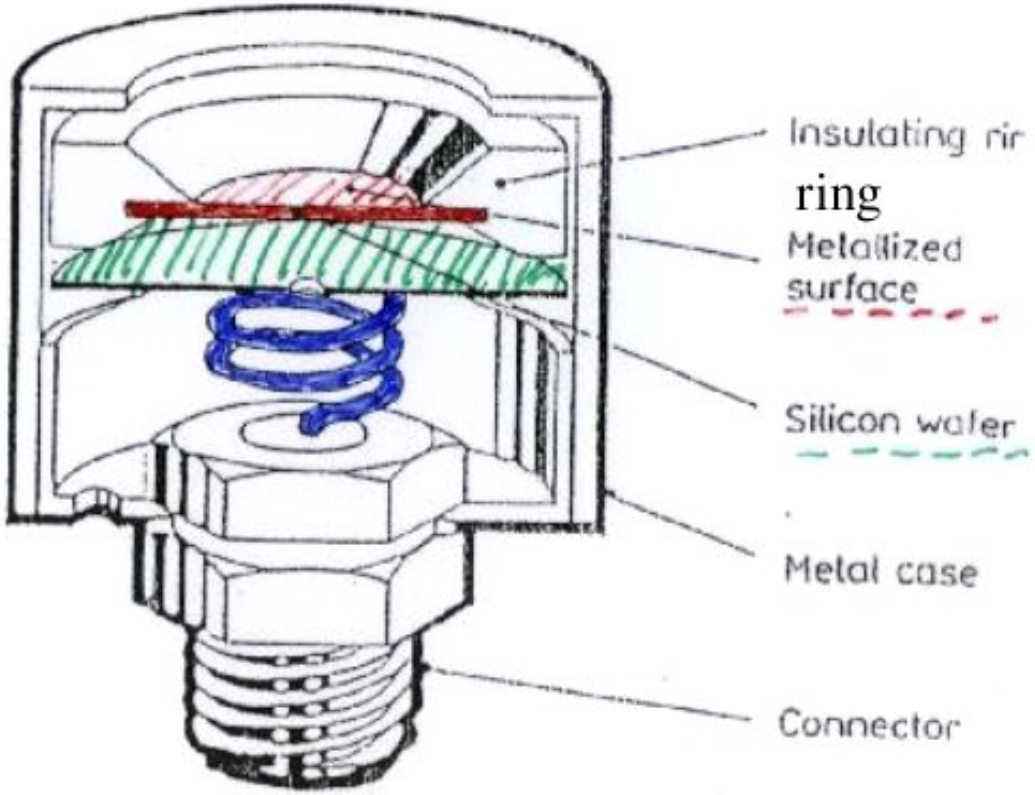

# 4.5.3. p-i-n detectors Ge(Li), Si(Li)

from 1960ies, trick: create a thick (cm) depletion layer with intrinsic conductivity by compensation

1. start with high-purity p-type Ge or Si, acceptor typically Boron
2. bring in contact with liquid Li bath ($350 - 400^\circ$ C) Li diffuses into Ge/Si
3. apply external field $\rightarrow$ positive Li-ions drift far into crystal and compensate B-ions locally

   typically $10^9$ cm$^{-3}$ Li atoms

   p-Si + $Li^+ \mathrel{\hat{=}}$ neutral
   $\rho = 2 \cdot 10^5$ $\Omega$cm possible
   i.e like true intrinsic material

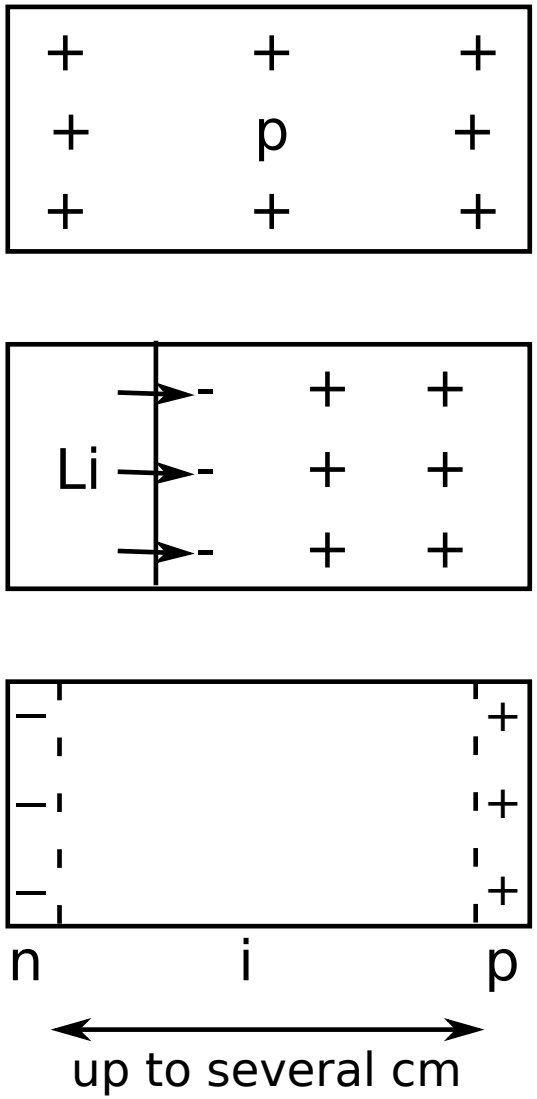

needs to be cooled permanently (liq. $N_2$) to avoid separation of Li from impurities by diffusion!

**application:** $\gamma$-spectroscopy

larger cross section for photo effect in Ge as compared to Si
$\rightarrow$ Ge(Li) preferred

however: full energy peak contains only order of 10 % of the signal in a 50 $cm^3$ crystal
(30 % in a 170 $cm^3$ crystal))

- resolution much better than NaI
- efficiency significantly lower

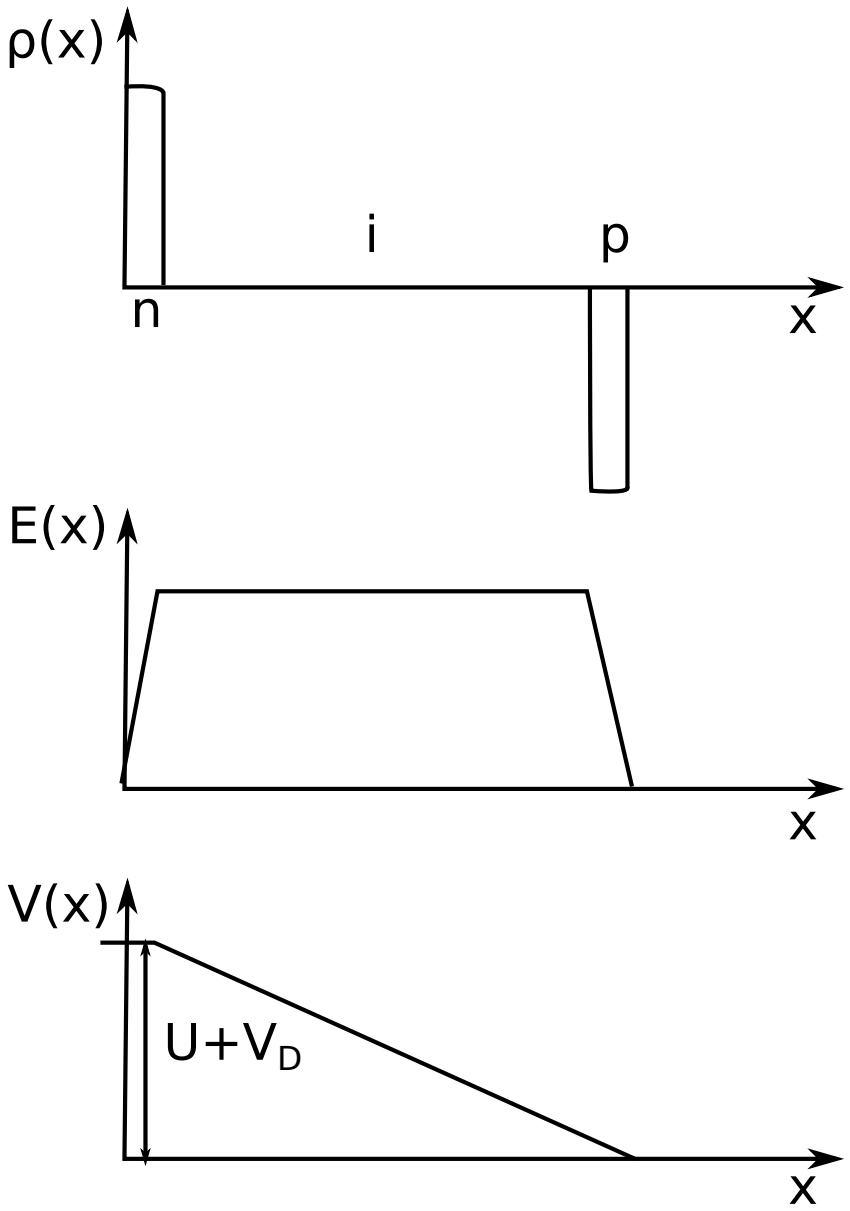


external voltage $U$ and diffusion voltage $V_D$

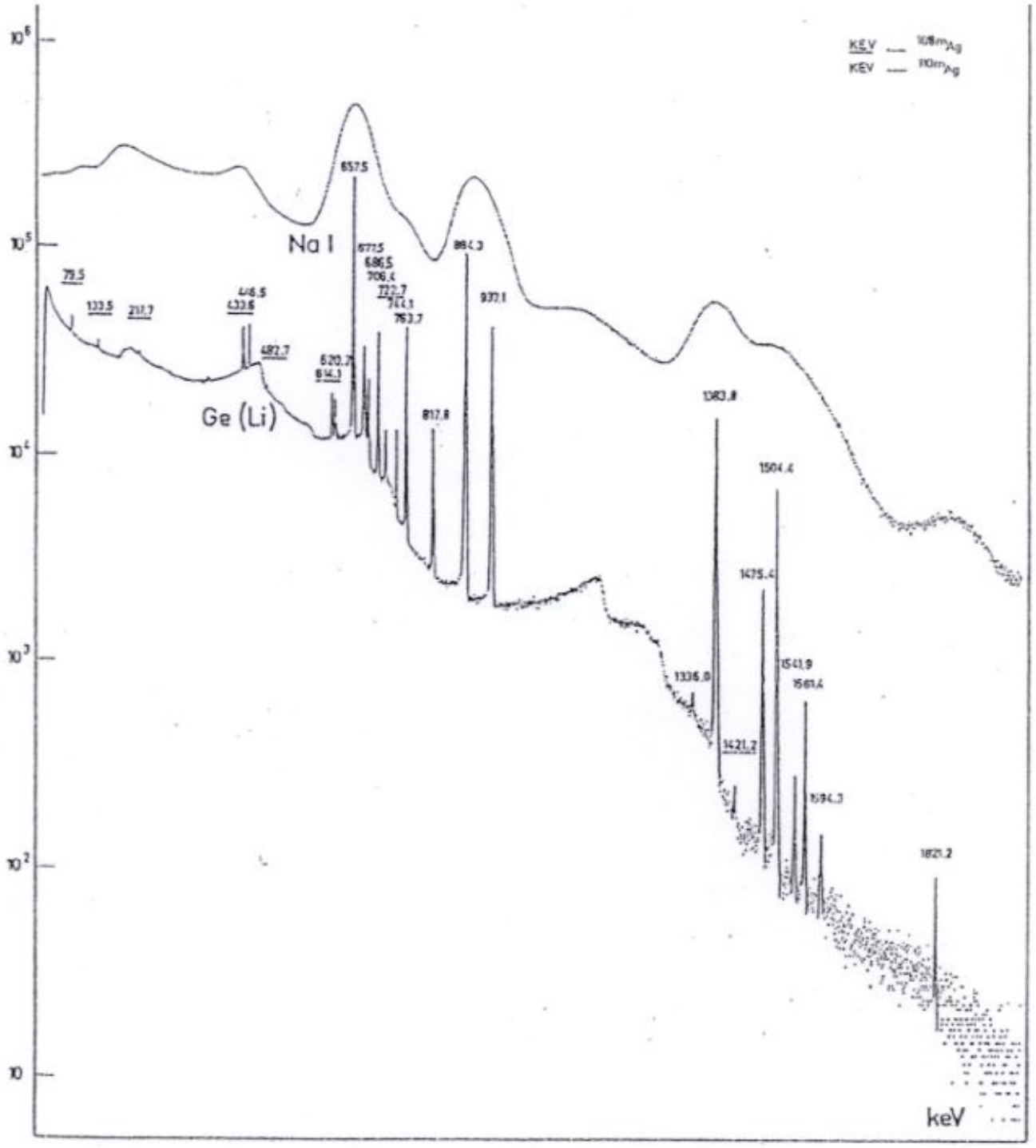


Ge(Li) detectors - a revolution in $\gamma$ spectroscopy in the mid 1960ies:
comparison of spectra obtained with NaI (state of the art technique until then) and Ge(Li)

comparative pulse height spectra recorded using a sodium iodide scintillator and a Ge(Li) detector source of $\gamma$ radiation: decay of $^{108m}$Ag and $^{110m}$Ag, energies of peaks are labeled in keV

# 4.5.4 High purity or intrinsic Ge detectors

from late 1970ies

similar to Li doped Ge or Si detectors, but dark current is kept low not by compensating impurities, but by making material very clean itself

by repeating the purification process (zone melting), extremely pure Ge can be obtained ($\leq 10^9$ impurity atoms per $cm^3$)
intrinsic layer like compensated zone in Ge(Li), similar sizes possible
advantage: cooling only needed during use to reduce noise

**other applications**

- low energy electrons
- strongly ionizing particles
- $dE/dx$ for particle identification

useful energy range determined by range of particle vs. size of detector

ranges of electrons, p, d, $\alpha$, ... in Si

particles stopped in 5 mm Si(Li) detector:

$\alpha$ up to 120 MeV kinetic energy
p up to 30 MeV
e up to 3 MeV

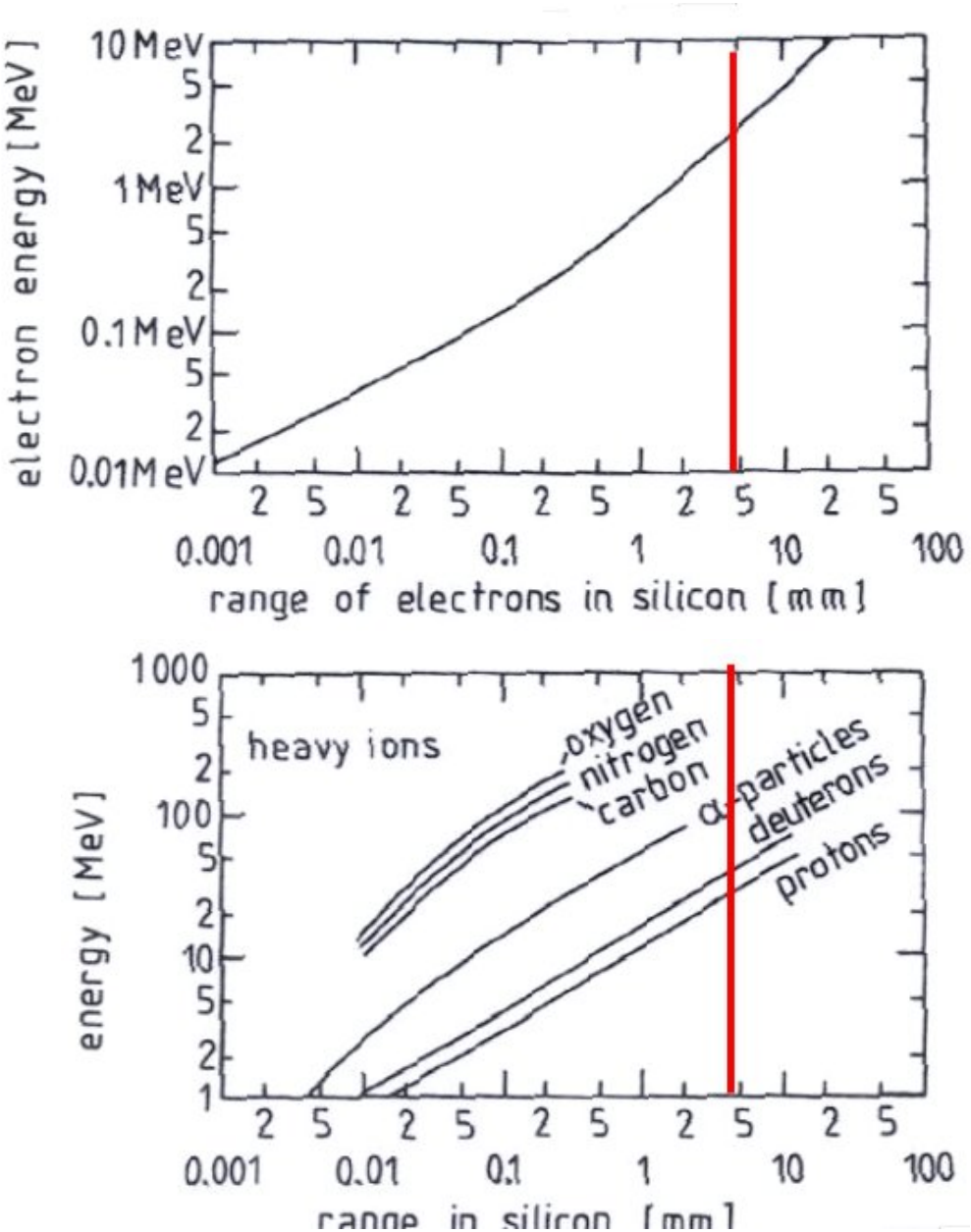


energy-range relation for electrons (top) and more massive particles (bottom)

# 4.5.5 Bolometers

how to increase resolution further?
use even finer steps for energy absorption, e.g. break-up of Cooper pairs in a semiconductor
operate at cryo-temperatures

instead of current one can measure temperature rise due to absorption of e.g. an X-ray,
couple absorber with extremely low heat capacity (HgCdTe) with semiconductor thermistor
$\rightarrow$ excellent energy resolution: 17 eV for 5.9 keV X-ray, i.e. $\Delta E/E = 2.9\,10^{-3}$
but low rate capability

applications: dark matter searches, astrophysical neutrinos, magnetic monopole searches

# 4.6 Position measurement with semiconductor detectors

## 4.6.1 Principle

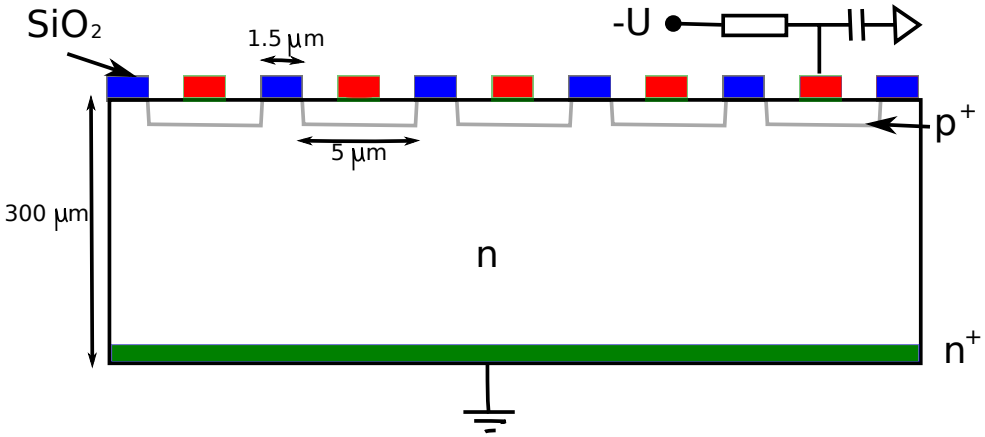


segmentation of readout electrodes into strips, pads, pixels
first usage in 1980ies
standard part of high energy experiments since LEP and Tevatron era

**limitations of position resolution**

- $\delta$-electrons can shift the center of gravity of the track
  estimate limit in Si for track incidence $\perp$ detector:
  $r_\delta$ range of $\delta$-electron
  energy of $\delta$-electron such that $N_\delta$ electron-hole pairs generated vs $N_p$ for primary track:
  assume $\delta \perp$ to primary track

$$\Delta x = \frac{N_\delta (r_\delta/2)}{N_\delta + N_p}$$

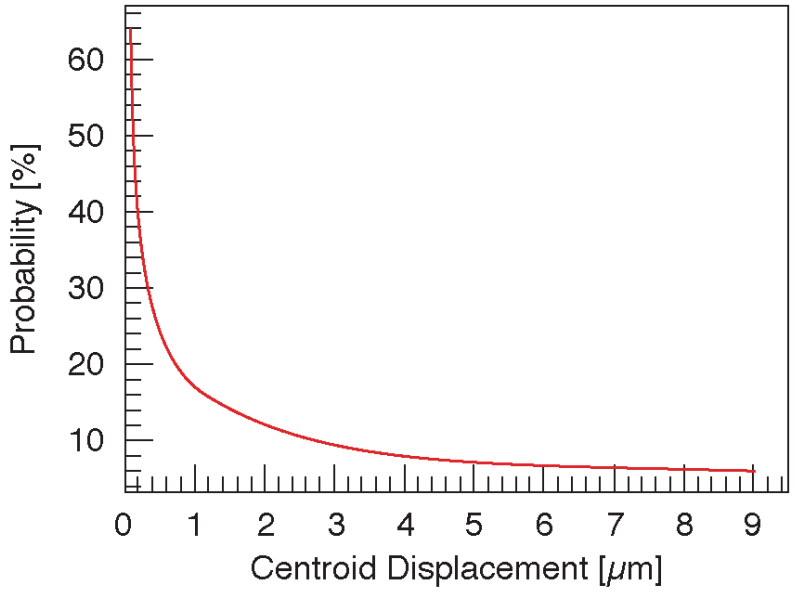


example:
100 $\mu$m Si, 5 GeV pion $\rightarrow$ 240 eV/$\mu$m $\rightarrow N_p = 6700$
10% probability for $\delta$ with $T_\delta > 20$ keV and $r_\delta = 5$ $\mu$m
$\rightarrow$ $\Delta x \approx 1$ $\mu m$
worse for thicker detector: see Fig for 300 $\mu$m Si

- energy loss (Landau) fluctuations have influence on position measurement

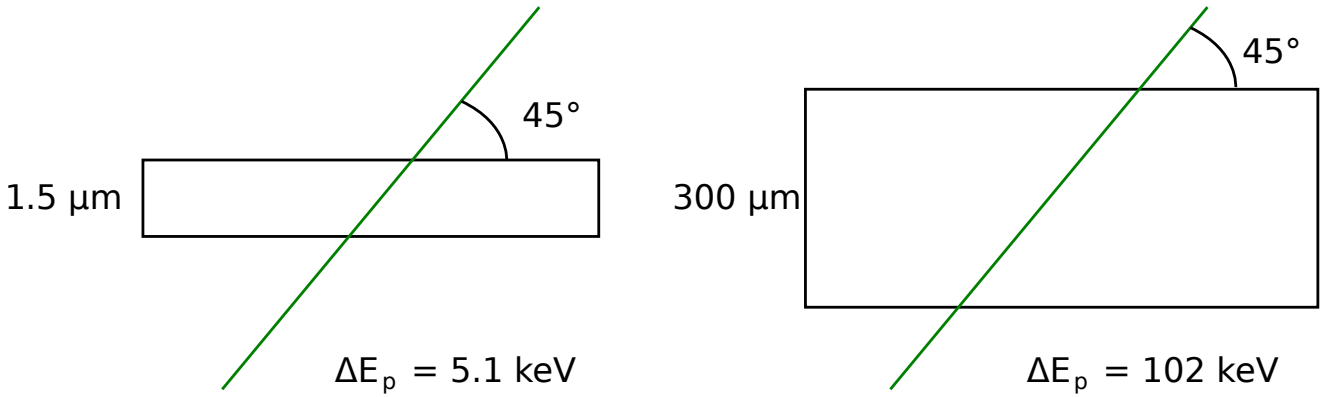


10 % probability for δ of 5 keV
→ Δx ≤ 4 µm but noise!

10 % probability for δ of 100 keV
→ Δx ≤ 87 µm but noise!

- noise: position measurement requires $S \gg N$
  if signal only on 1 strip (or pad), resolution $\sigma_x = \Delta s/\sqrt{12}$, independent of $S/N$
  if signal on several strips ⇒ more precise position by center-of-gravity method (see below), but influenced by $S/N$
- diffusion: smearing of charge cloud (see gaseous detectors, transverse diffusion)
  initially helps to distribute signal over more than one strip
  but 2-track resolution and $S/N$ deteriorate with diffusion
- magnetic fields: Lorentz force on drifting electrons and holes: track signal is displaced if $E$ not parallel $B$, increasing displacement with drift length

## One Strip Clusters


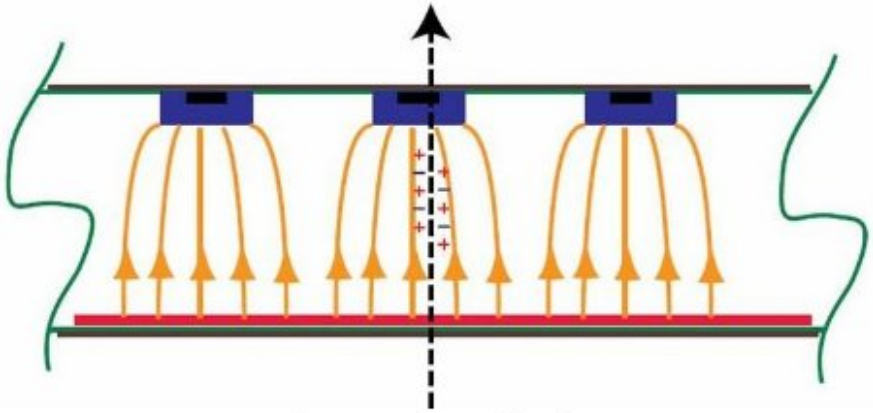

$\Delta s$: strip pitch

$\sigma_x = \Delta s/\sqrt{12}$

## Two Strip Clusters

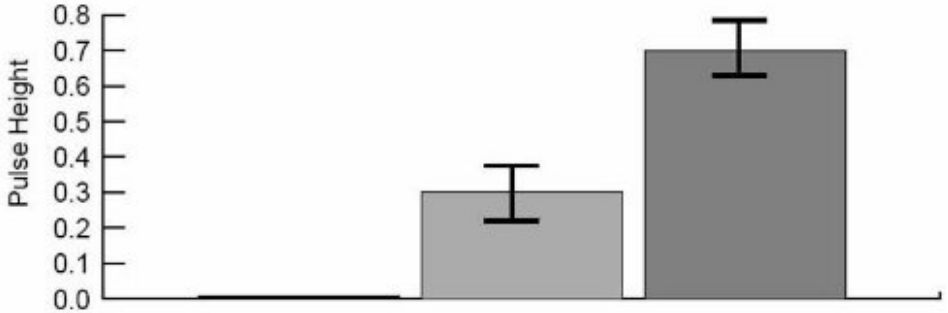


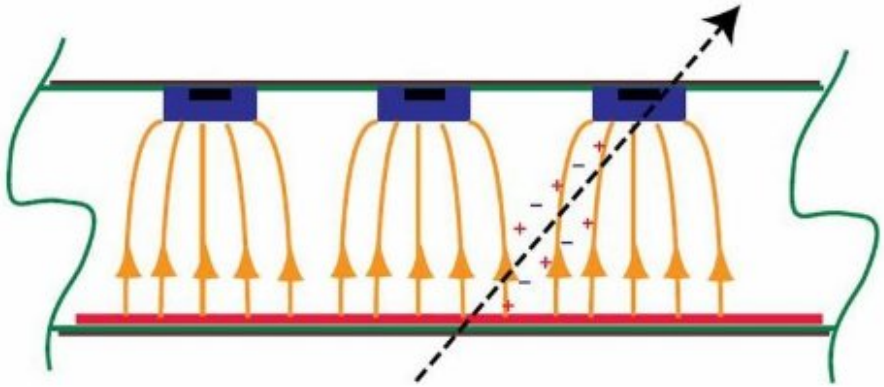

centroid resolution

$\sigma_x \approx (\Delta s/2)(N/S)$

charge distribution registered for a semiconductor detector with or without magnetic field

no field

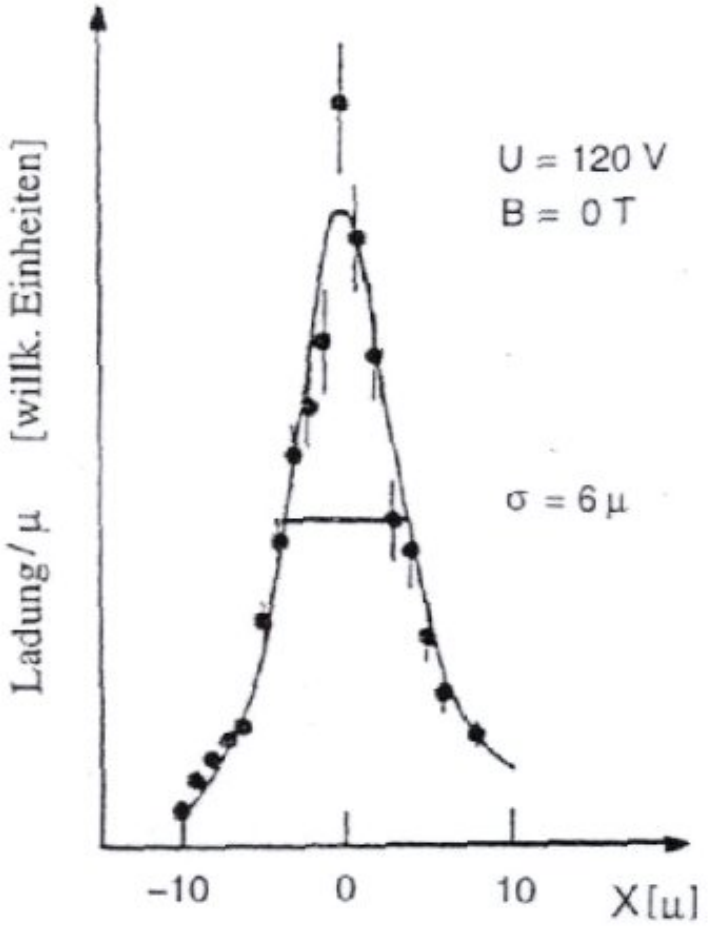


$B = 1.68\ T$

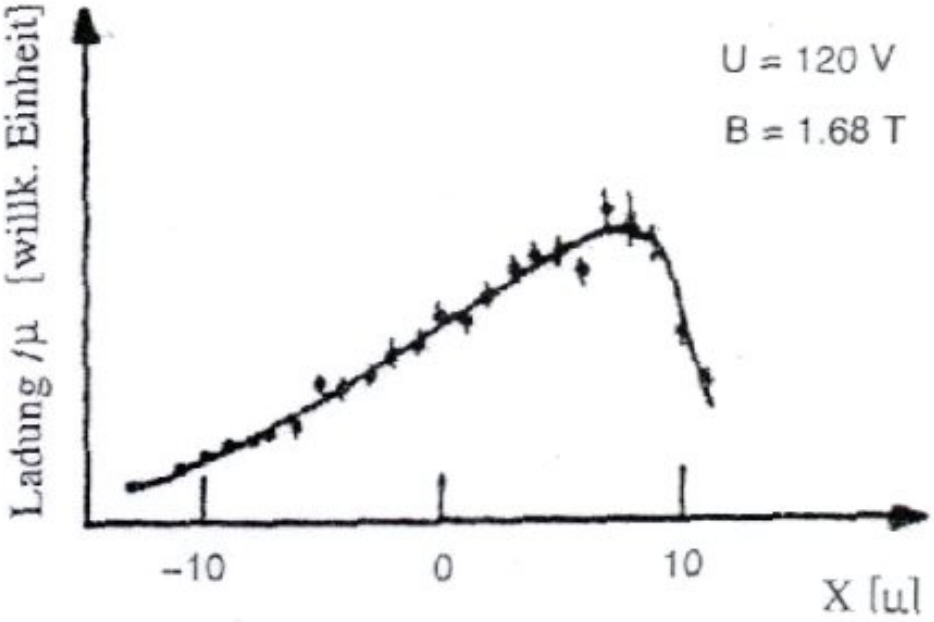

# Si vertex detectors

main applications:

- tracking of particles close to primary vertex before multiple scattering
  $\Rightarrow$ good angular resolution
- identification of secondary vertices
  c, b, $\tau$ decays $\tau = 10^{-12} \ldots 10^{-13}$ s,
  $\gamma c\tau \cong \gamma \cdot 30\ \mu$m

'b-tagging' for top or Higgs decays

example: 4 layers microstrips of H1 experiment $\Longrightarrow$

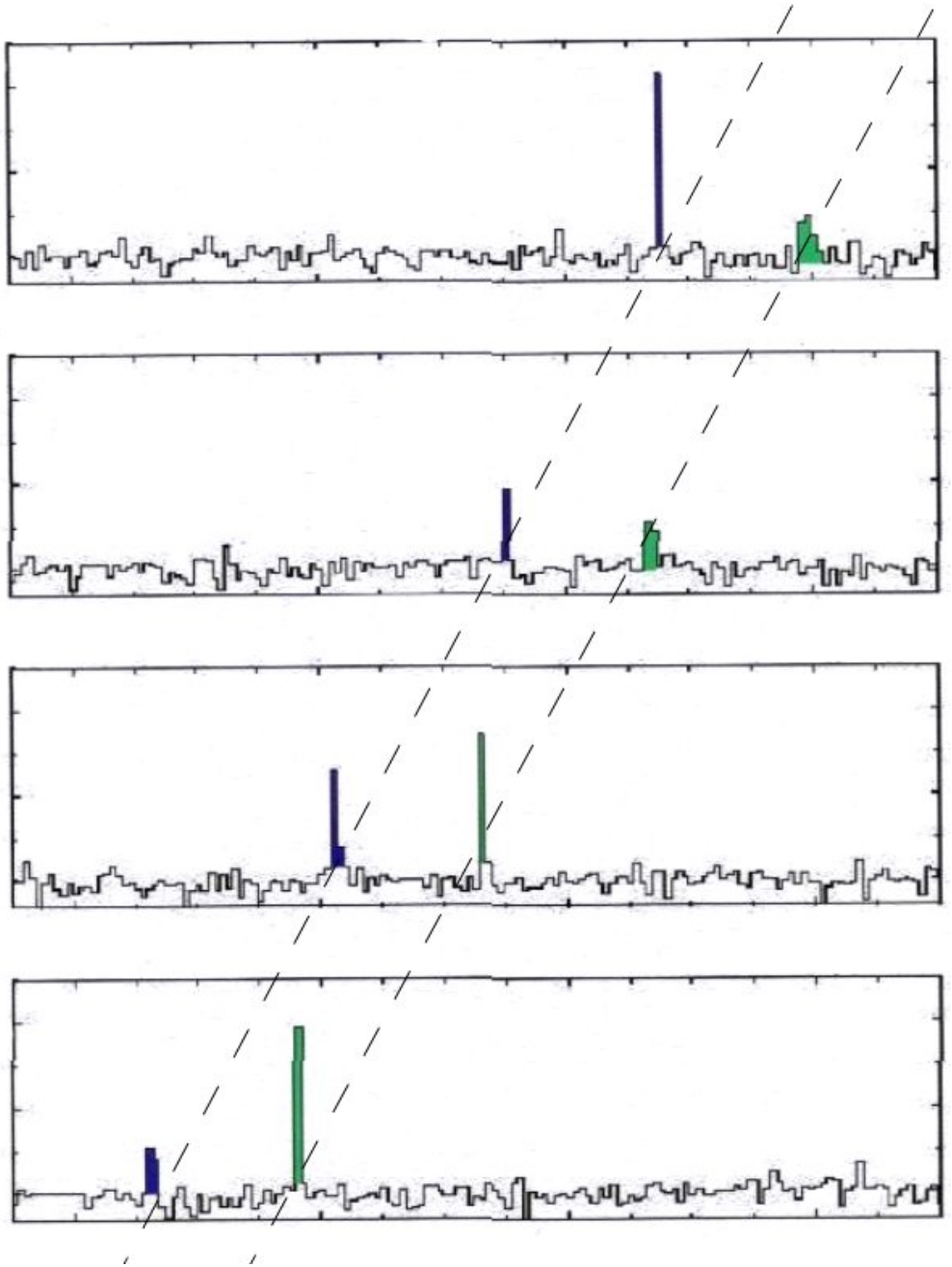

example: CDF

discovery top quark
3 Si-layers at
r = 1.5, 5-10, 20-29 cm
total active area approx. 10 $m^2$

$D^{\pm} \to K\pi\pi$ mass peaks
before and after $7\sigma$ vertex cut

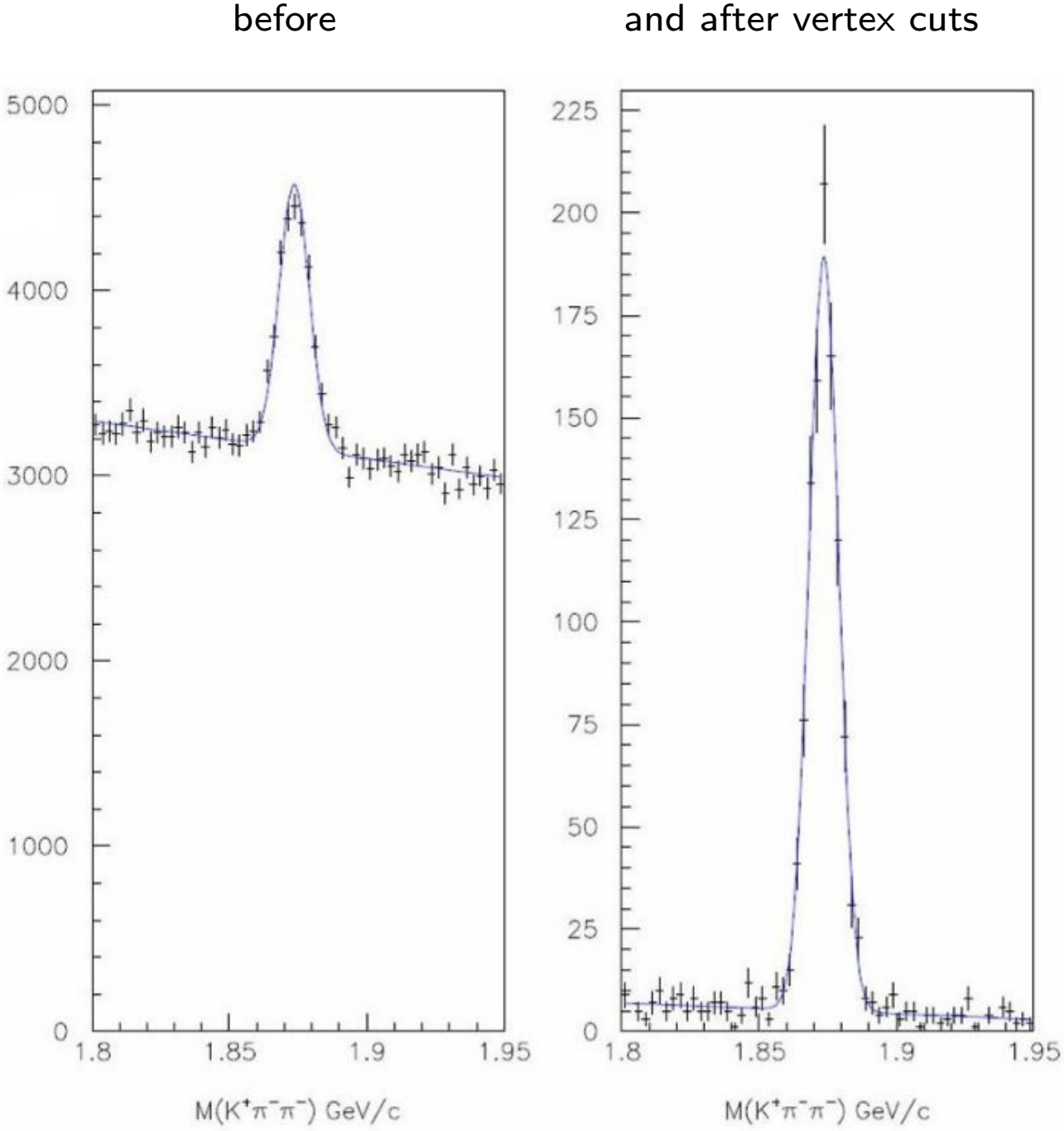

example (CDF): detection of 2 b-jets from $t\bar{t}$-decay

$$
\begin{aligned}
p + \bar{p} \rightarrow & t\bar{t} + X \\
& \hookrightarrow \bar{b} + W^+ \\
& \qquad \hookrightarrow e^+ + \nu_e \\
& \hookrightarrow b + W^- \\
& \qquad \hookrightarrow q\bar{q} \text{ (2 jets)}
\end{aligned}
$$

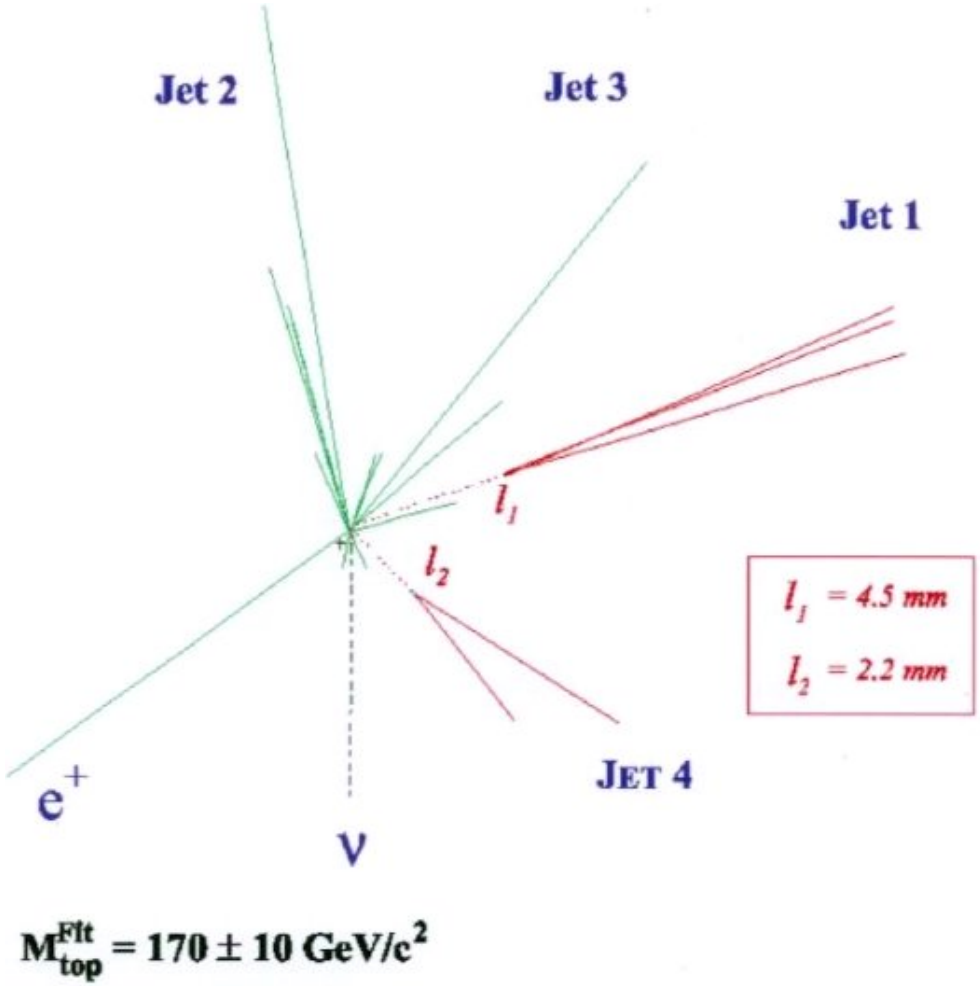

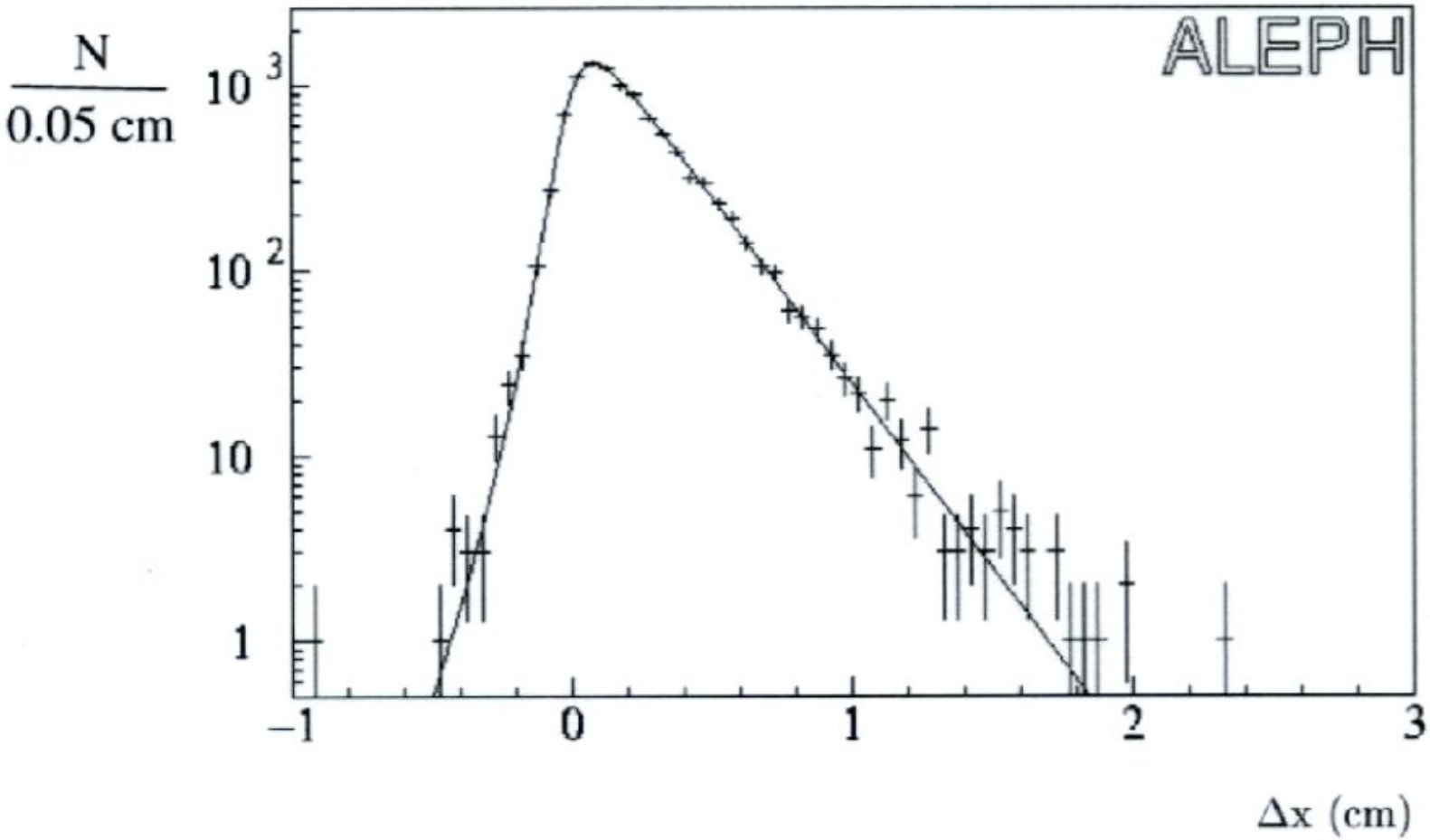


distribution of secondary vertices typical for charm decays in ALEPH.

how to use it: make a cut at e.g. $x > 3\sigma$ of vertex resolution $\rightarrow$ secondary vertex

critical for detection of secondary vertices:
impact parameter resolution

'impact parameter' $b$: closest distance from (extrapolated) track to primary vertex

$$\frac{\sigma_b}{\sigma_1} = \frac{r_2}{r_2 - r_1}$$

$$\boxed{\sigma^2 = \left(\frac{r_1}{r_2 - r_1}\sigma_2\right)^2 + \left(\frac{r_2}{r_2 - r_1}\sigma_1\right)^2 + \sigma_{MS}^2}$$

$$\frac{\sigma_b}{\sigma_2} = \frac{r_1}{r_2 - r_1}$$

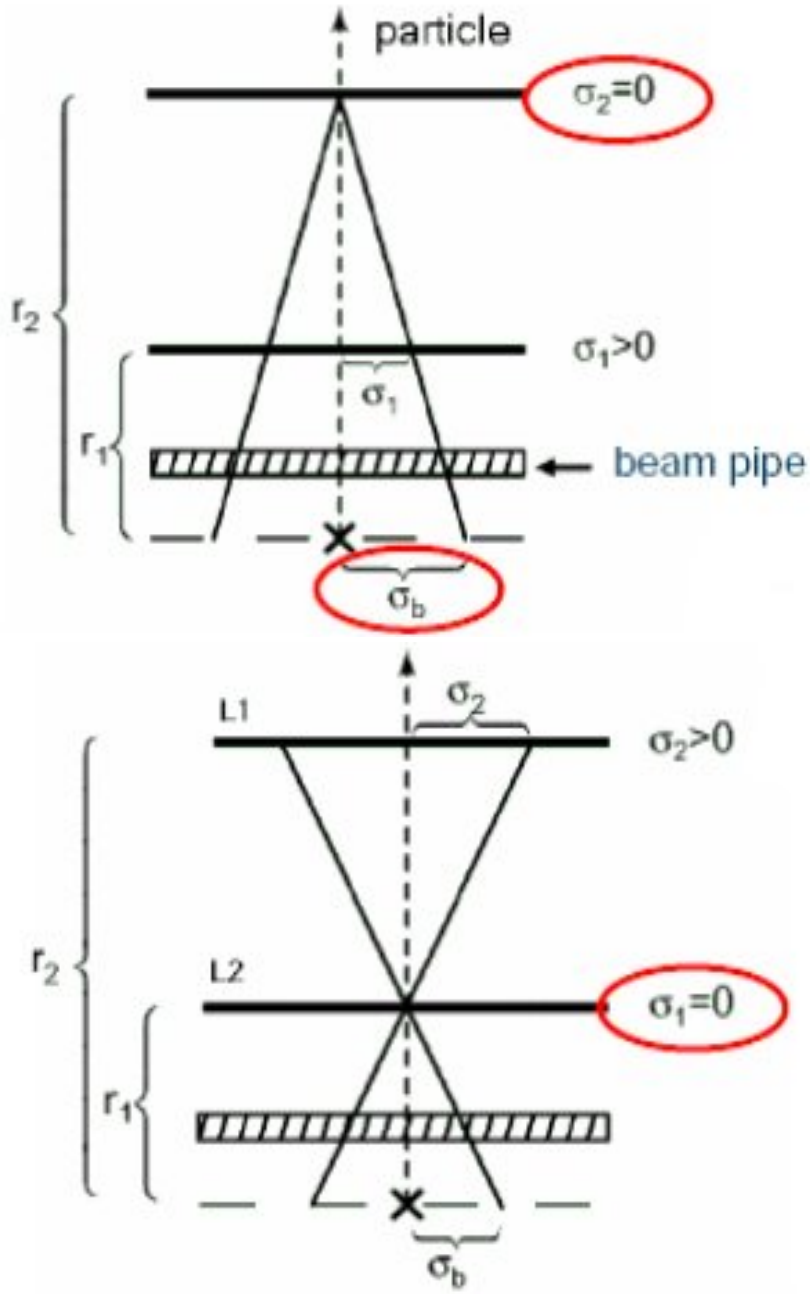


optimum resolution for $r_1$ small, $r_2$ large and $\sigma_1$, $\sigma_2$ small
make contribution of multiple scattering small, as little material as possible $\sigma_{MS} \propto \frac{1}{p}\sqrt{\frac{X}{X_0}}$

practical values $< 100$ $\mu$m for $p > 1$ GeV/c

# 4.6.2 Micro-strip detectors (about 1983)

principle and segmentation see above

typical pitch $20 - 50\ \mu$m

width of charge distribution (for $\perp$ incidence) $\cong 10\ \mu$m

signal in 300 $\mu$m Si: $\cong 25\,000\,e$ for minimum ionizing particles

order 100 channels/cm$^2$

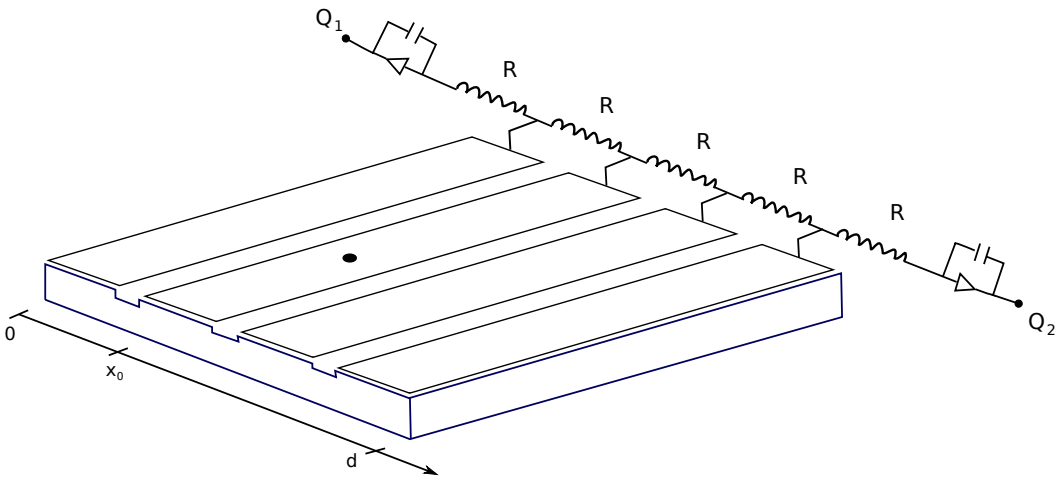


**read-out:**

- resistor network for charge division

$$\langle x \rangle = \frac{Q_2}{Q_1 + Q_2} d$$

charge sensitive preamplifier

disadvantages:

- only 1 hit per event and detector
- $R$ has to be large enough for good $S/N$
- slow due to $RC$ of resistor chain

- **individual read-out of all strips:**

  charge-sharing by capacitive coupling between strips $\cong 1$ pF/cm

  $\Rightarrow$ signal on neighboring strip a few % of central signal

  typical position resolution $\sim 10\ \mu$m

  vertex resolution determined by

  - position resolution
  - lever arm
  - multiple scattering
  - momentum $p$ or $p_\perp$, respectively track curvature in magnetic field
  - effect of Lorentz force on drifting charge

  typical value (H1 detector):

  $$\sigma_{vtx} = 27\ \mu\text{m} \oplus \frac{98\ \mu\text{m}}{p_\perp\ (\text{GeV/c})}$$

  $\oplus$: addition in quadrature

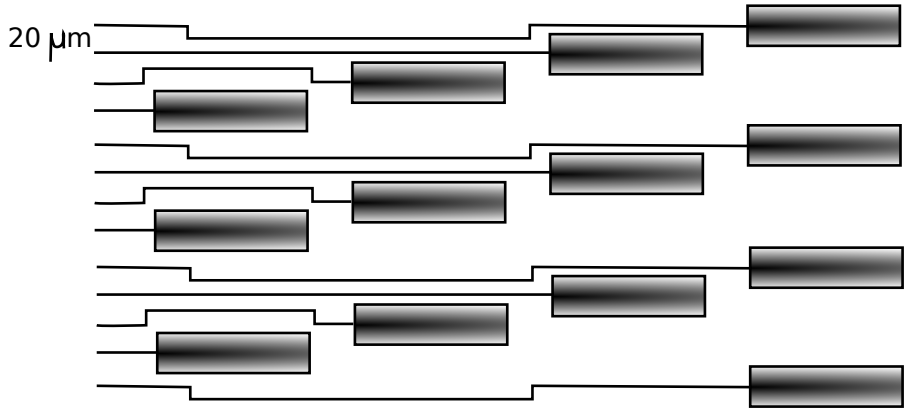


contact pads for readout electronics

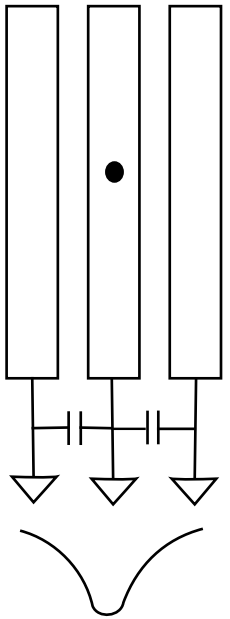

# 4.6.3 Double-sided micro-strip detectors

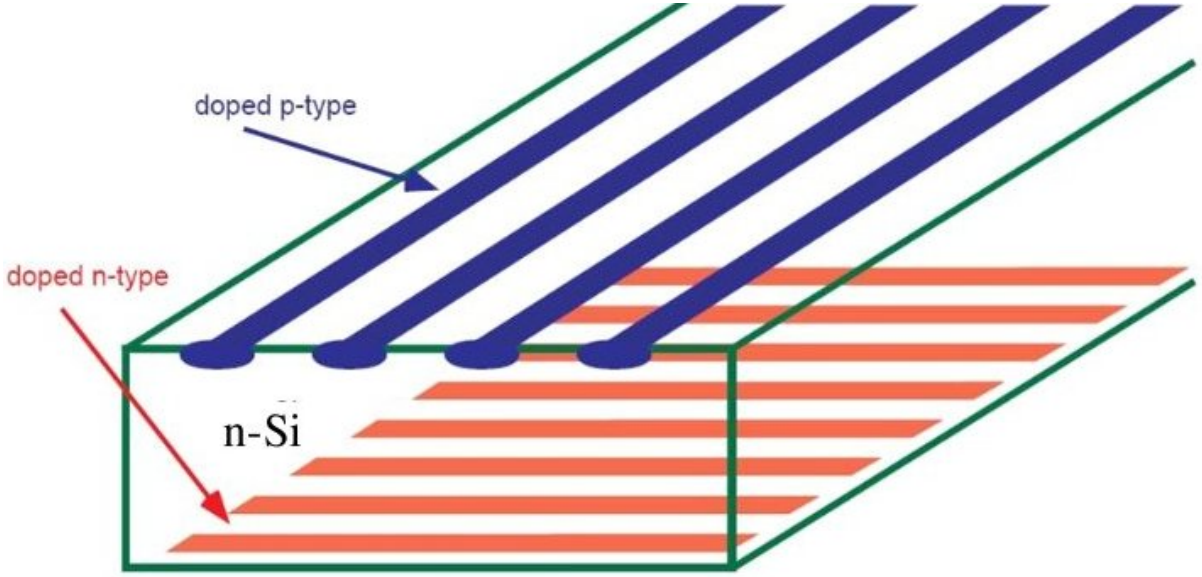


between $n^+$ side strips, additional strips are needed for insulation:
$SiO_2$ surface layer: positive space charge $\Rightarrow$ $e^-$ layer in n-material
$p^+$ blocking electrodes for separation of $n^+$ strips

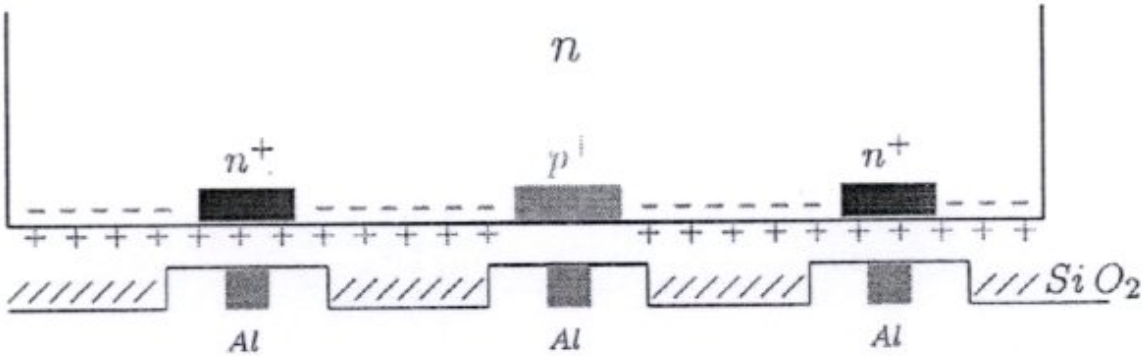


used in:
DELPHI, ALEPH, H1, ZEUS, HERA-B, CDF, D0

# Example: Delphi vertex detector

3 coaxial layers of double-sided micro-strips, capacitive coupling, 6.3, 9.0, 10.9 cm from beam axis

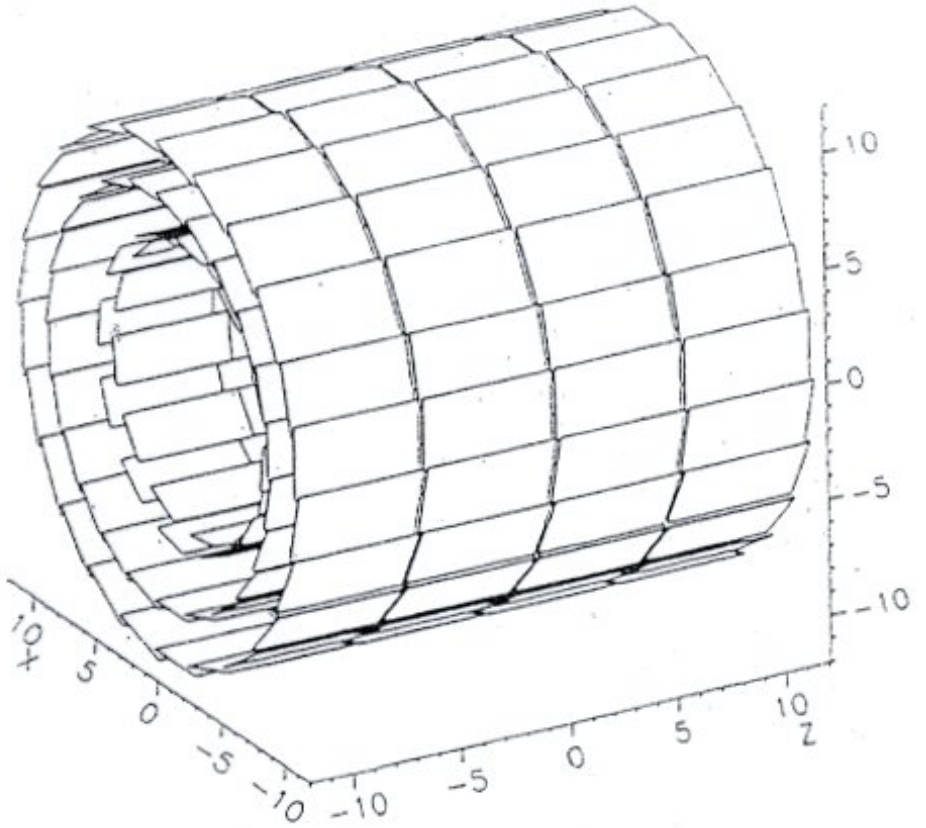


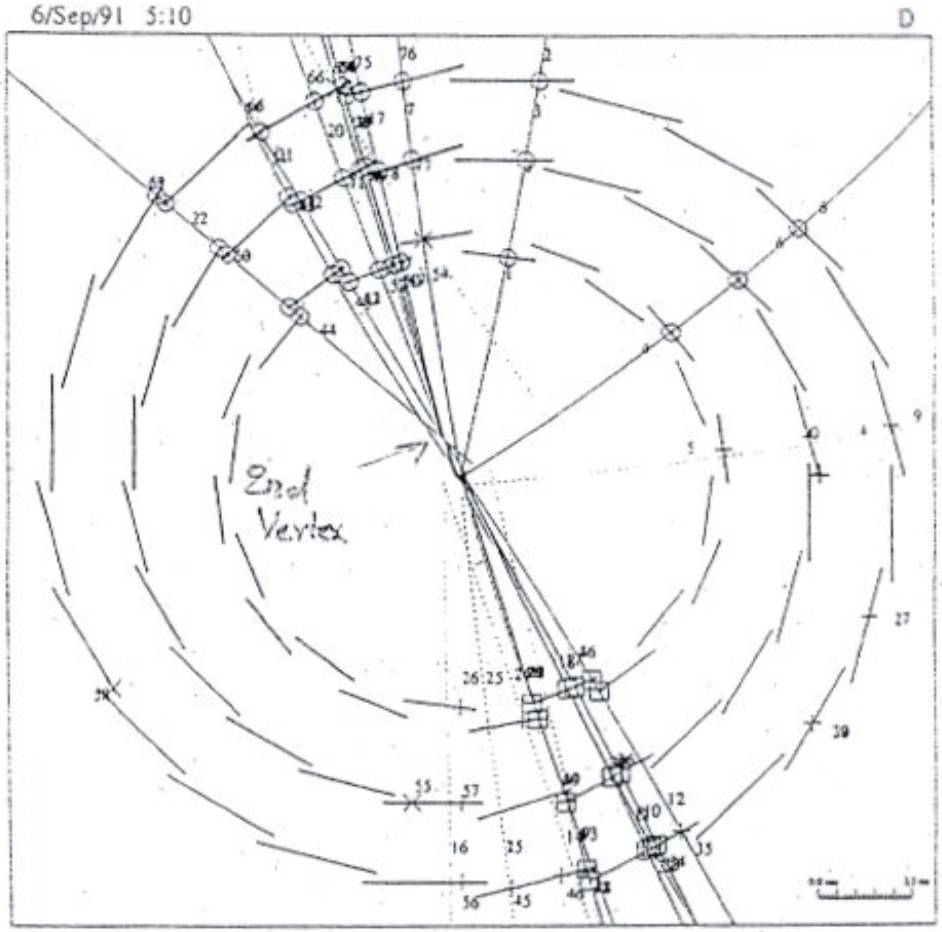


event recorded by the Delphi micro-vertex detector

# 4.6.4 Silicon drift detectors

proposed by Gatti and Rehak in 1984, first realized in 1990ies

potential inside wafer has parabolic shape (see next page), superimpose linear electric field

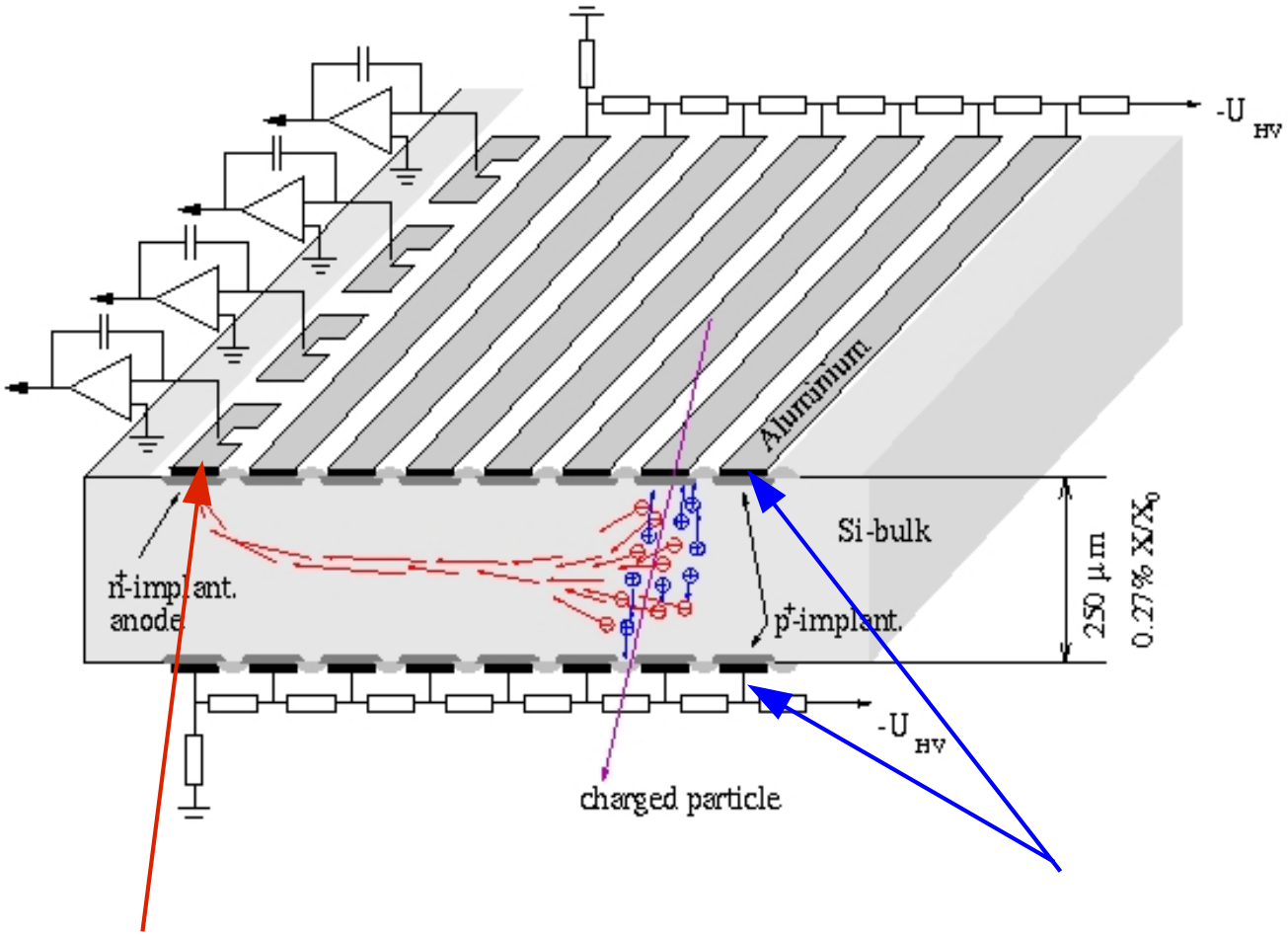


wafer can be fully depleted by reverse bias voltage on a small n+ anode implanted on wafer edge

n-type bulk Si with p+ electrodes on both flat sides

analog to gaseous drift chambers: charge carriers drifting in well-defined E-field

measurement of drift time
$\Rightarrow$ position of ionizing track

typical drift time: a few $\mu$s for $5 - 10$ cm

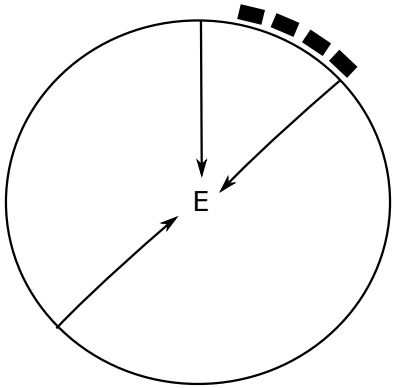


first example CERES at SPS:
radial Si drift-chamber

readout: $1^\circ$ sectors in $\varphi$, 256 time samples (flash ADC) for determination of $r$, equivalent of 1 plane in a TPC

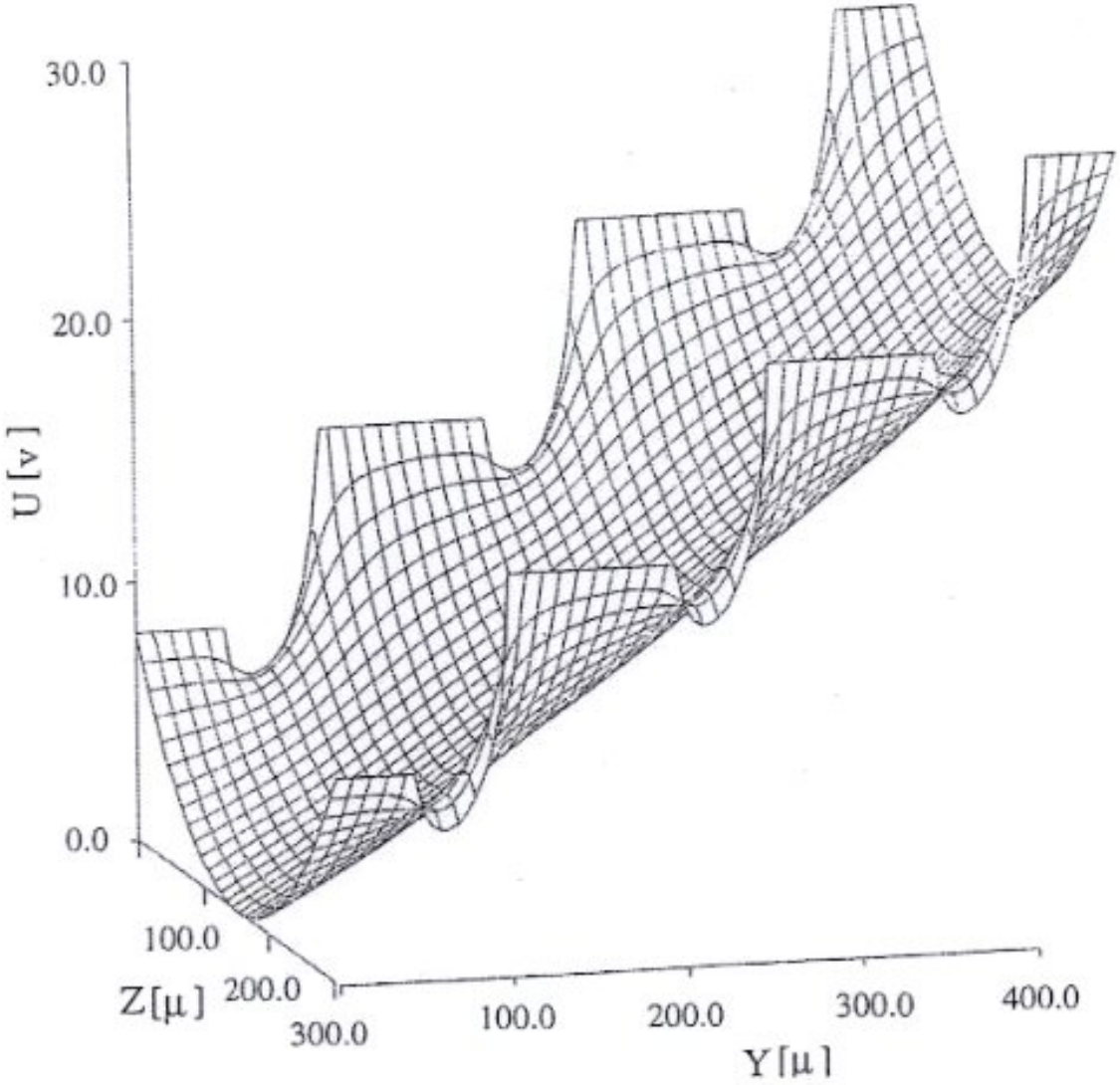


potential shape in Si drift-chamber:
trough-like shape due to positive space charge in depletion area, slope from external voltage divider

# CERES 4 inch Si drift detector

event display

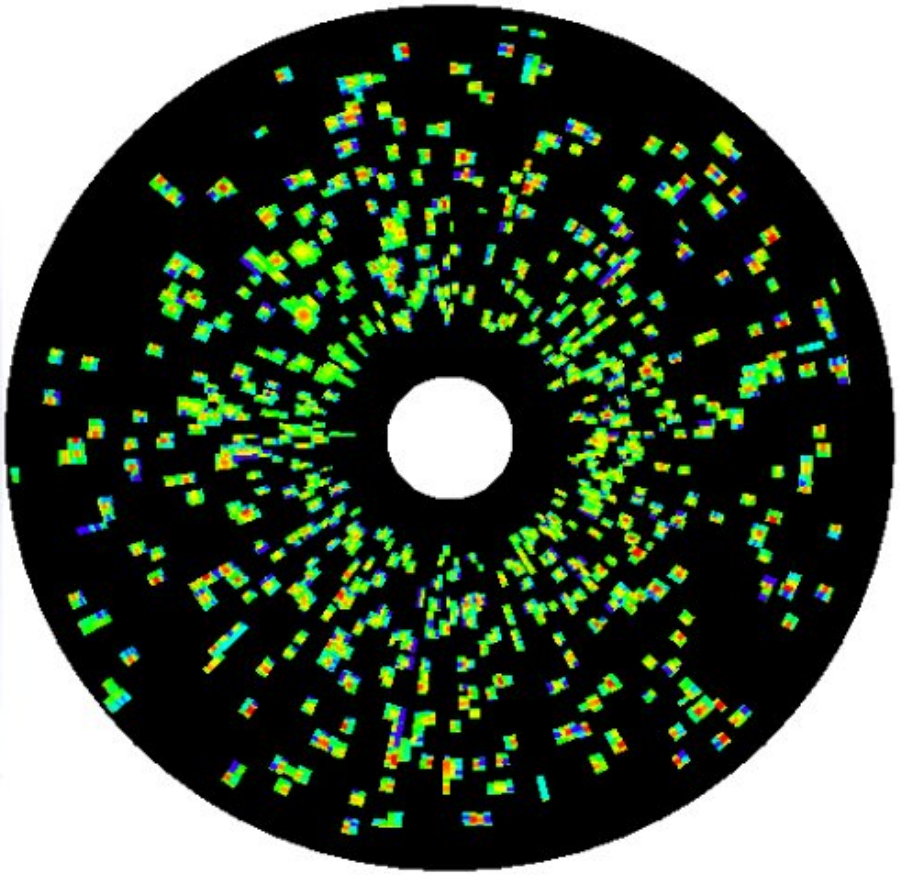

| | |
|---|---|
| active area | 52 $cm^2$ |
| granularity | 360 anodes $\times$ 256 time bins |
| | $=$ 92 160 pixels |
| max. number of resolved hits | $2 \cdot 10^4$ |
| wafer thickness | 250 $\mu$m |
| radiation length | 0.27% of $X_0$ |
| multiple scattering | $\approx$ 0.54 mrad @ 1 GeV/c |

# 4.6.5 Pixel detectors

- principle: like micro-strips, but 2-dimensional segmentation of $p^+$ contacts: 'pixel'
  each pixel connected to bias voltage and readout electronics

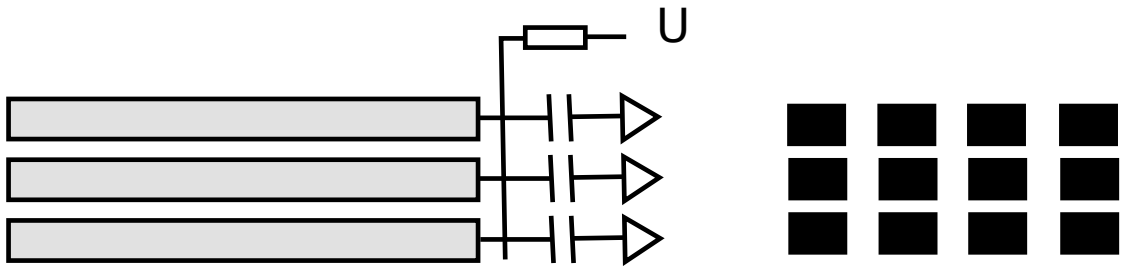


- advantage: 2-dim information like double-sided micro-strip,
  but more simultaneous hits per detector allowed
  low capacity and thus low noise $\Rightarrow$ good $S/N$
- disadvantage: large number of read-out channels $\Rightarrow$ expensive, large data volume
  pixel contacts are complicated ('bump bonding' or 'flip chip' technologies)
- typical pixel areas $\sim 2000\ \mu m^2 \rightarrow$ order 5000 channels/cm$^2$
  square ($150 \times 150\ \mu m^2$)
  rectangular ($50 \times 300\ \mu m^2$)
- hit resolution: $\Delta x/\sqrt{12}$ and $\Delta y/\sqrt{12}$

examples: all LHC experiments

## bump bonding

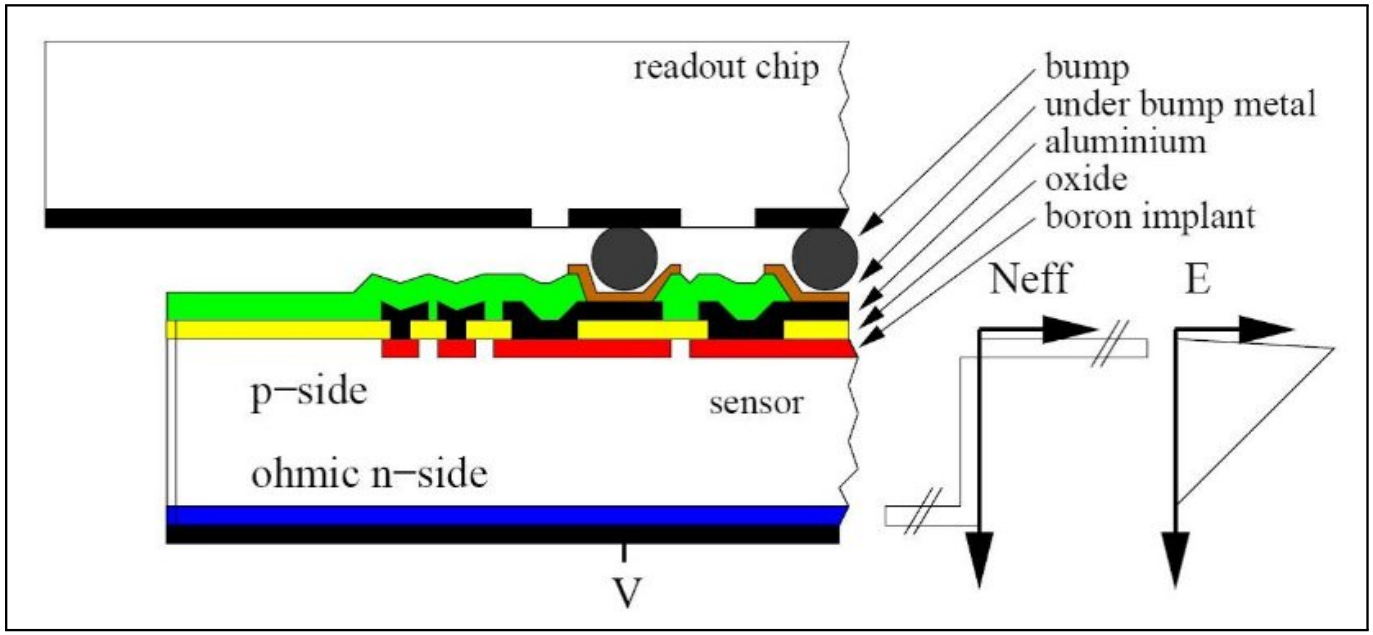


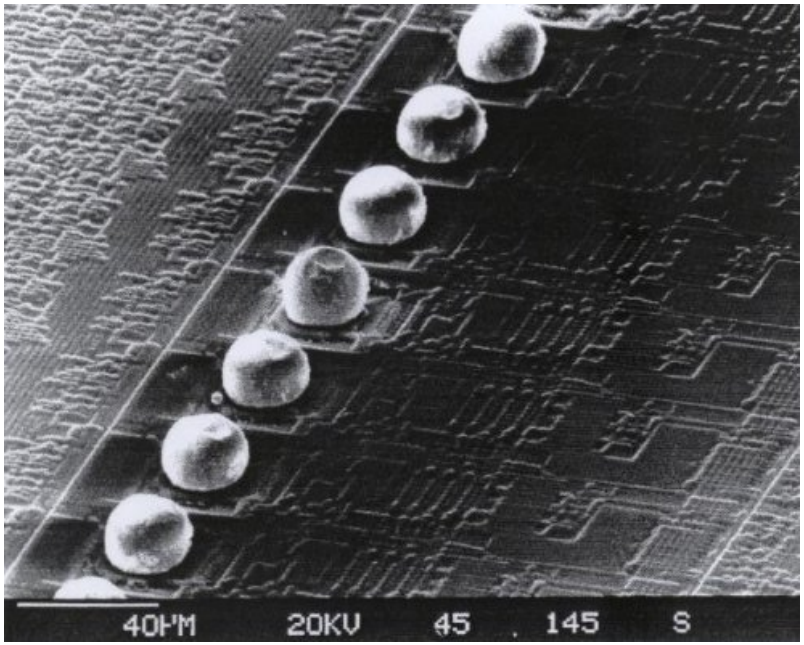


SEM photograph of solder bumps on an Omega3 chip

connection pixel chip ↔ readout chip

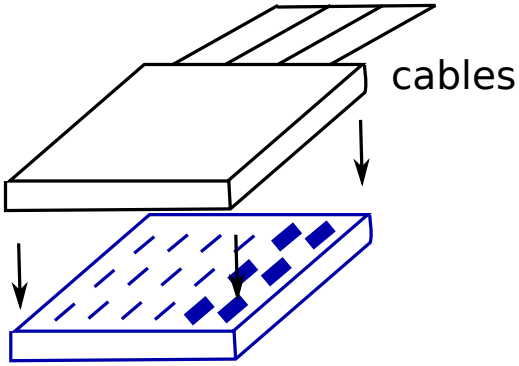

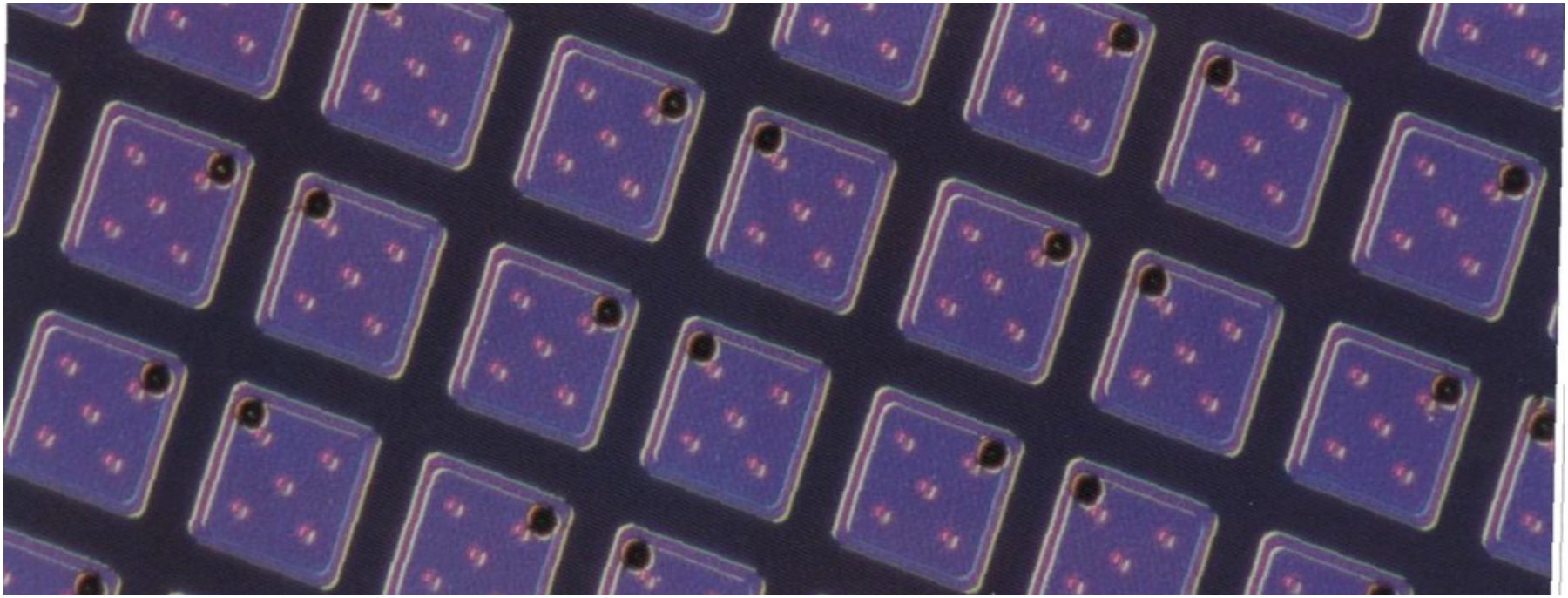

pixel detectors depend on the bump-bonding technique, which PSI adapted and miniaturized
contact between pixel and microchip is a 17 $\mu m$ solder ball of indium
microscope image shows pixels with the indium balls (dark points).

prototype Si pixel telescope

7(9) Si pixel detectors
0.5 M (0.7 M) channels
+ Si $\mu$strip planes

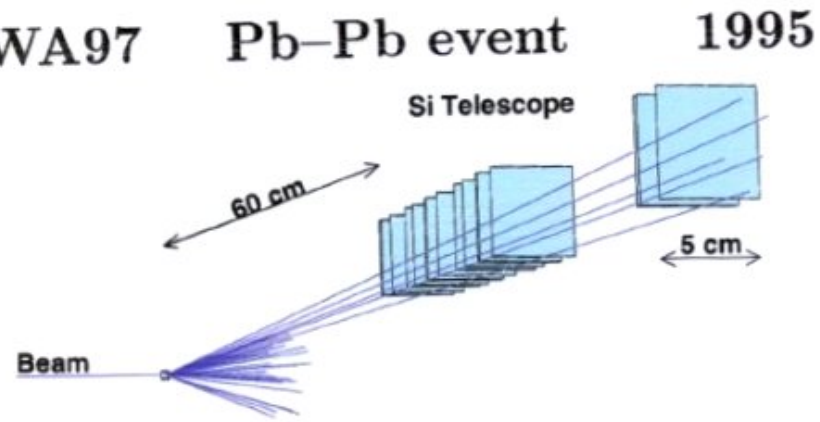


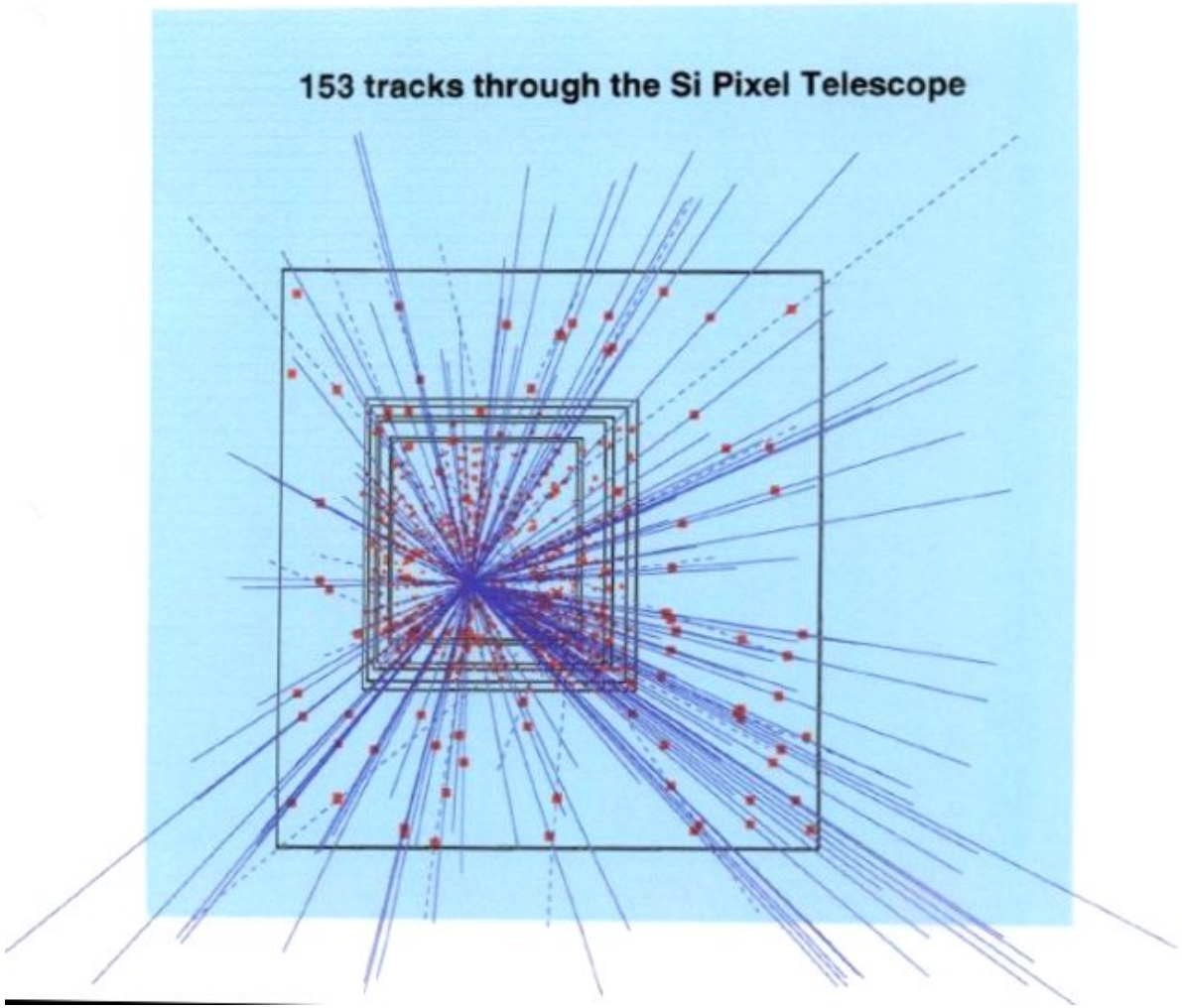

# 4.6.6 putting it all together: the LHC experiments use Si pixels, strips, and drift

the challenge at LHC:

high rate, high hit density, radiation damage

$\sim$ 1000 tracks every 25 ns or $10^{11}$/s

$\Rightarrow$ high radiation dose

$10^{15} \frac{n_{eq}}{\text{cm}^2 \cdot 10\text{a}}$ @ LHC

or

600 kGy (60 Mrad)
1 kGy = 1 J/g

through the ionization of mips
in bulk silicon

LHC $\cong 10^6 \times$ LEP in track rate!
detectors in ATLAS and CMS need to be replaced by 2018

14 TeV pp-collisions seen with the ATLAS pixel detector

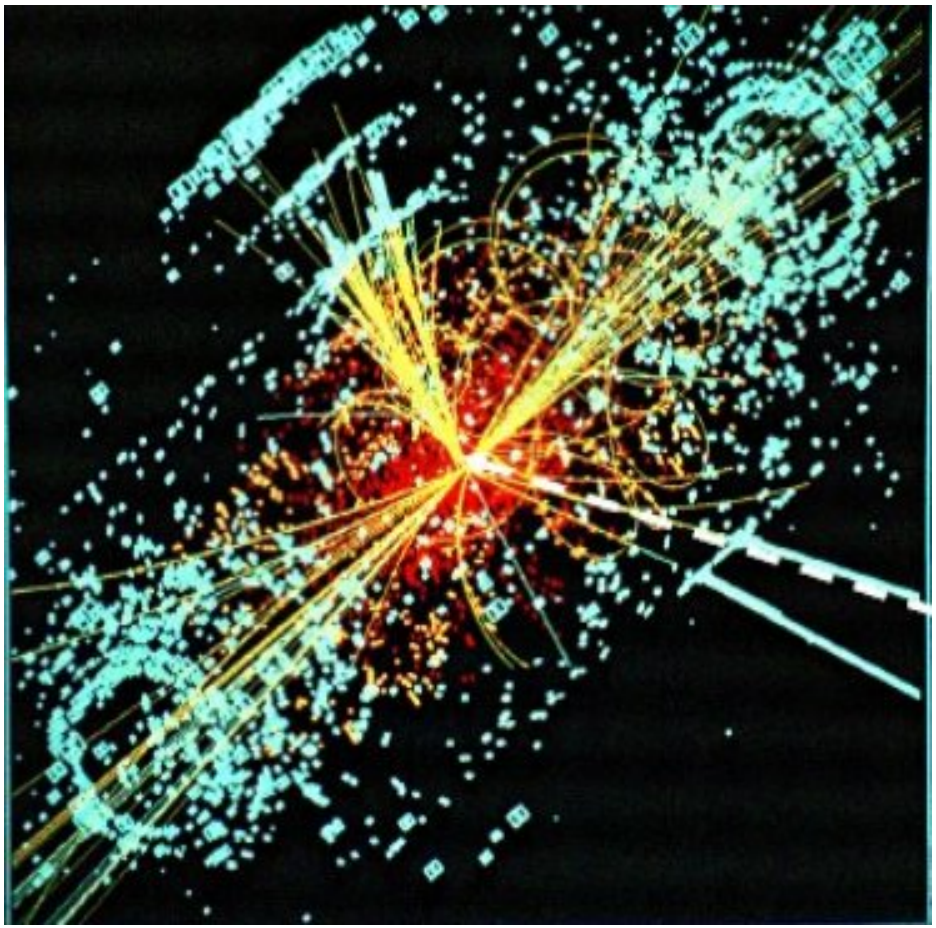

# Tasks for pixel detectors in LHC experiments

- pattern recognition and tracking

  precision tracking point (3D); can do in one pixel layer the equivalent of $3-4$ strip layers

  momentum measurement before much material (mult. scattering)
  e.g. ATLAS: $\sigma(p_t)/p_t = 0.03\,\% p_t\ (\mathrm{GeV/c}) \oplus 1.2\%$

- vertexing

  find primary vertex (can use all tracks, get 10 $\mu$m precision in $x, y$ and 50 $\mu$m in $z$)

  find secondary vertex (c,b) (few tracks, get 50 $\mu$m in $x, y$ and 70 $\mu$m in $z$)

  impact parameter for tracks not from primary vertex (electrons from semileptonic D and B decays

# tracking detectors: ATLAS

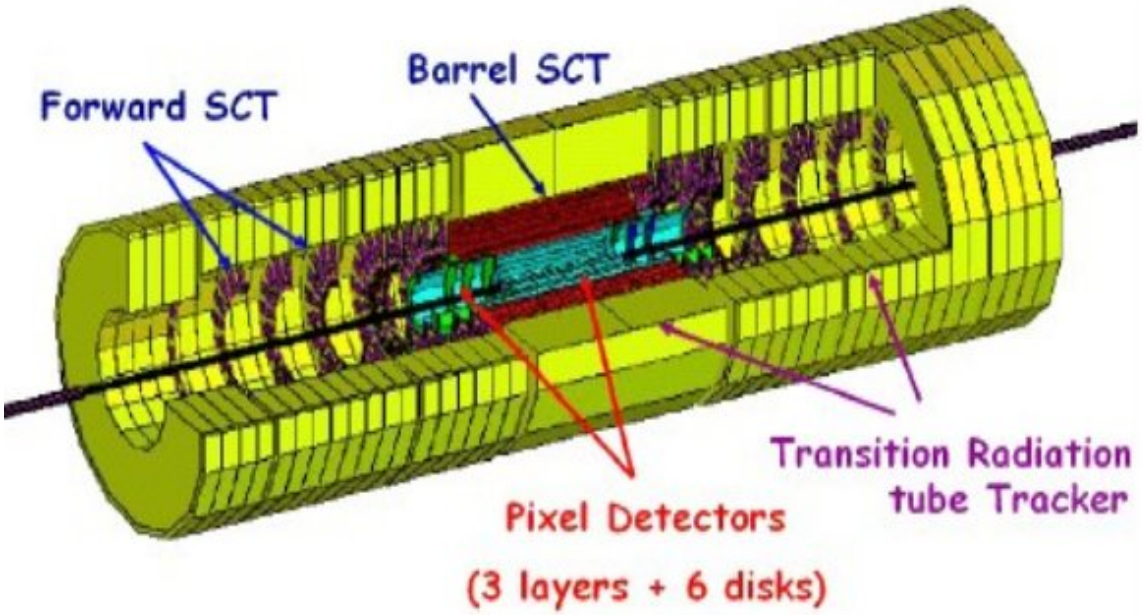


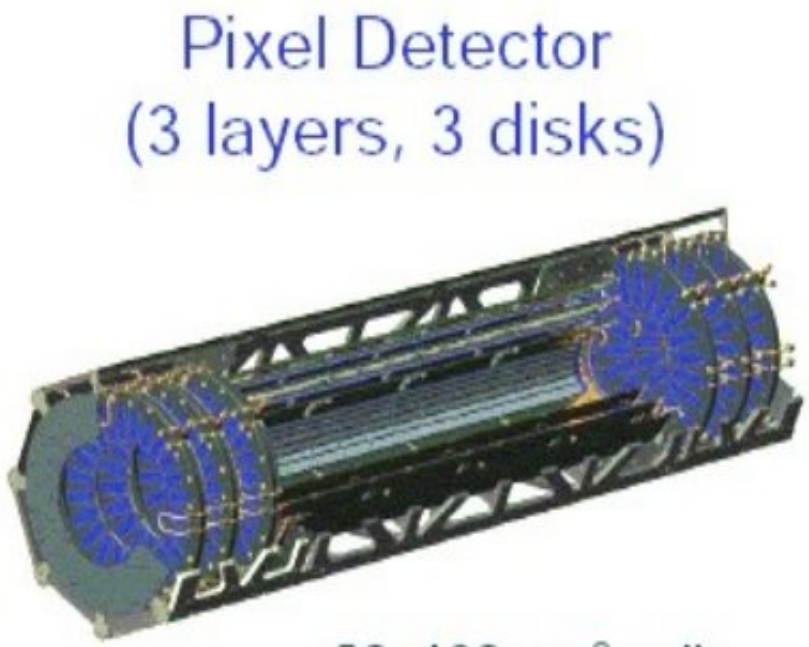


| | points | $\sigma(R\phi)$ $\mu$m | $\sigma(Rz)$ $\mu$m |
|---|---|---|---|
| pixel | 3 | 12 | 60 |
| SCT | 4 | 17 | 580 |
| TRT | 36 | 170 | - |

Silicon Pixel Detector $\sim$ 1.8 m$^2$
Silicon Strip Detector $\sim$ 60 m$^2$
Transition Radiation Tracker $\sim$ 300 m$^2_{eq}$

# ATLAS micro strip detector (15 million strips)

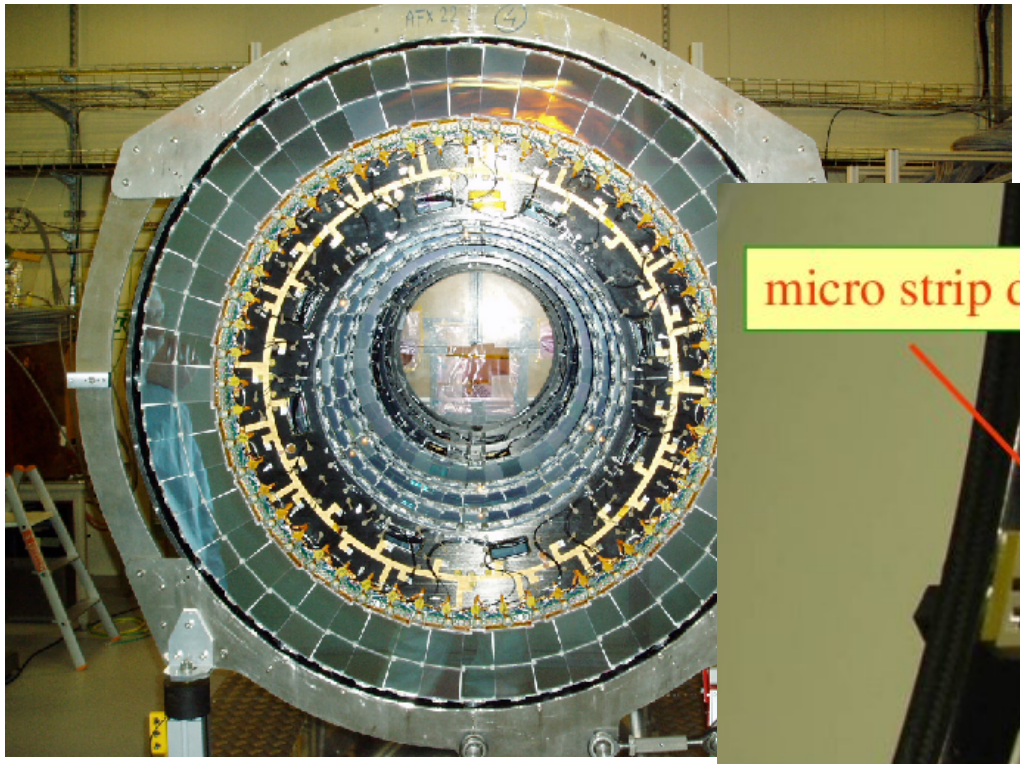

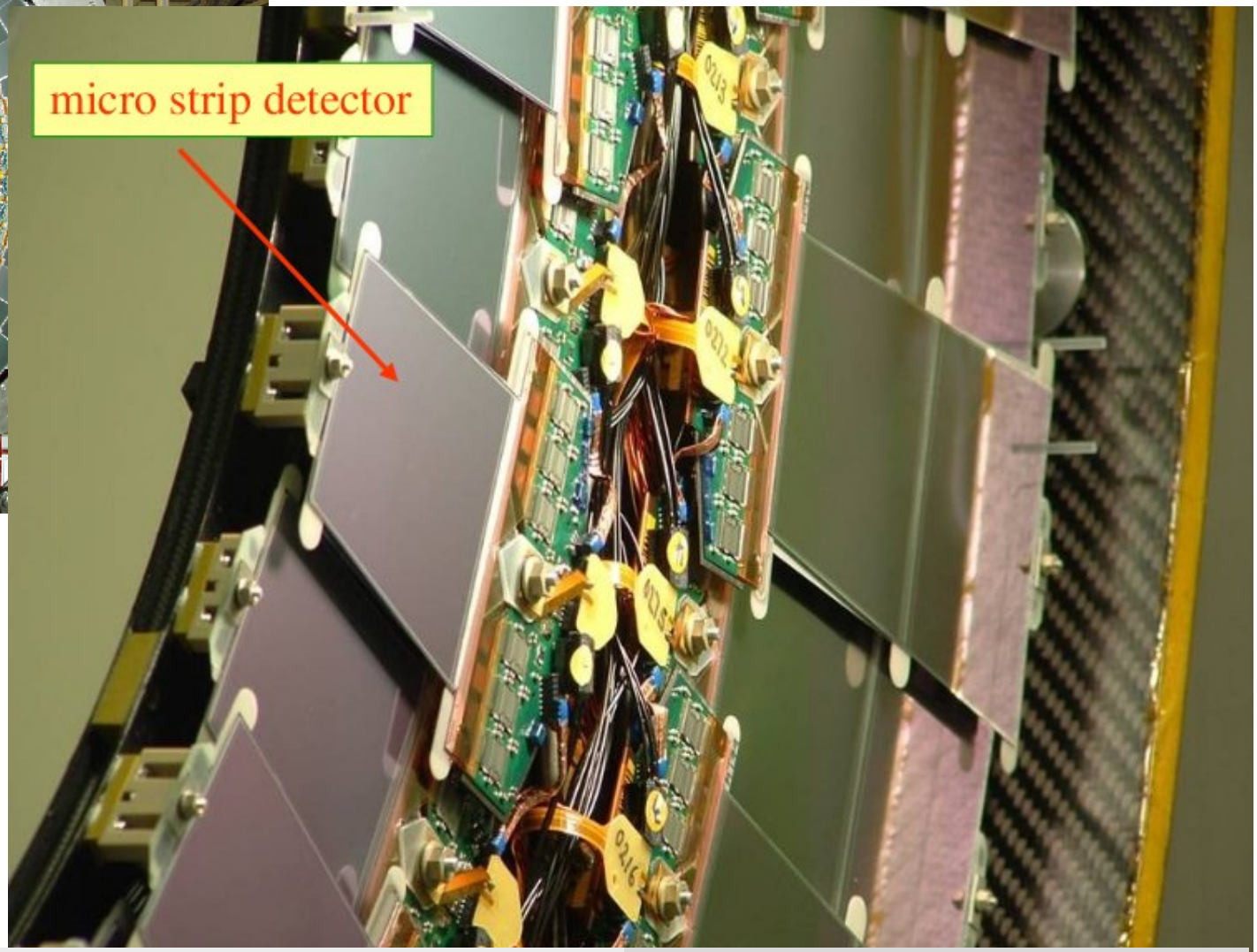


Freiburg, MPP München

# ATLAS pixel detector: 5 cm from collision point

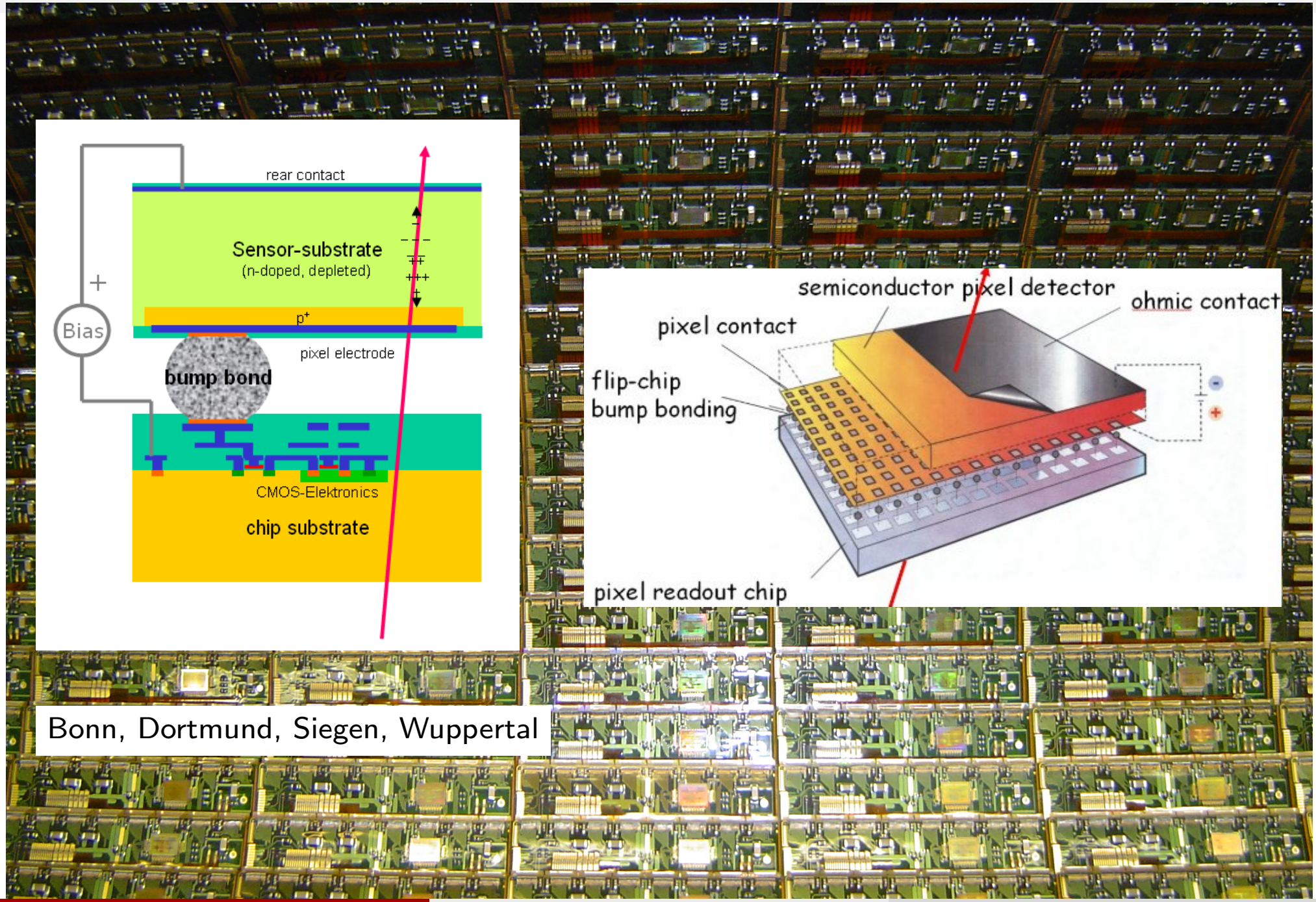

# ATLAS pixel detector

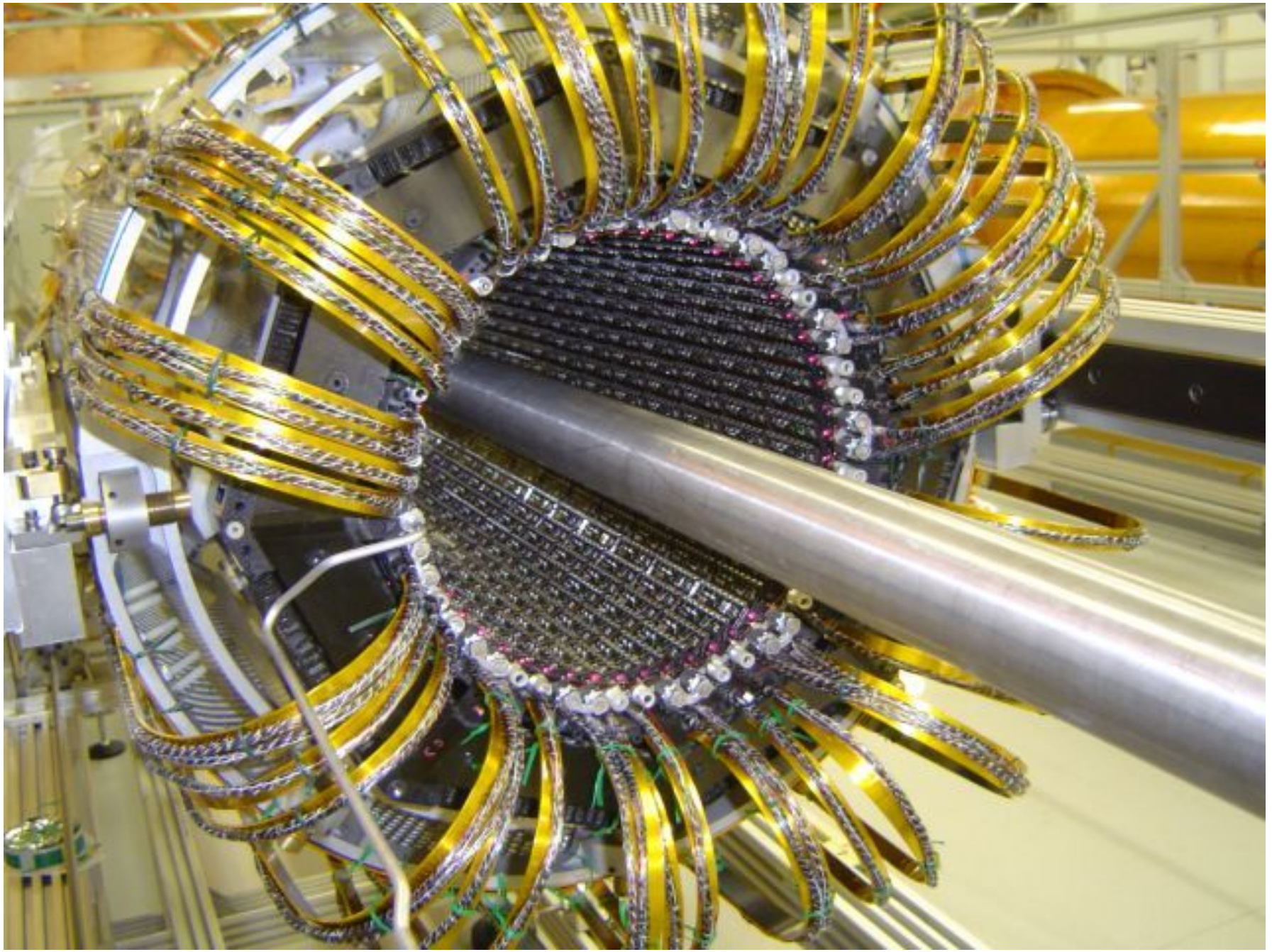

# tracking detectors: CMS

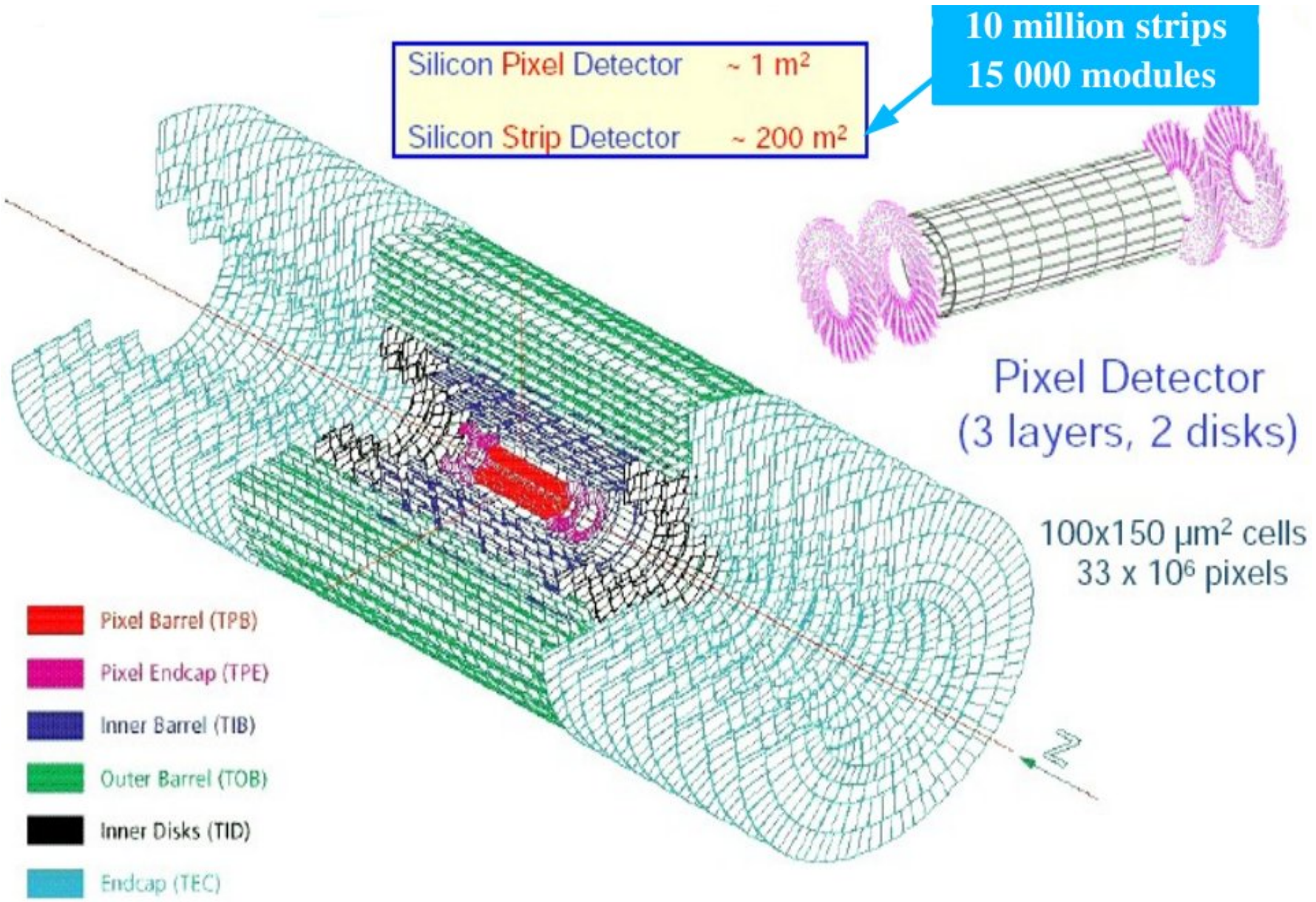

# CMS tracker-supermodule and -endcap

assembly and tests of supermodules (petals)
(Aachen, Hamburg, Karlsruhe)

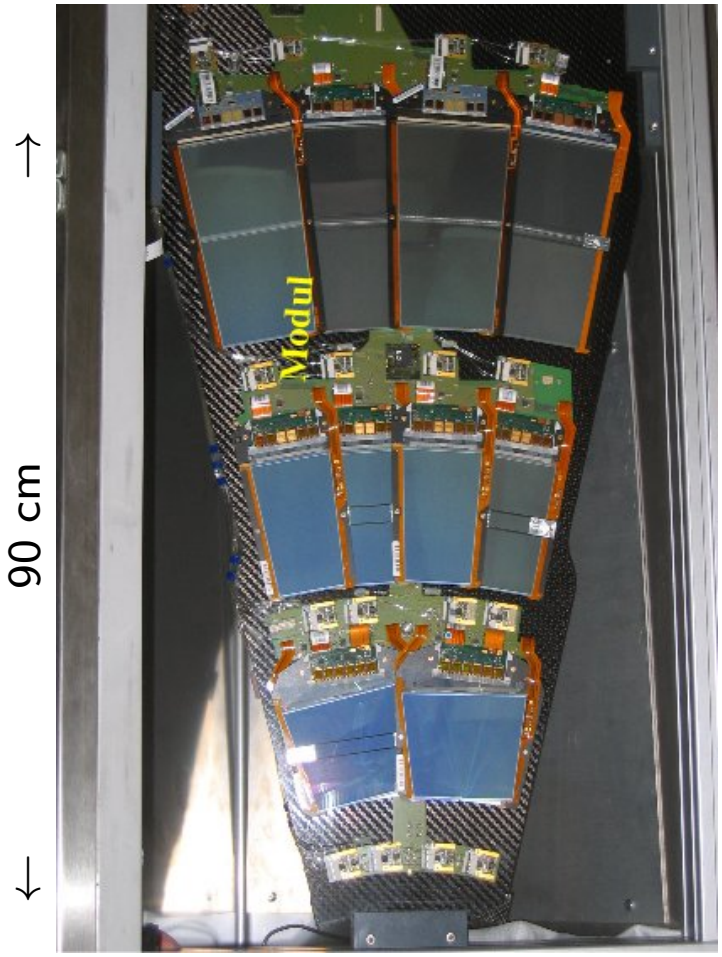


134 petals assembled
(mechanics + electronics + cooling)
288 petals tested

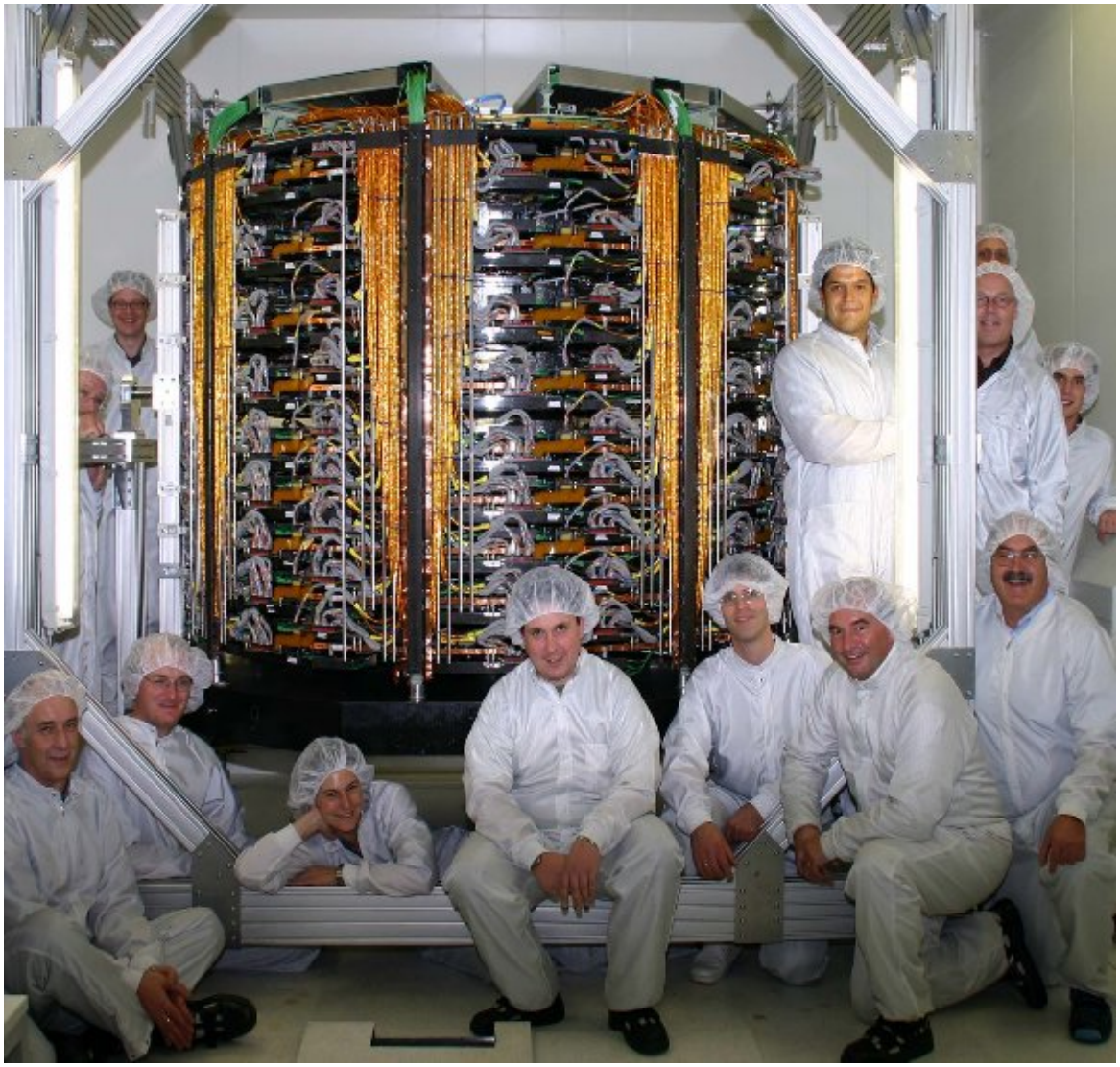

integration of tracker-end cap (Aachen)
end cap (with 144 petals) before transport to CERN

# inner tracking detectors: ALICE

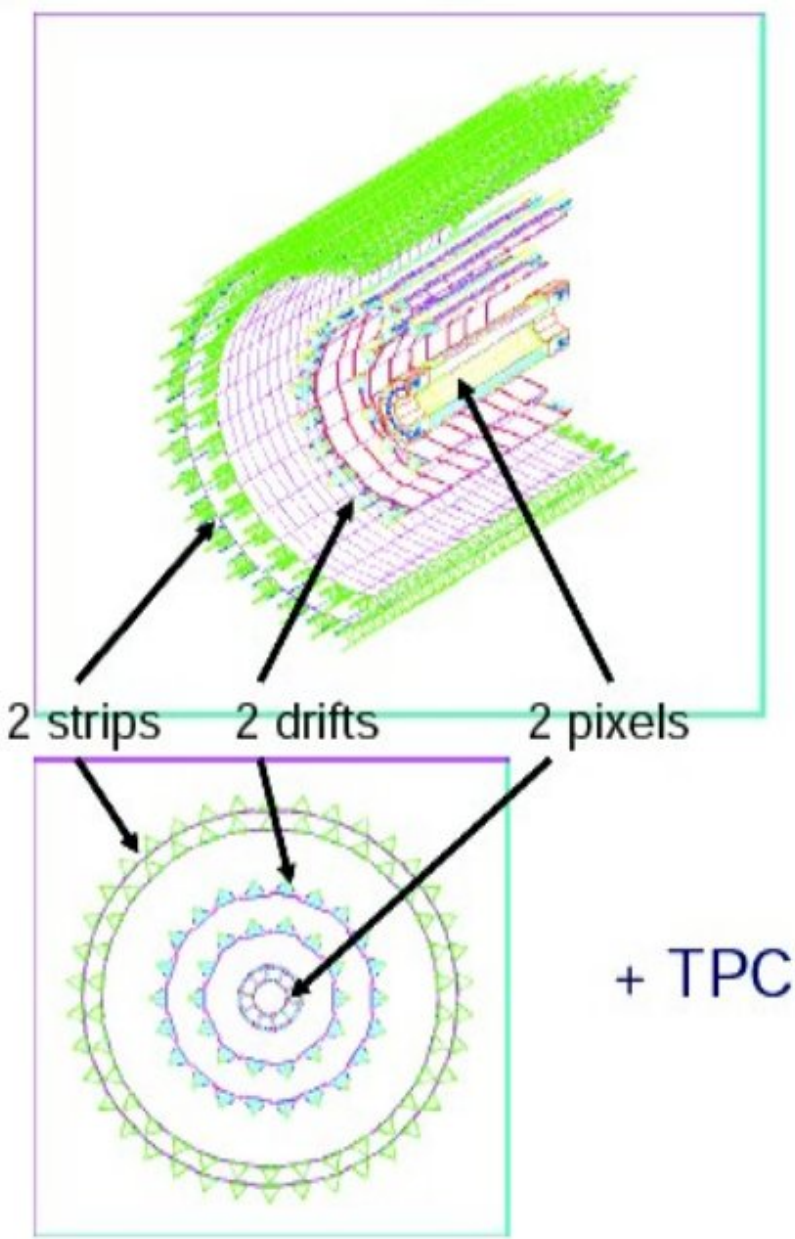


+ TPC

| | |
|---|---|
| Silicon Pixel Detector | ~ 0.2 m² |
| Silicon Drift Detector | ~ 1.3 m² |
| Silicon Strip Detector | ~ 4.9 m² |

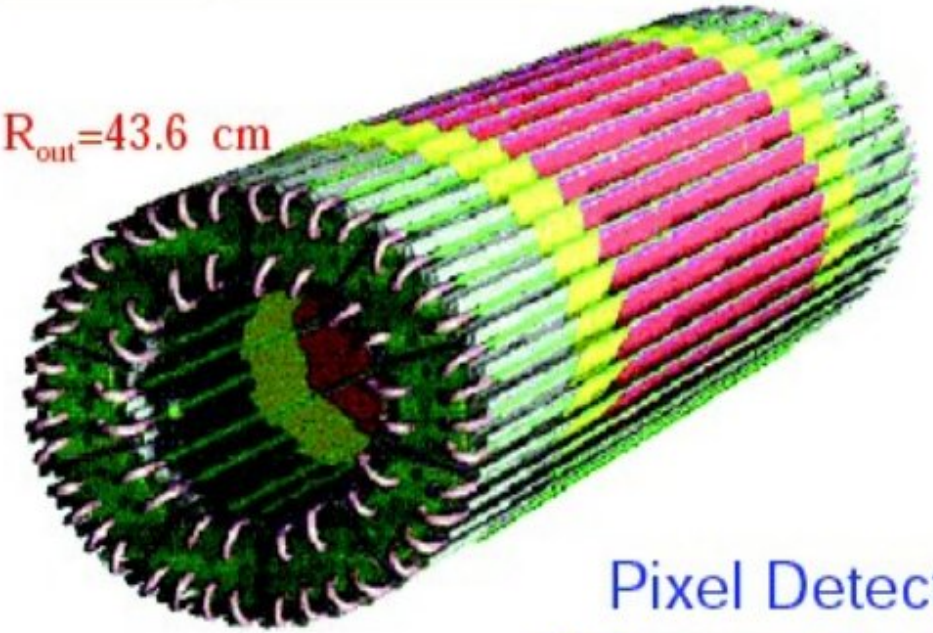


Pixel Detector
(2 layers, no disks)

50x450 µm² cells
10 x 10⁶ pixels

# ALICE ITS

inner tracker system

| layer | type | $r$(cm) | $\pm z$(cm) | area (m$^2$) | ladders | lad./stave | det./lad. | tot. channels |
|---|---|---|---|---|---|---|---|---|
| 1 | pixel | 4 | 16.5 | 0.09 | 80 | 4 | 1 | 5 242 880 |
| 2 | pixel | 7 | 16.5 | 0.18 | 160 | 4 | 1 | 10 485 760 |
| 3 | drift | 14.9 | 22.2 | 0.42 | 14 | - | 6 | 43 008 |
| 4 | drift | 23.8 | 29.7 | 0.89 | 22 | - | 8 | 90 112 |
| 5 | strip | 39.1 | 45.1 | 2.28 | 34 | - | 23 | 1 201 152 |
| 6 | strip | 43.6 | 50.8 | 2.88 | 38 | - | 26 | 1 517 568 |

dimensions of the ITS detectors (active areas)

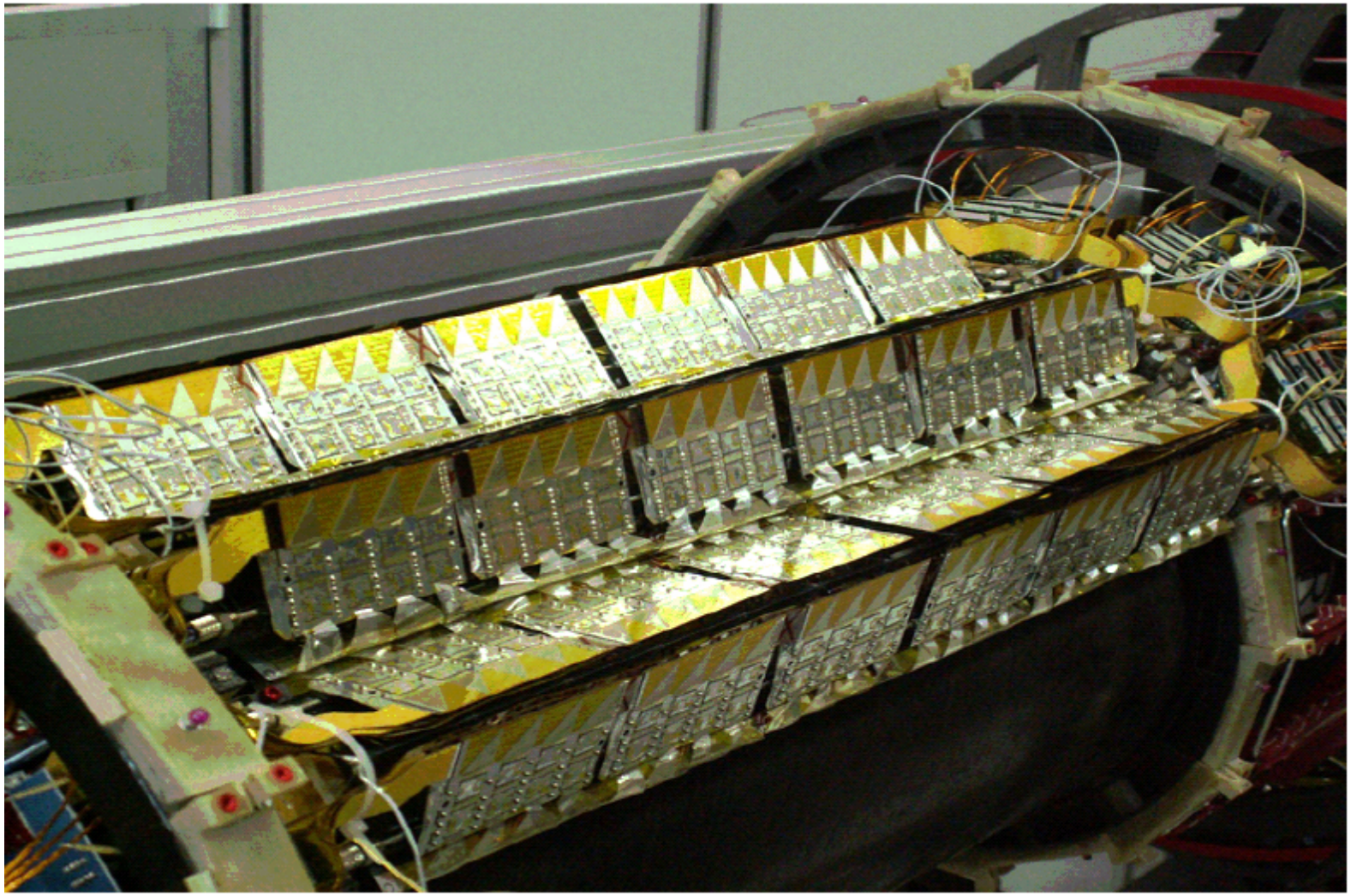

6 layers
3 technologies:
pixel, drift, strips

# main issue for ALICE: minimal material

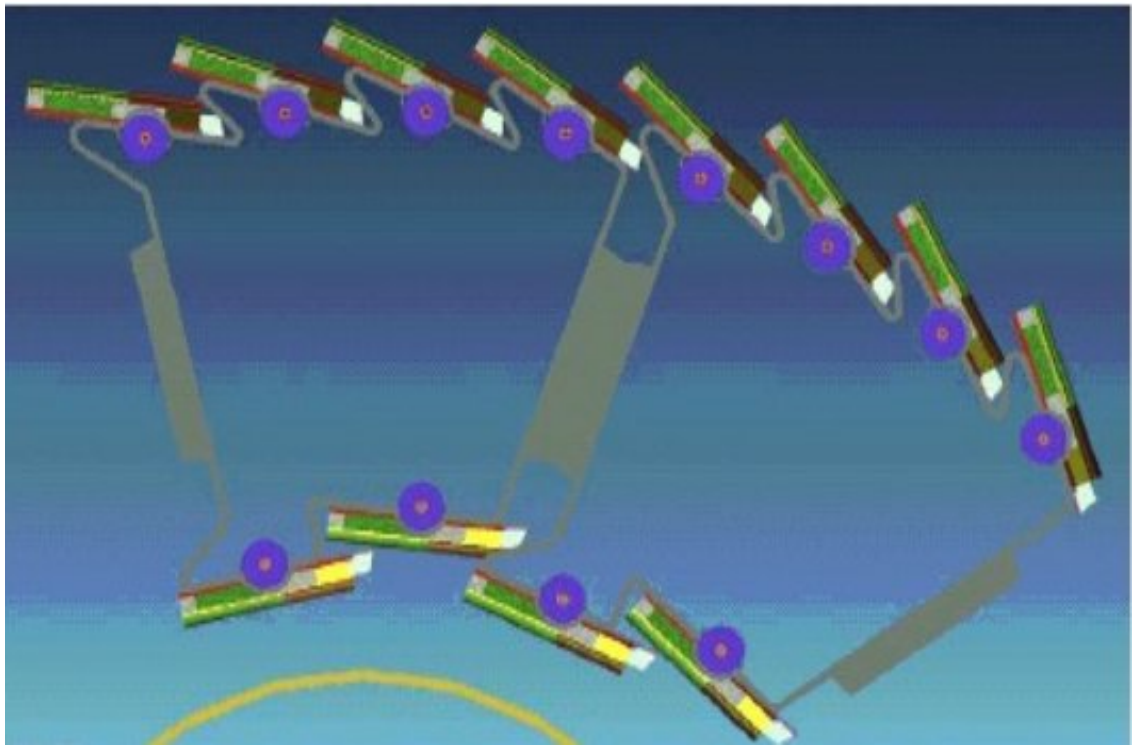

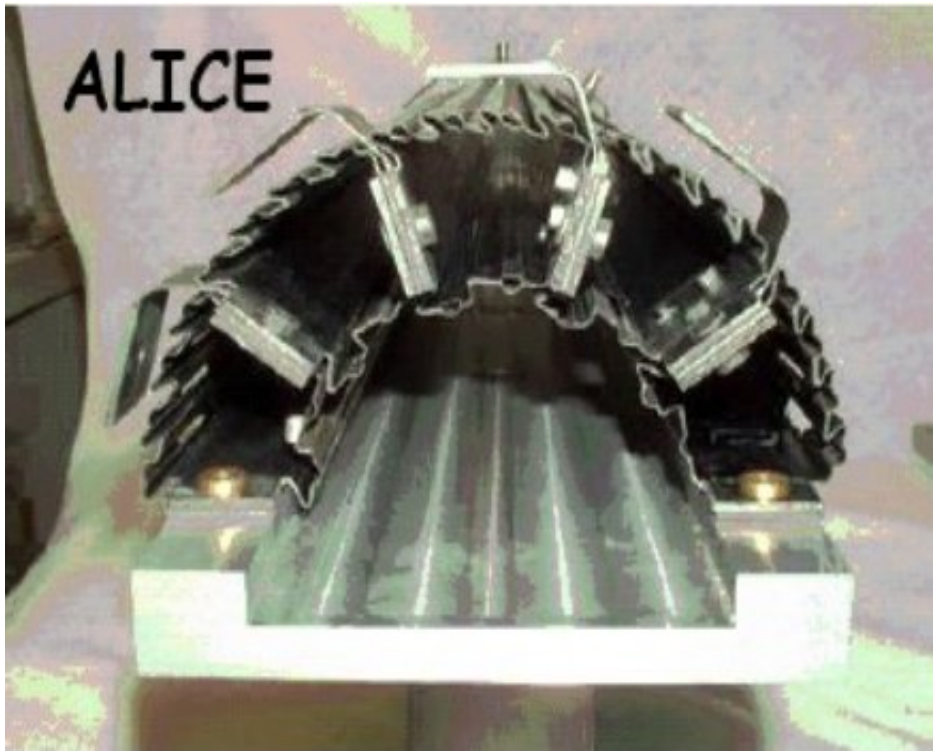


very light-weight carbon fiber support structure
(200 $\mu m$, $\sim$ 0.1% $X_0$)

| | |
|---|---|
| sensor | 200 $\mu$m |
| IC | 150 $\mu$m |
| cooling ($C_4F_{10}$) @ RT | 0.3% $X_0$ |
| (PHYNOX tubes, wall 40 $\mu$m) | |

total $X_0$ per layer $\sim$ 0.9%
(ATLAS, CMS $>$ 2%)

# the LHCb Vertex Locator (VELO)

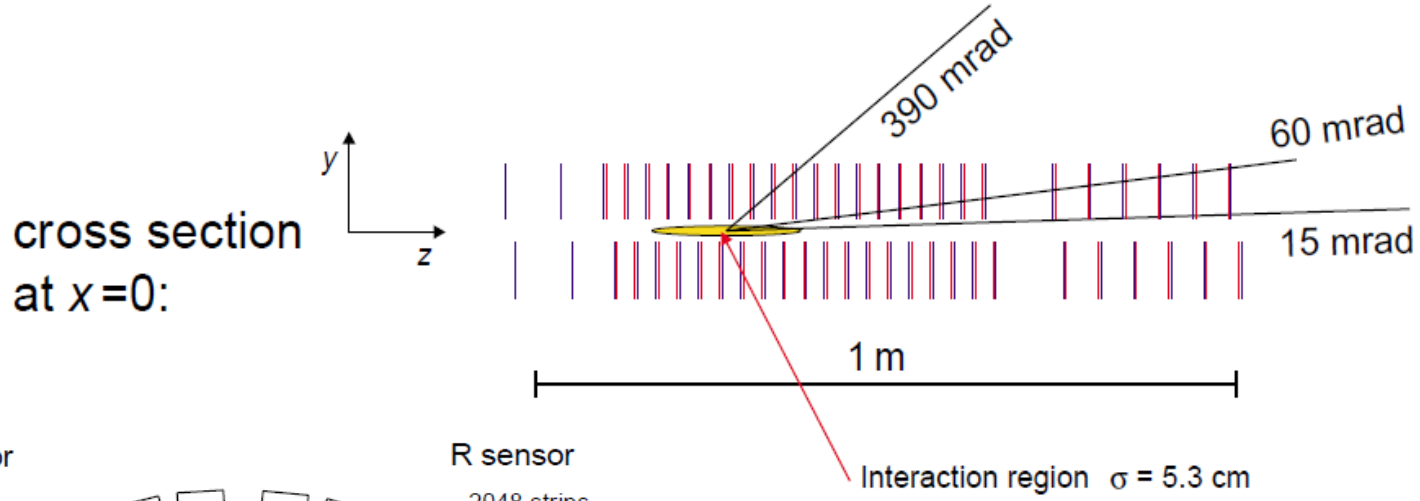


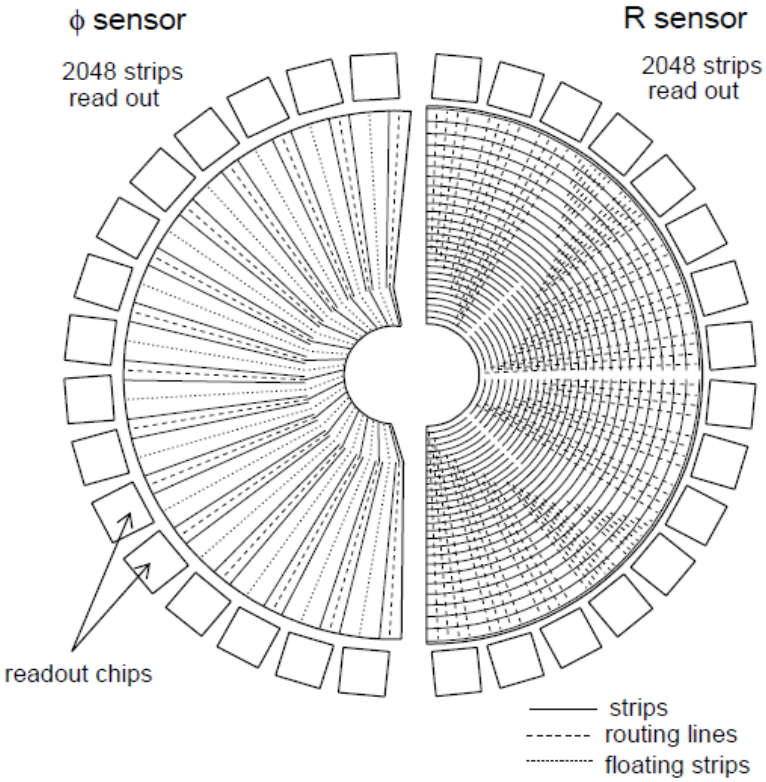


25 stations of R and phi sensors

pitch 40-100 mm

signals routed to outer radius where electronics (chips) sits

innermost active structure 7 mm from the beams!

- smaller than aperture required for LHC beams during injection $\rightarrow$ the 2 detector halves opened during injection (29 mm) and closed thereafter (reproducible to 10 µm)

operation in secondary vacuum, shield detector against RF pickup from beams and vice versa

# the LHCb Vertex Locator (VELO)

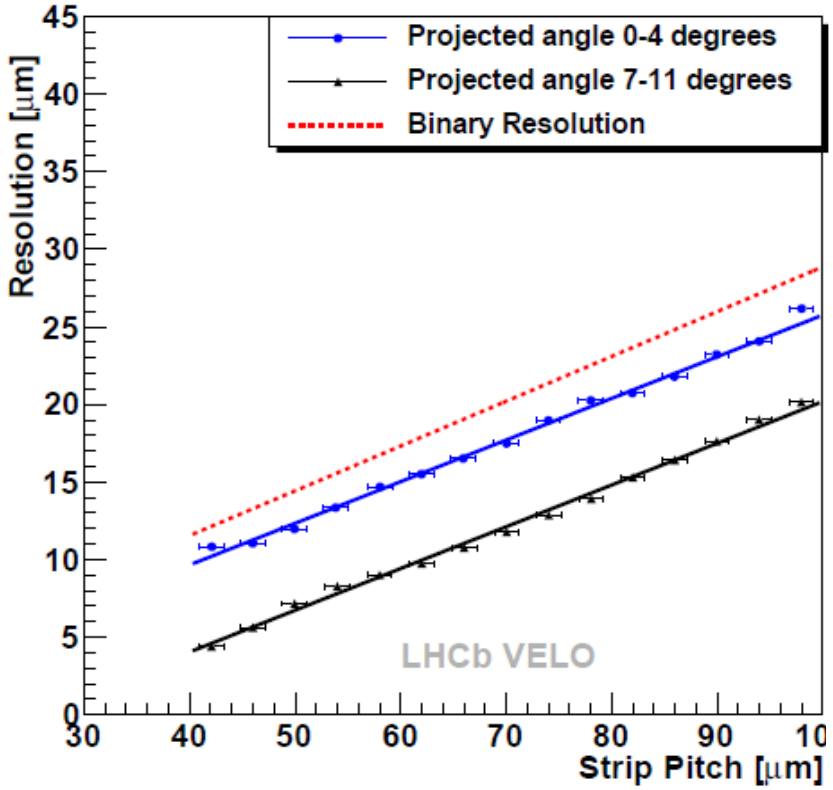


⇐ single hit resolution depending on strip pitch

primary vertex resolution as function of number of tracks contributing to vertex ⇓

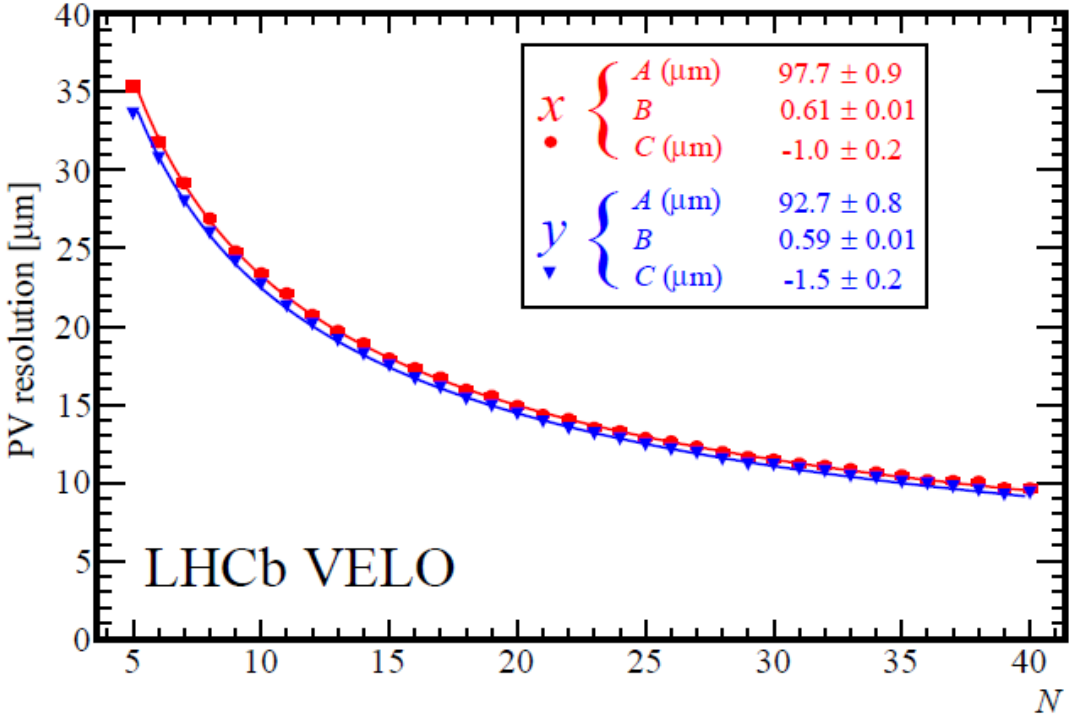


secondary vertices: impact parameter resolution limited by multiple scattering in detector ) 3.2% $X_0$ → better 35 μm

# Further Reading


- Rossi, Fischer, Rohe, Wermes, **'Pixel Detectors: From Fundamentals to Applications'** Springer Berlin-Heidelberg-New York, 2006, (ISBN 3-540-283324)
- G. Lutz, **'Semiconductor Radiation Detectors'** Springer Berlin-Heidelberg-New York, 1999
- E. Heijne, **'Semiconductor Micro-pattern Pixel Detectors: A Review of the Beginnings'** NIM A465 (2001) 1-26
- N. Wermes, **'Pixel Detectors for Tracking and theirs Spin-off in Imaging Applications'** NIM A541 (2005) 150-165, e-Print Archive: physics/0410282
  and
  **'Pixel Detectors'** in LECC2005 Heidelberg 2005, Electronics for LHC and future experiments e-print Archive: physics/0512037

# 4.6.7 CCD, charge-coupled device

MOS structure (metal-oxide-silicon)

many independent and separately switchable gates (electronically shielded potential wells) on $SiO_2$ over p-substrate

- pixels $50 \times 50\ \mu m^2$ (or even $20 \times 20$), act at low voltage (2 V) as capacitors storing charges produced by ionizing tracks

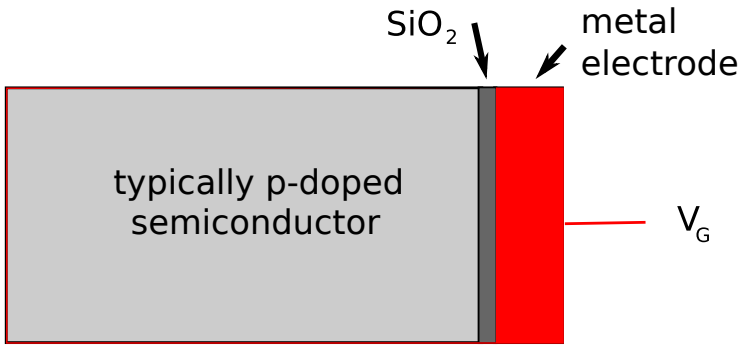


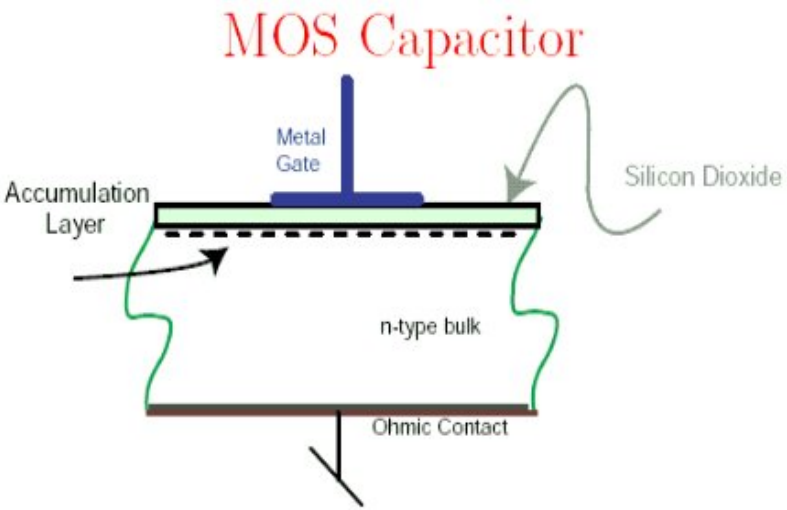


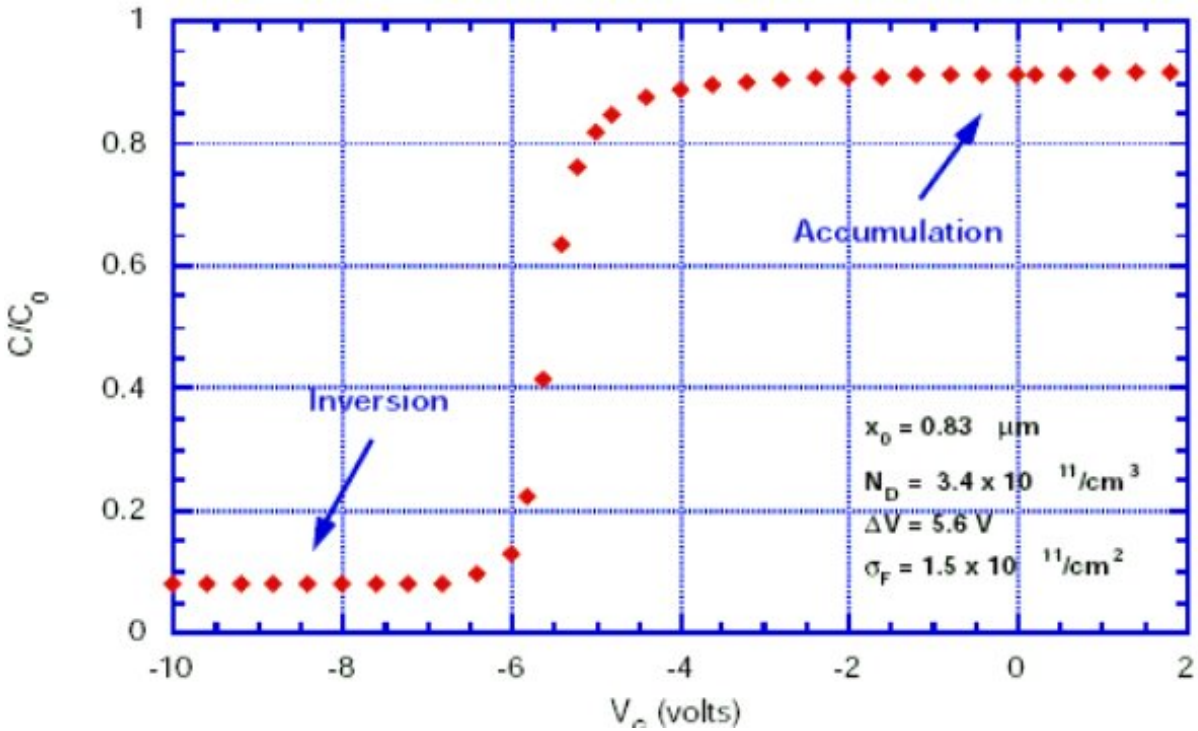


MOS high frequency C-V characteristic curve (n-type bulk)

# Band model of MOS contact

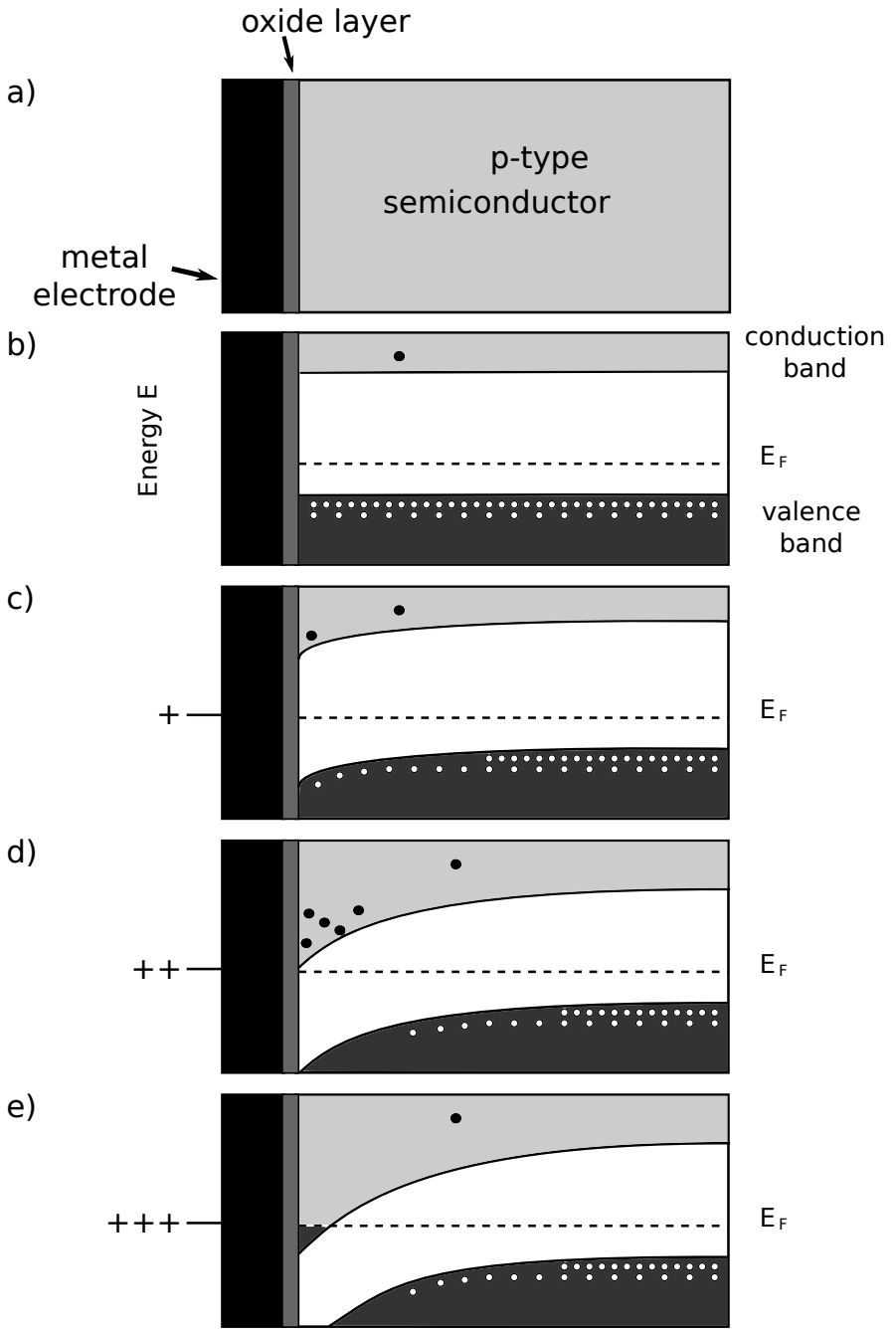


b) energy levels without external field

c) small positive bias: depletion near surface (like at p-n junction)
high resistance space charge zone, can store charge

d) higher positive bias: band are lowered towards interface, in thin layer conduction goes from p to n "inversion"

e) further increase of potential: conduction band dives below Fermi level $\rightarrow$ degenerated Fermi gas – conducting

- **serial readout**:

  make use of fact that boundary becomes conducting at higher voltage (5-10 V)

  charge follows a wandering potential well produced by a pulse sequence applied to the gates, until it reaches charge-sensing preamplifier

2 or 3-phase clock
typical frequency 8 MHz

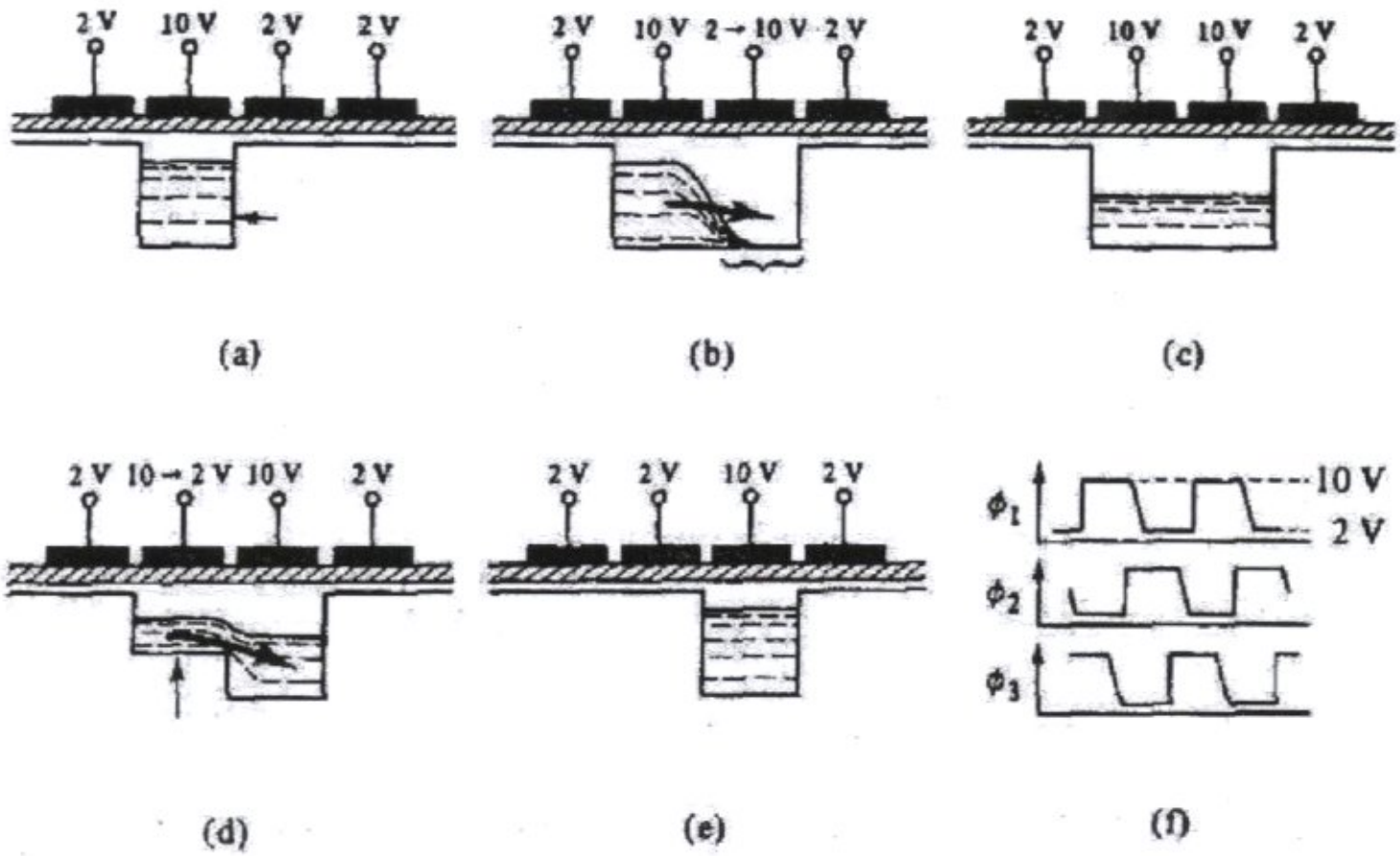

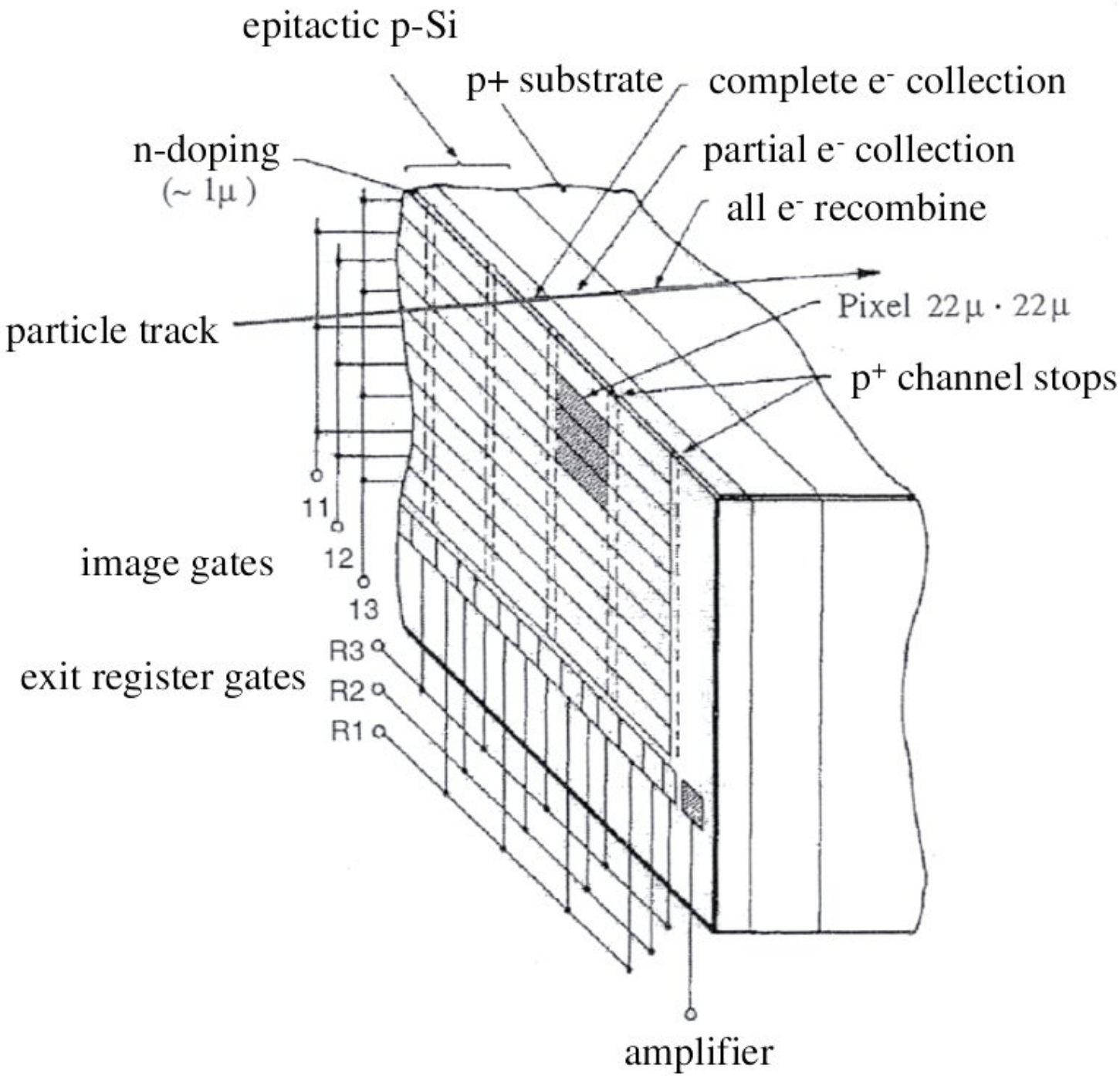
epitactic p-Si
p+ substrate
complete e⁻ collection
n-doping
(~ 1μ)
partial e⁻ collection
all e⁻ recombine
particle track
Pixel 22μ · 22μ
p⁺ channel stops
11
12
13
image gates
R3
R2
R1
exit register gates
amplifier

# CCD - principle of operation I

a detailed look at the charge storage and charge transfer process

**1. charge storage**

incident light generates charge, i.e. electron-hole pairs.
if light is incident on a localized section of p-type silicon, below a positive contact, charge will accumulate.

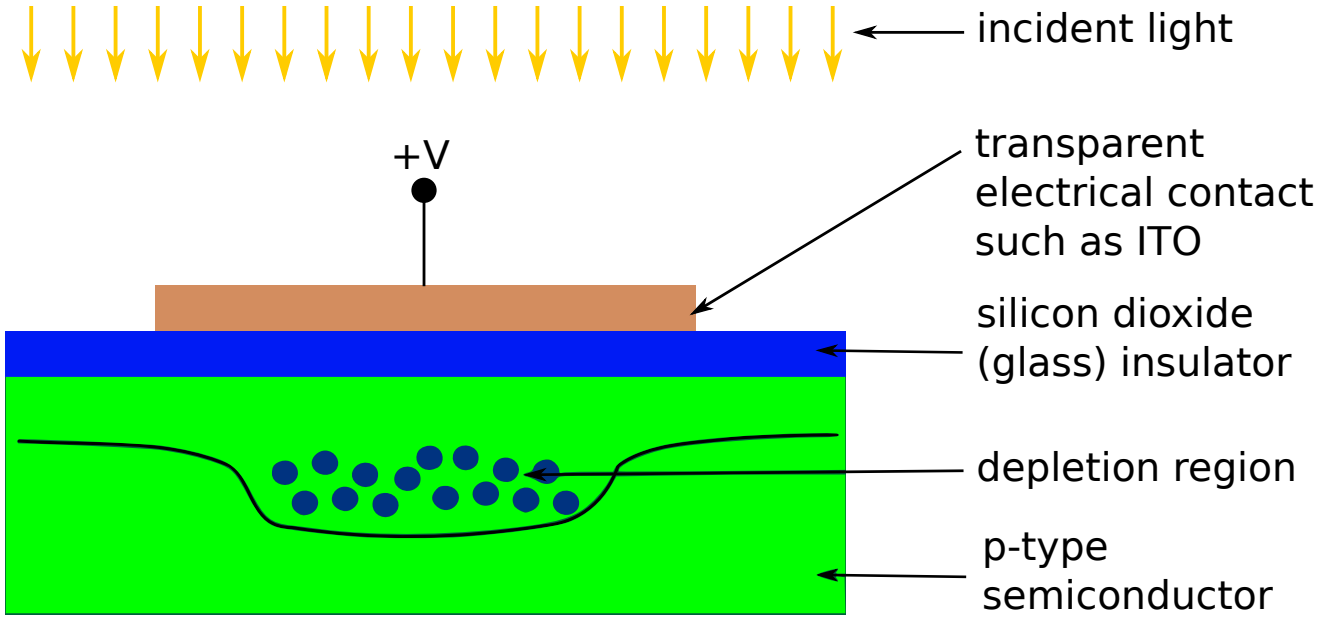

# CCD - principle of operation II

**2. charge transfer**

as voltage on adjacent well is increased, the width of the well increases and the charge becomes shared between the two electrodes

removing voltage from the first well decreases the charge stored below it

the charge packet is therefore transferred to the adjacent electrode

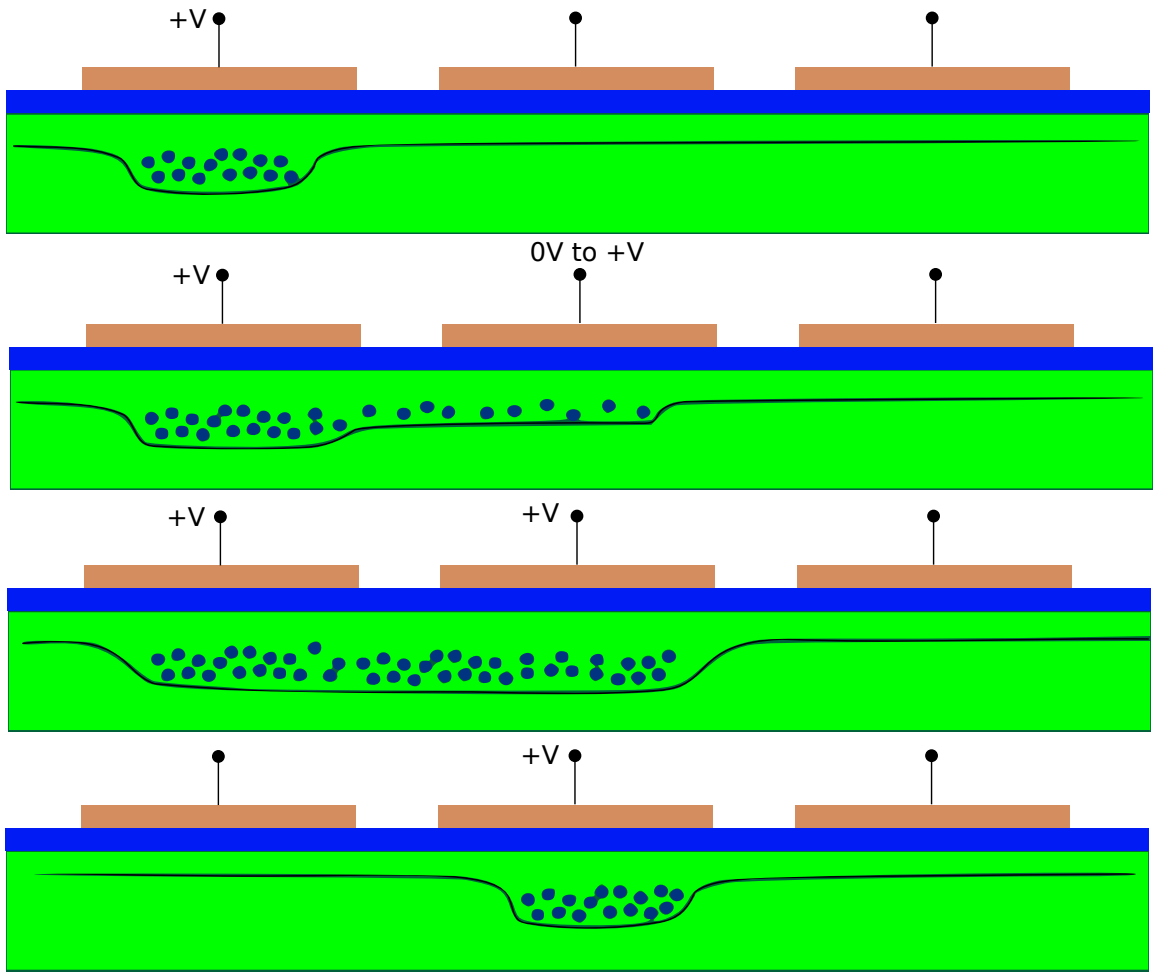

# optical imaging with CCD arrays

charge creation by incident light prior to charge transfer, amount of charge represents integration of light.

charge packet transfer: electrodes are grouped into sets of three or four. These 'phases' remove the charge from the detecting part of the device to the digitizing part.

example of a clocking sequence for a three phase arrangement.

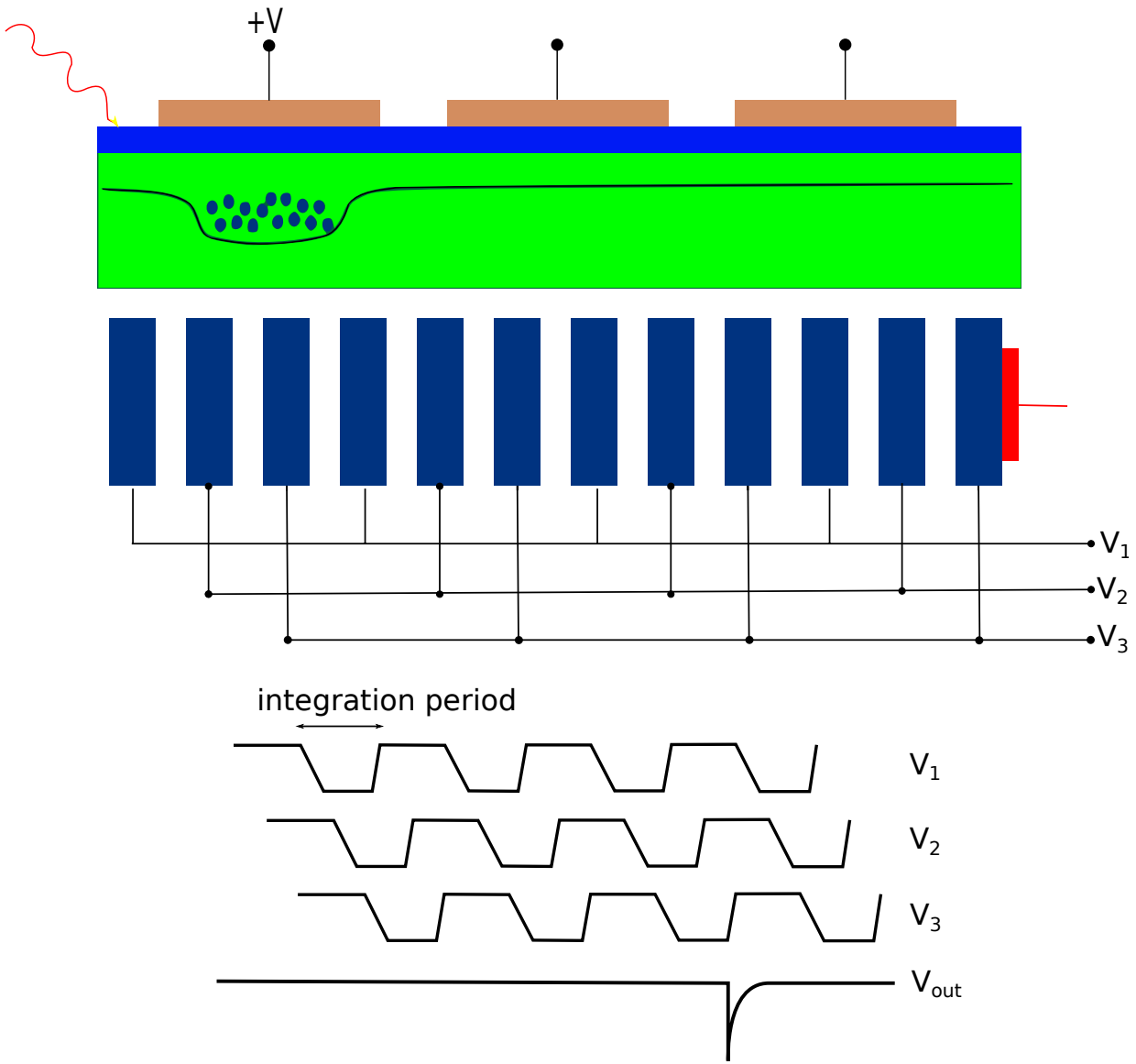

# CCD arrays I

2-dimensional images are digitized using a 2-dimensional array of CCD elements. There are 3 different methods of sequentially reading and storing the spatial light patterns that fall onto the array.

**1. full frame CCD**
accumulated charge shifted vertically row by row to serial read-out register, for each row the read-out register must be shifted horizontally $\rightarrow$ 'progressive scan'
disadvantage: smearing of image due to light falling on sensor while transferring accumulated charge (could use mechanical shutter in addition)

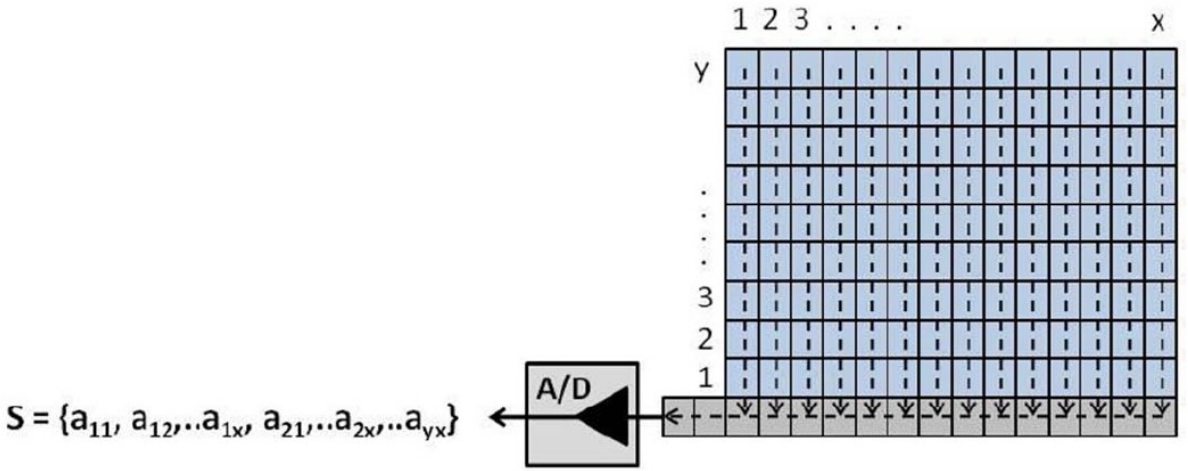

# CCD arrays II

**2. frame transfer**

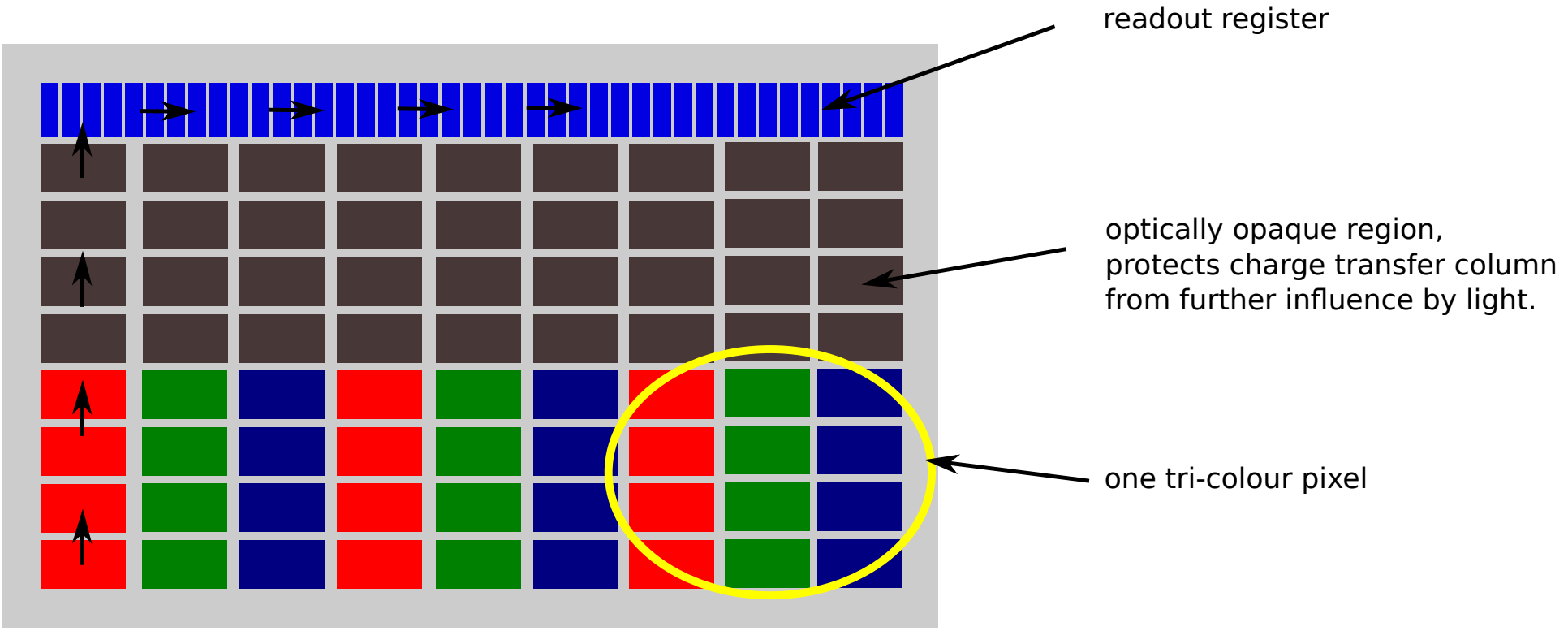


two part sensor, half of the array is used as storage region and protected from light
'up and out' - data are read-out and digitized frame by frame $\rightarrow$ high resolution, slow transfer

# CCD arrays III

**3. interline transfer**

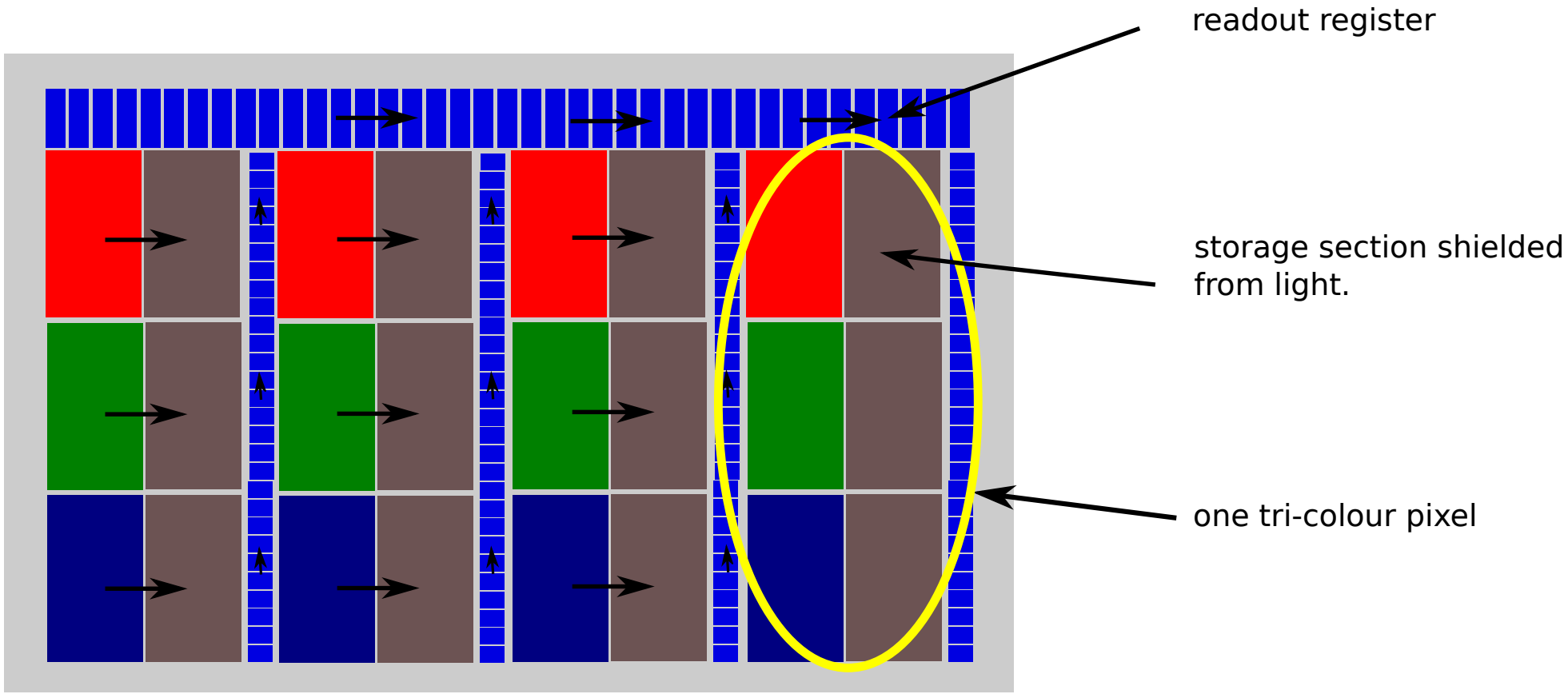


charge transfer channels adjacent to each photodiode, 'over, up and out' - data are read-out and digitized line by line $\rightarrow$ lower resolution (reduced image area), fast transfer reducing image smear

CCD principle conceived by Boyle and Smith at Bell Labs in 1970

## The Nobel Prize in Physics 2009

**"for groundbreaking achievements concerning the transmission of light in fibers for optical communication"**

**"for the invention of an imaging semiconductor circuit – the CCD sensor"**

Photo: U. Montan

**Charles K. Kao**

1/2 of the prize

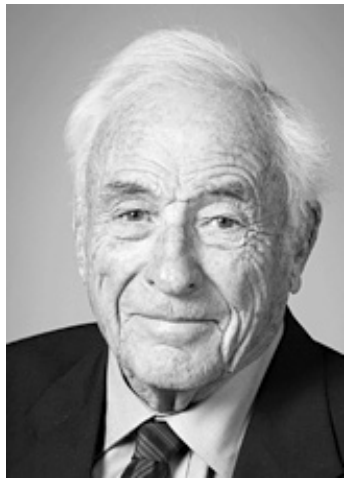

Photo: U. Montan

**Willard S. Boyle**

1/4 of the prize

Photo: U. Montan

**George E. Smith**

1/4 of the prize

# a large state of the art CCD camera

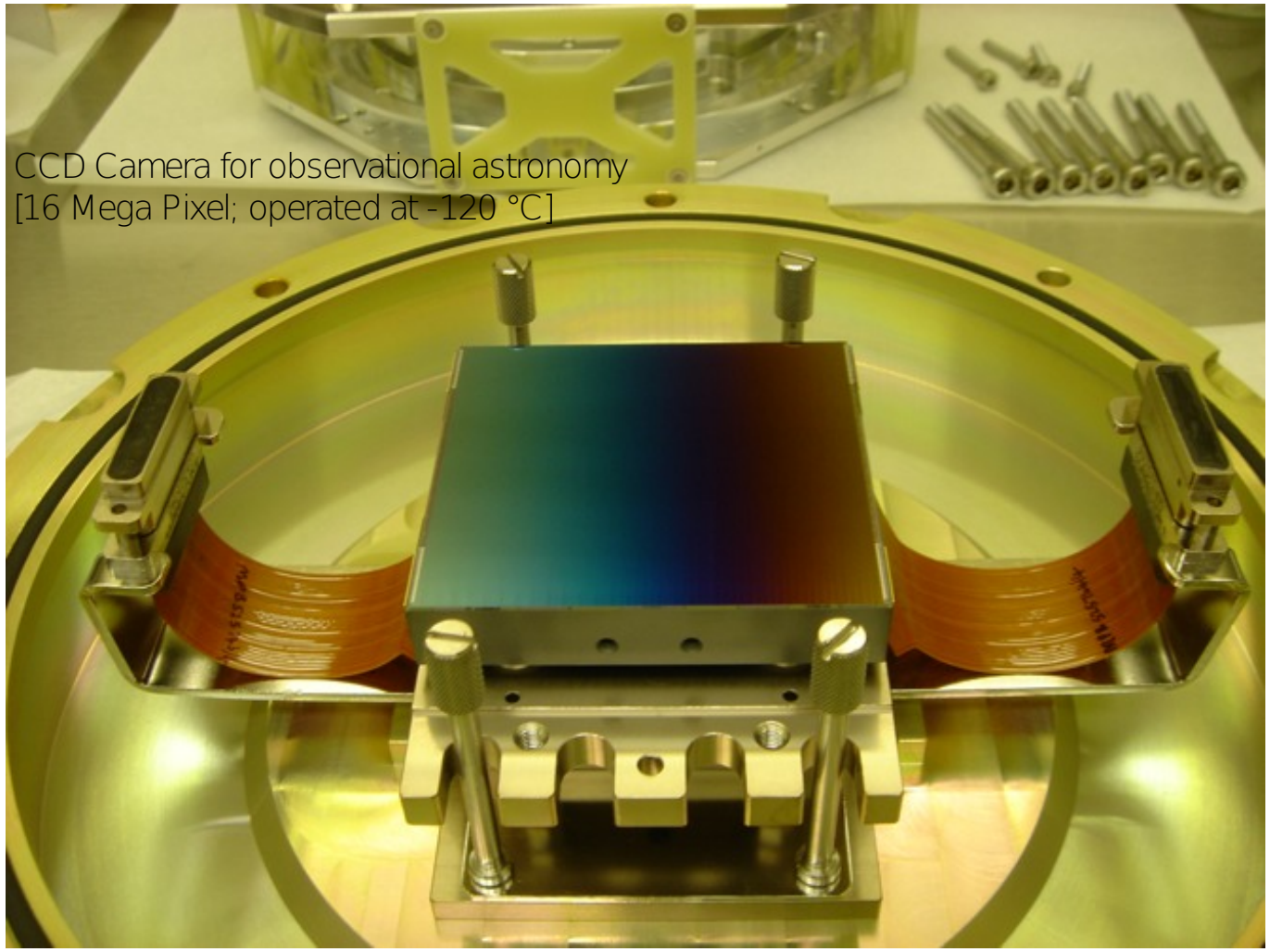

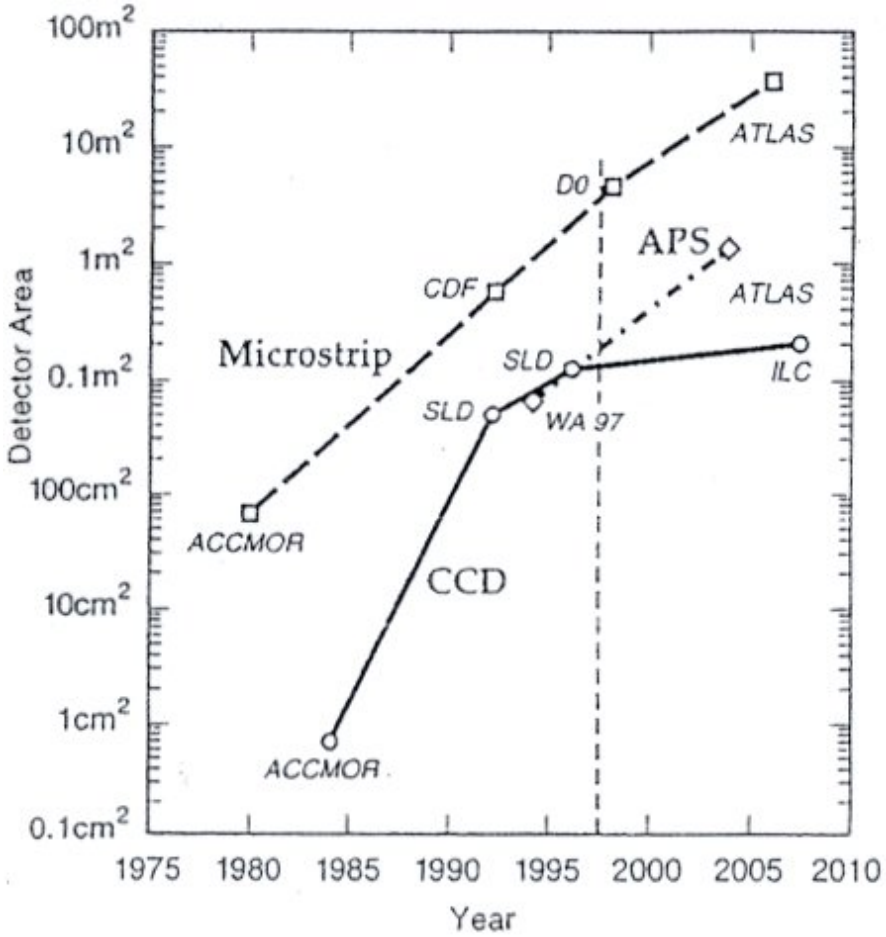


active area of the silicon vertex/tracking detectors as function of time. Micro-strip detectors retain the capability of largest area coverage.

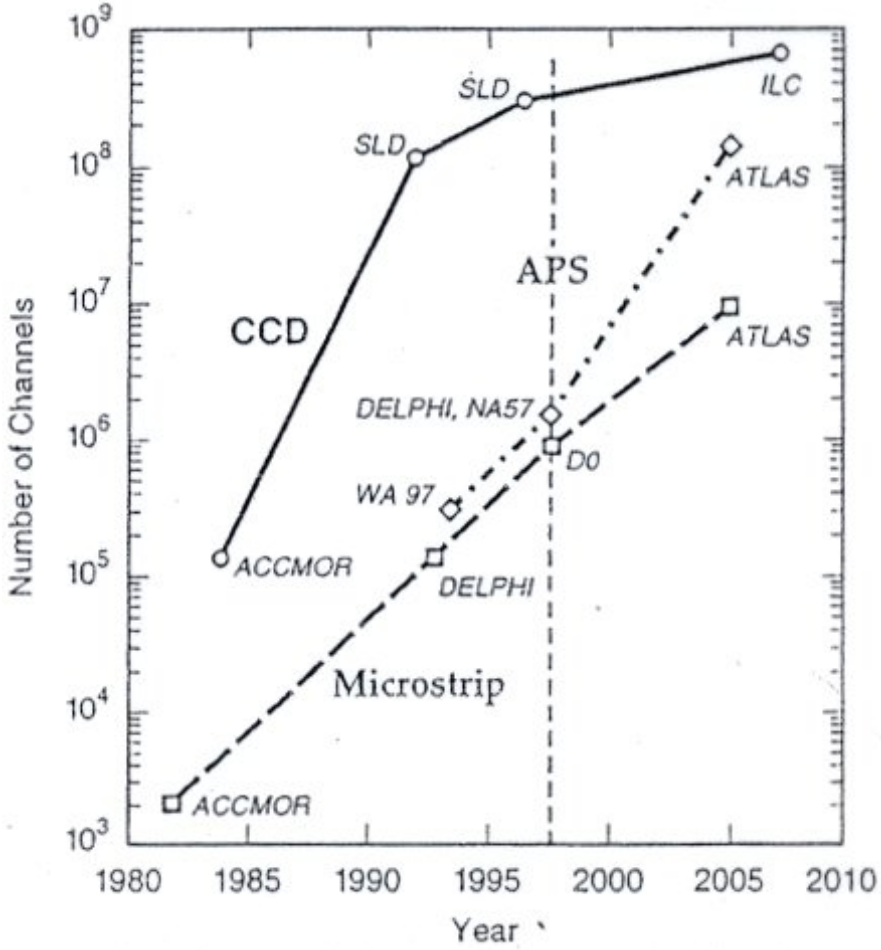


number of channels in the silicon vertex/tracking detectors as function of time. CCD-based pixel detectors retain the capability of finest granularity, but APS ('Active Pixel Sensors') detectors may come close in the long-term future.
2015: now they are

Figs from C.J.S. Damerell, Rev. Sci. Instr. 69 (1998)1570

# 4.7 Radiation damage

major issue at LHC: with design luminosity of $10^{34}/\text{cm}^2\text{s}$ at radius of 10 cm
over 10 years of running accumulated radiation dose $10^{15}\, n_{eq}/\text{cm}^2$ equal 600 kGy
Super LHC (SLHC) possibly from 2019: 10 times the dose of LHC

intensive irradiation R&D program over past $15 - 20$ years to study and minimize effects

- Si sensors
- electronics
- glue and other material

**radiation damage in Si sensors**:
when e.g. a 1 MeV neutron hits Si nucleus $\rightarrow$ recoil kinetic energy of Si 30 keV

compare to typical binding of Si in crystal lattice of $15 - 25$ eV

similarly, incident pions in few hundred MeV range form $\Delta$ resonance when hitting p or n

decay momentum of 200 MeV/c gives recoil to decay p or n of about 2 MeV

NIEL (non-ionizing energy loss) dislocates Si-atoms from their lattice positions

for one 1 MeV neutron about $10^3$ atoms in region of about 100 nm are displaced

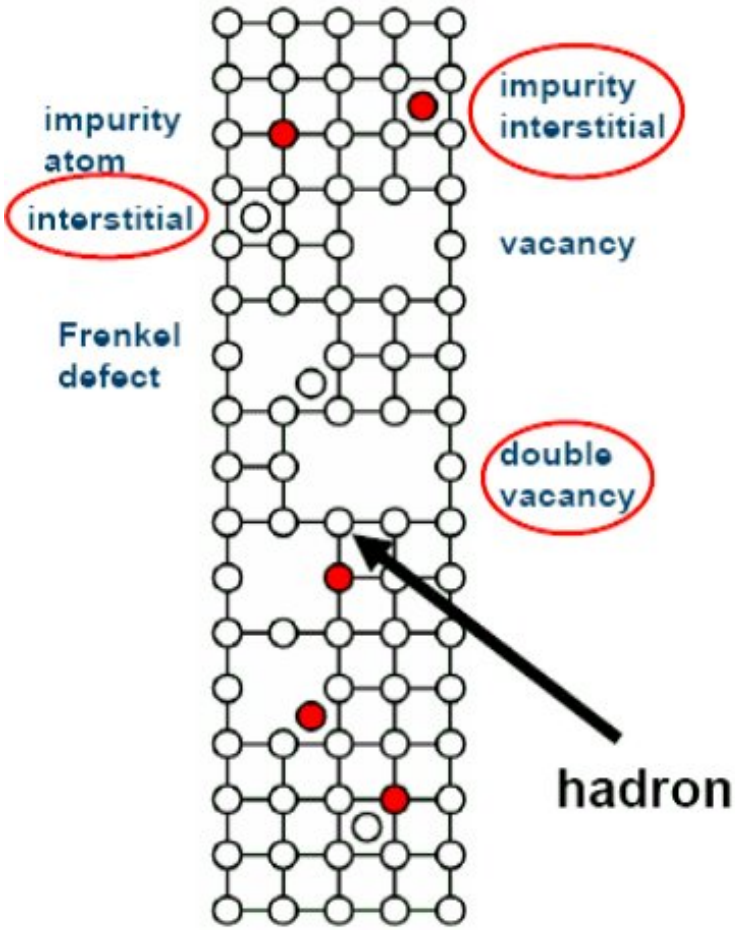

- generation and recombination of levels in band gap → increase of leakage current
  $I = I_0 + \alpha\phi V$ with $\alpha = 2 \cdot 10^{-17}$ A/cm$^2$ for particle flux $\phi$ (per cm$^2$) and volume $V$
  increased detector noise, worse resolution ($S/N$)
- creation of trapping centers → trapping of signal charge by recombination
- change of space charge in depleted region → change of effective doping
  in extreme case type inversion n-type → p-type

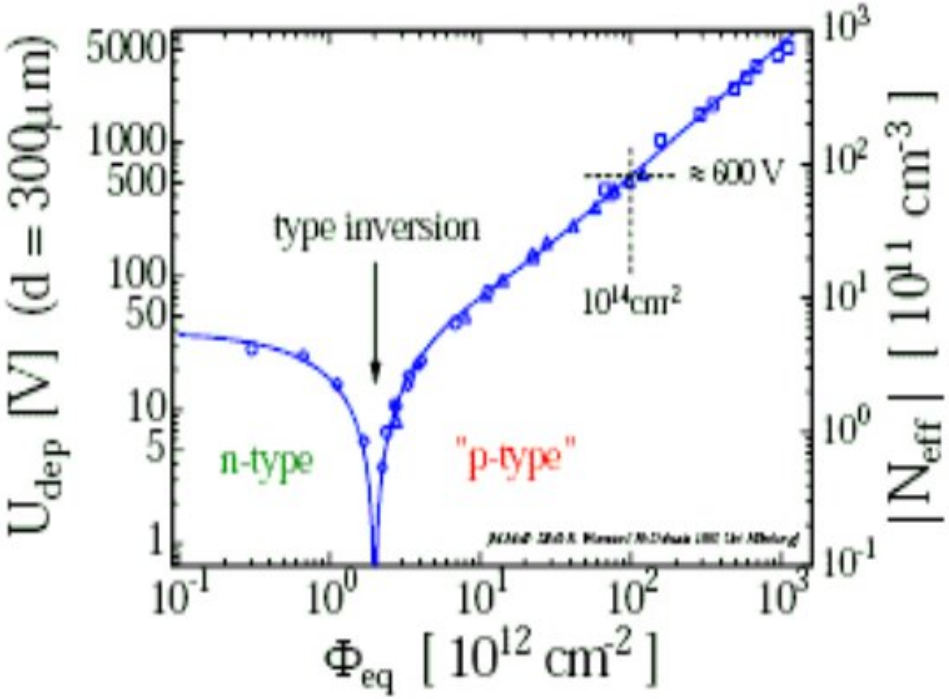


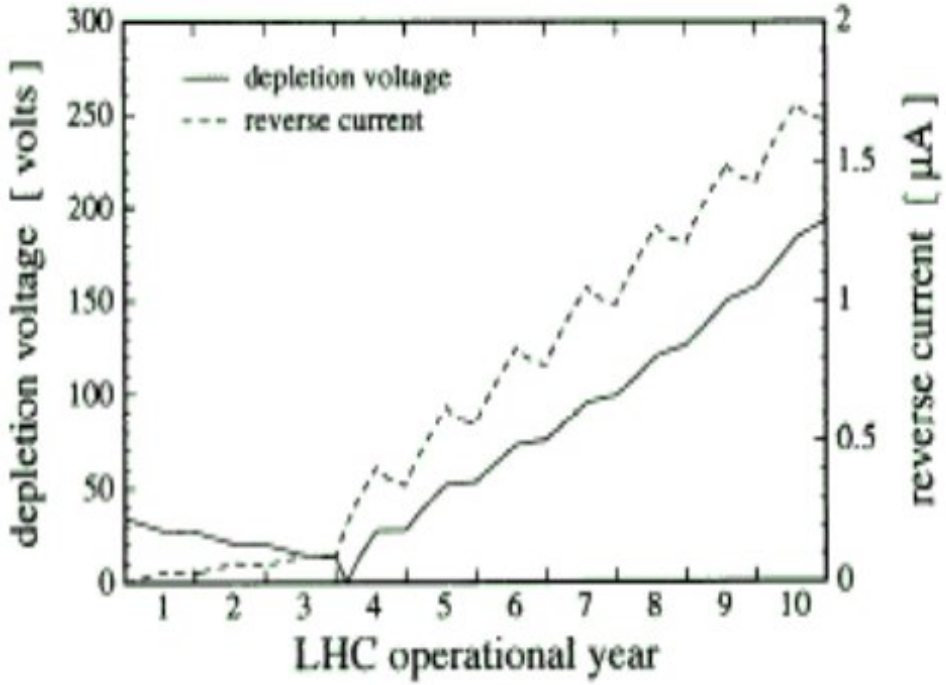


can operate detector up to about $10^{14} n_{eq}/\text{cm}^2$ as for $U > 600$ V discharge
this would be only one year at LHC nominal luminosity → not good enough!

## after irradiation complicated time dependence of damage:

- for irradiation without type-inversion slow healing of damages (months)
- after type-inversion:

  - for first week, effective doping concentration decreases at room temperature (beneficial annealing)

  - after that, doping concentration slowly increases (reverse annealing); can be minimized by keeping detector cool in between running periods

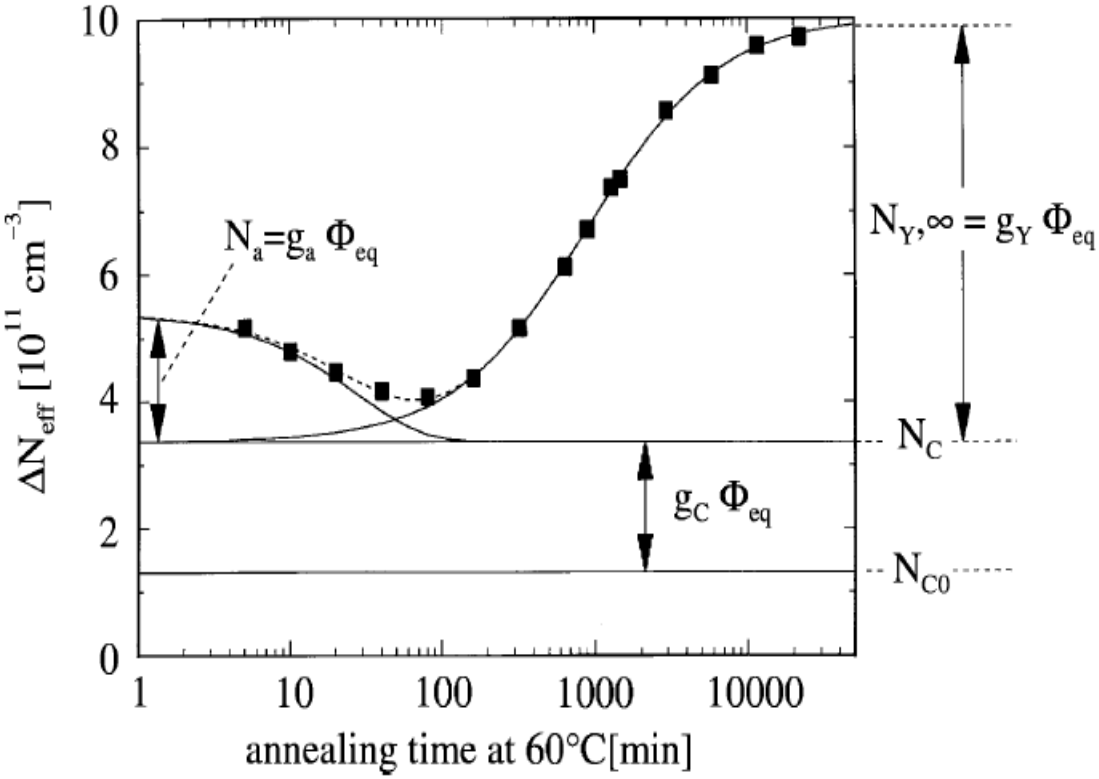

## the solutions for LHC:

**1. oxygenated Silicon** = deliberate addition of impurities to bulk material, i.e. enrichment of Si substrate with oxygen
- electrically active defects capture vacancies in stable and electrically neutral point defects
- reduces radiation induced increase in full depletion voltage for irradiation with charged hadrons

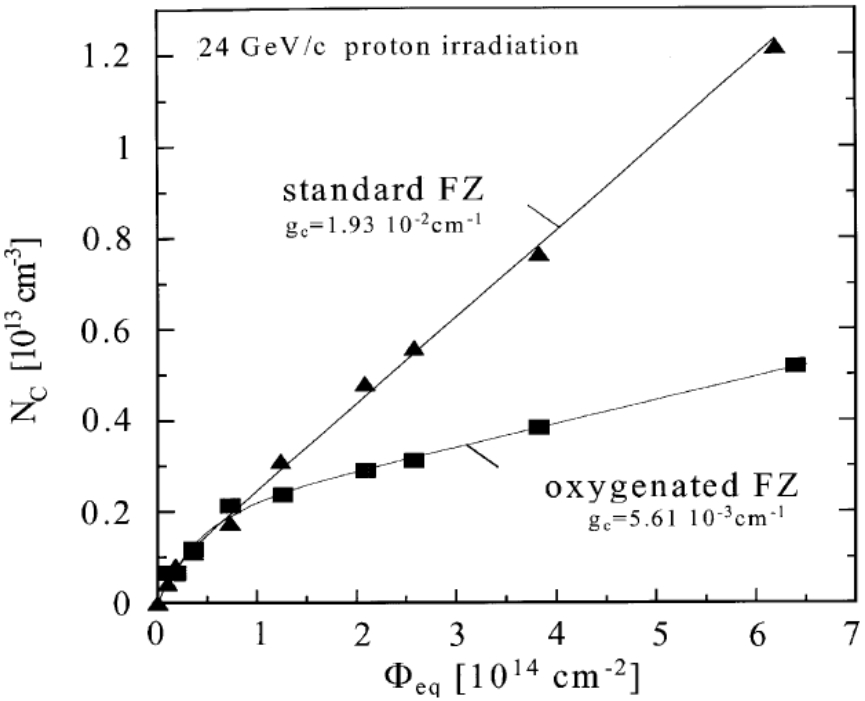


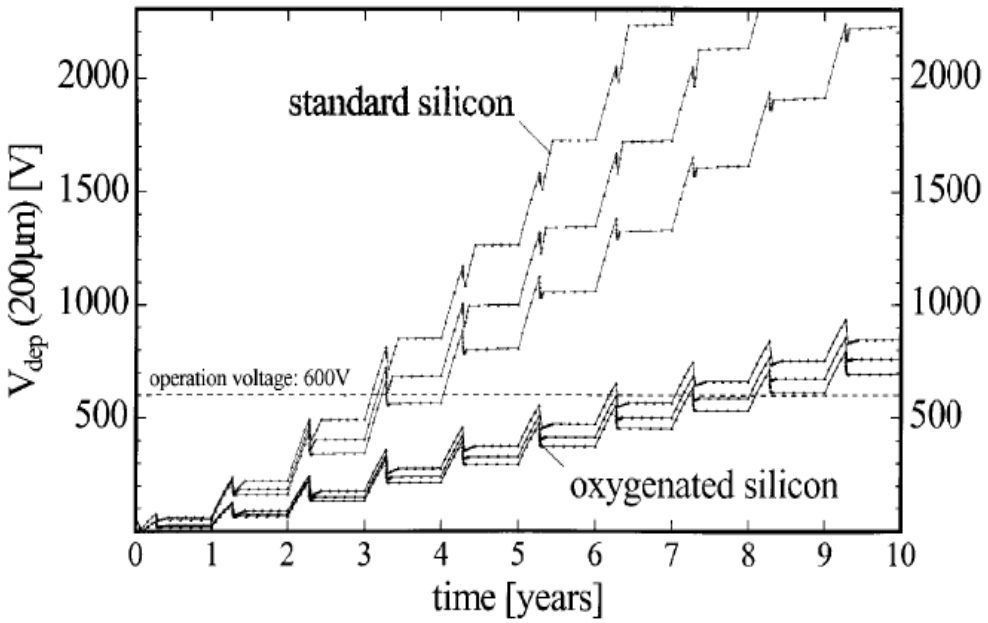


RD48, G. Lindström et al., NIM A465 (2001) 60

# measuring the effective depletion depth after irradiation

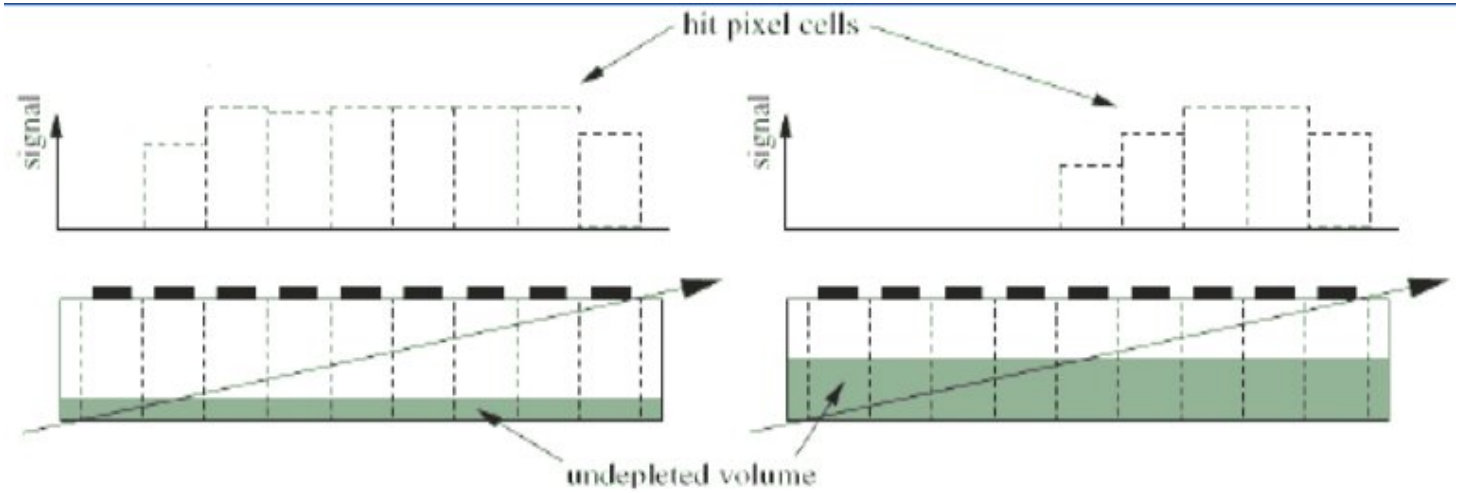


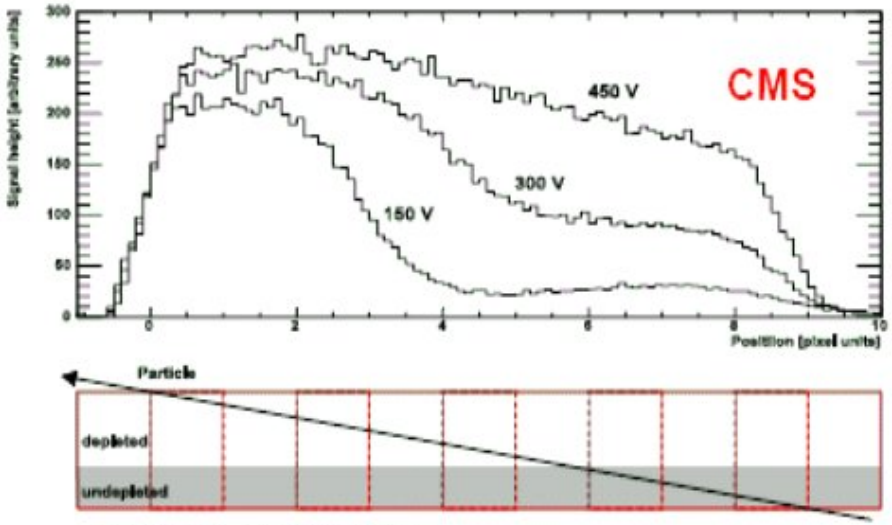


V.Chiochia, M. Swartz et al.
arxiv.org/abs/physics/0409049, IEEE NSS 04 in Rome

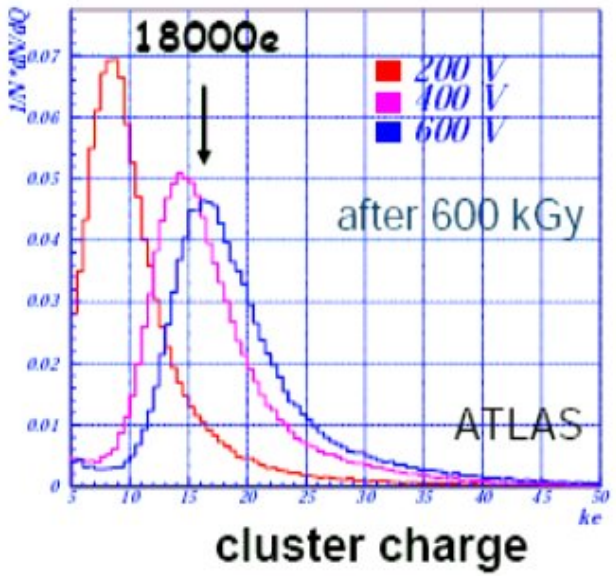

**2. use of n+ in n (all LHC pixel detectors):**

n+ implants in n-type Si

after type-inversion depletion region grows from n+ side → can operate detector partially depleted when full voltage cannot be applied any longer

plus, usage of guard rings around sensor at ground potential to protect sensitive frontend electronics from discharges

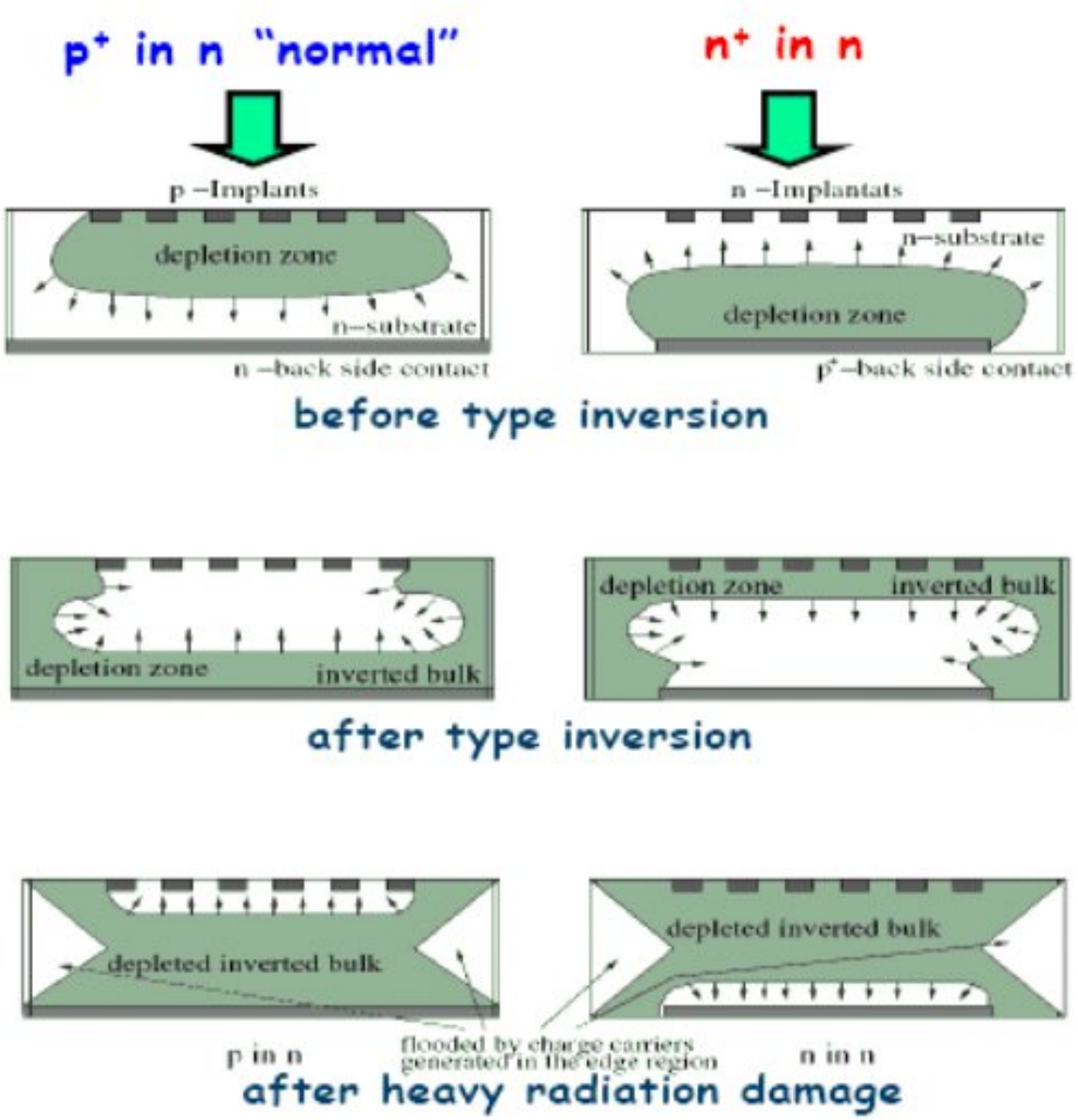


L. Andricek et al., NIM A409 (1998) 184

# long-term prospects 1: Diamond detectors

($E_{gap} = 5.45$ eV)

much better behavior after irradiation

- lower leakage current
- increased mean free path for charge carrier trapping
- radiation hard up to $5 \cdot 10^{15}$ cm$^2$

but: can produce only thin detectors (less than 300 $\mu$m)
worse $S/N$, a lot of R&D needed

can already produce cheap material by evaporation (chemical vapor deposition)

# long-term prospects 2: 3D - silicon detectors

(see e.g. C. DaVia, CERN courier Jan/Feb 2003):
proposed by Sherwood Parker in 1995: p+ and n+ electrodes penetrate silicon bulk

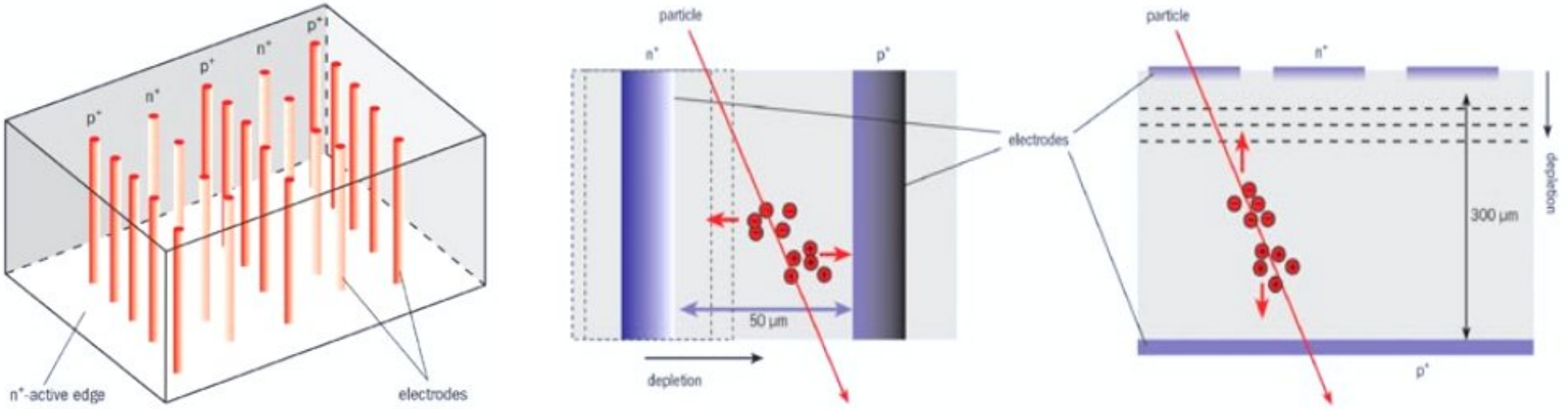


the same charge as in planar detector is collected in shorter time over shorter distance and with 10 times less depletion voltage

| design parameter | 3D | planar |
|---|---|---|
| depletion voltage (V) | $< 10$ | 70 |
| collection length ($\mu$m) | $\sim 50$ | 300 |
| charge collection time (ns) | $1 - 2$ | $10 - 20$ |
| edge sensitivity ($\mu$m) | $< 10$ | $\sim 300$ |

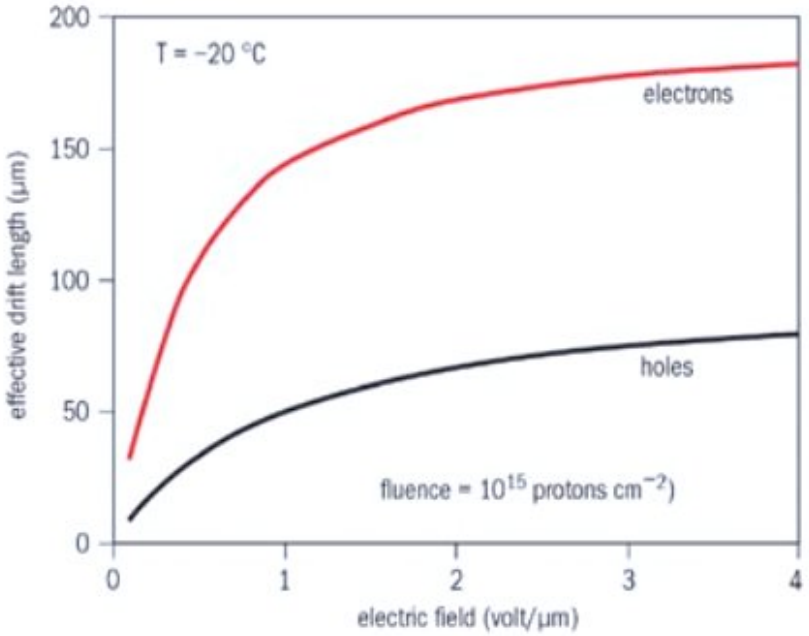


generally, electric field in sensor must be as large as possible $\rightarrow$ maximizes drift velocity $\rightarrow$ maximizes effective drift length before charge is trapped by defects $L_{drift} = v_{drift} \cdot \tau_{tr}$ with a trapping time $\tau_{tr}$

drift lengths decrease linearly with fluence, device with larger drift length becomes inefficient at high radiation levels.
in detector with segmented electrode (pixels), larger fraction of signal generated by charge carrier drifting towards it
in irradiated detector, electrons travel farther before being trapped, therefore advantageous to collect signal at n+ electrode

deep reactive ion etching to 'drill' holes in silicon with thickness/diameter = 20 : 1, means holes into 300 $\mu$m substrate can be 'drilled' 50 $\mu$m apart

fill holes with poly-crystalline Si doped with B or P, which is then diffused into the surrounding pure silocon to make electrodes

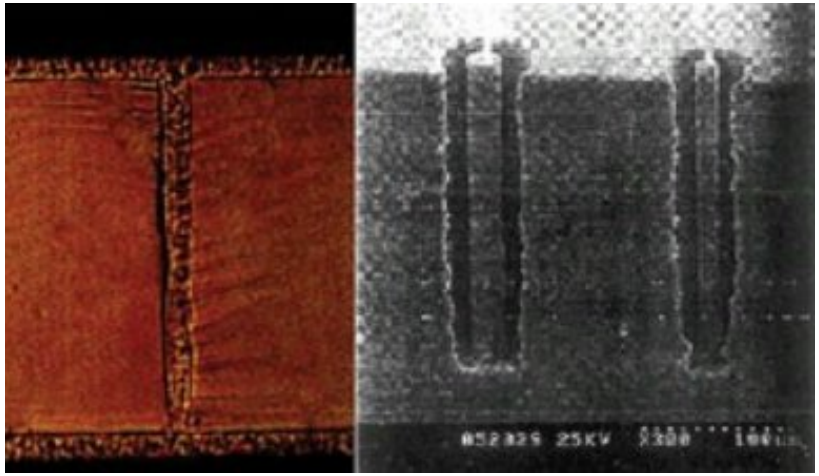

right: 290 $\mu$m deep etching followed by deposition of 2 $\mu$m poly-crystalline Si
left: broken wafer showing filled electrode holes

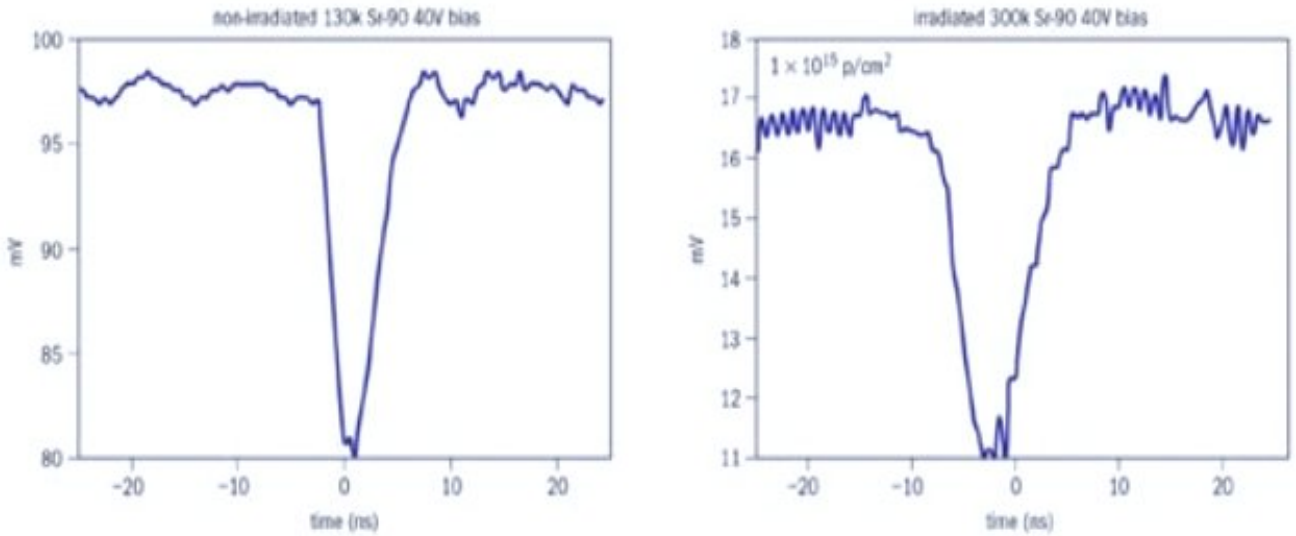


3D silicon sensor before and after irradiation: signal smaller but response still fast

3D sensor in the process of fabrication: 1 set of electrodes completed in hexagonal pattern
bottom: active edge filled with dopant to form electric field inside sensor $\rightarrow$ deplete within a few microns of edge

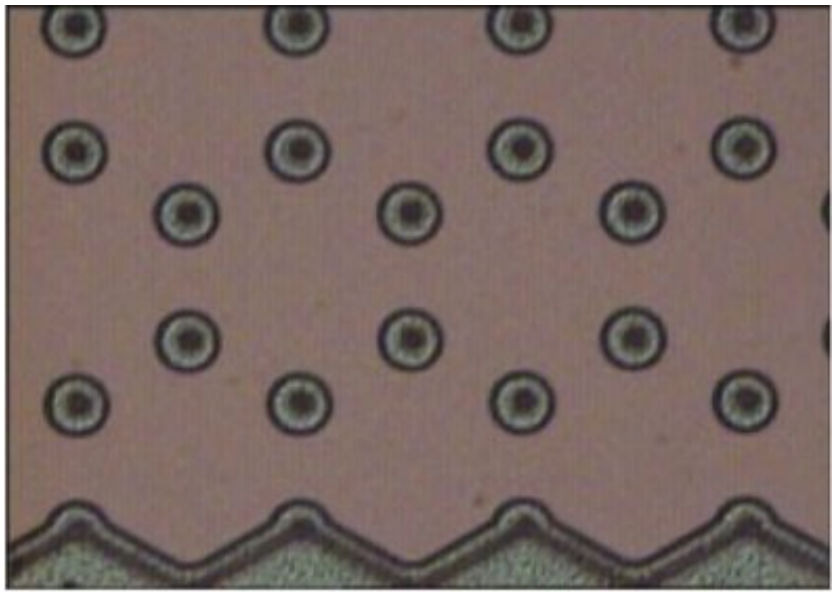

technology also important for X-ray imaging, e.g., in molecular biology (protein folding)